

University of Montana

ScholarWorks at University of Montana

Graduate Student Theses, Dissertations, &
Professional Papers

Graduate School

2002

Sedimentary record of Late Cretaceous through Paleocene evolution of the Bighorn Basin Wyoming

Jesse H. Mitchell

The University of Montana

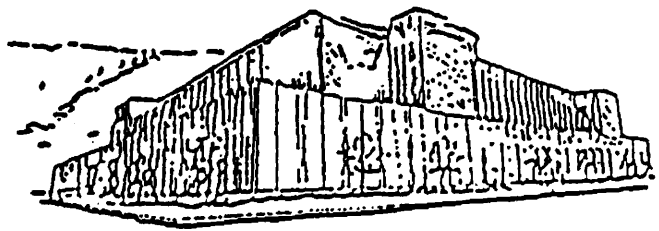
Follow this and additional works at: <https://scholarworks.umt.edu/etd>

Let us know how access to this document benefits you.

Recommended Citation

Mitchell, Jesse H., "Sedimentary record of Late Cretaceous through Paleocene evolution of the Bighorn Basin Wyoming" (2002). *Graduate Student Theses, Dissertations, & Professional Papers*. 7100.
<https://scholarworks.umt.edu/etd/7100>

This Thesis is brought to you for free and open access by the Graduate School at ScholarWorks at University of Montana. It has been accepted for inclusion in Graduate Student Theses, Dissertations, & Professional Papers by an authorized administrator of ScholarWorks at University of Montana. For more information, please contact scholarworks@mso.umt.edu.



Maureen and Mike
MANSFIELD LIBRARY

The University of **MONTANA**

Permission is granted by the author to reproduce this material in its entirety,
provided that this material is used for scholarly purposes and is properly cited in
published works and reports.

*** Please check "Yes" or "No" and provide signature ***

Yes, I grant permission
No, I do not grant permission

Author's Signature *[Signature]*

Date 12-31-02

Any copying for commercial purposes or financial gain may be undertaken only with
the author's explicit consent.

**Sedimentary record of Late Cretaceous through Paleocene evolution of
the Bighorn basin, Wyoming**

by

Jesse H. Mitchell

B.S., University of Wisconsin Madison, 1995

Presented in partial fulfillment of the requirements

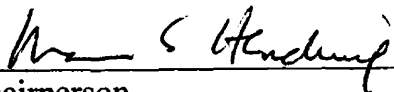
for the degree of

Master of Science

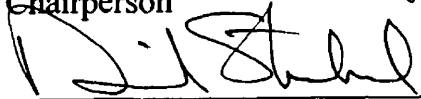
The University of Montana

2002

Approved by:



Chairperson



Dean, Graduate School

12-31-02

Date

UMI Number: EP37901

All rights reserved

INFORMATION TO ALL USERS

The quality of this reproduction is dependent upon the quality of the copy submitted.

In the unlikely event that the author did not send a complete manuscript and there are missing pages, these will be noted. Also, if material had to be removed, a note will indicate the deletion.

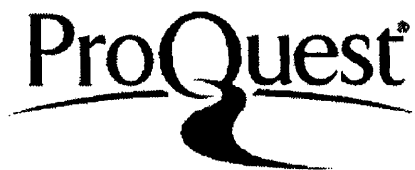


UMI EP37901

Published by ProQuest LLC (2013). Copyright in the Dissertation held by the Author.

Microform Edition © ProQuest LLC.

All rights reserved. This work is protected against
unauthorized copying under Title 17, United States Code



ProQuest LLC.
789 East Eisenhower Parkway
P.O. Box 1346
Ann Arbor, MI 48106 - 1346

Sedimentary record of Late Cretaceous through Paleocene evolution of the Bighorn basin, Wyoming

Director: Marc Hendrix MSH

Three stratigraphic sections were measured in the southern Bighorn basin, Wyoming in the latest Cretaceous Montana Group and Paleocene Fort Union Formation. These sections were analyzed in terms of lithofacies, sandstone petrofacies, and paleocurrent trends, and were subdivided into sequences. The Montana Group of the Bighorn basin consists of the Cody Shale, the Mesaverde Formation, including tongues of the Claggett Shale and the Teapot Sandstone, the Meeteetse Formation, including a tongue of the Lewis Shale, and the Lance Formation. The Fort Union Formation is not subdivided into members in the southern Bighorn basin.

Six sequences (S1-S6) were identified in these formations. These sequences record both the final retreat of the Cretaceous Western Interior Seaway in the Bighorn basin and contemporaneous influences of local tectonics. Sequences S1 - S2 appear to be controlled by relative sea level changes together with autocyclic processes such as delta lobe switching. Sequences S3 - S5 are primarily controlled by tectonic movement of the Absaroka thrust sheet and the Washakie uplift to the west. Sequence S6 clearly indicates tectonic control, with a basal angular unconformity in the eastern part of the basin proximal to the Bighorn uplift.

Paleocurrent and provenance data from S1-S6 provide further evidence of an evolving tectonic landscape. Paleocurrent data from the Sequences S1-S5 indicate uninterrupted eastward flow toward the Cretaceous Western Interior Seaway. Sandstones are of uniform composition in the southern portion of the basin, consisting of quartz-chert rich clastics, consistent with a sedimentary source in the Idaho-Wyoming fold thrust belt to the west. Sandstone samples in the northeastern part of the study area contain a higher percentage of plagioclase, possibly due to input from the Elkhorn Mountains volcanics of Montana. In contrast, paleocurrent data of the uppermost strata of S5 at Greybull indicate northwestern axial flow, indicating structural definition of the Bighorn basin by early Paleocene. Sandstone compositions may reflect unroofing of Mesozoic strata overlying the Bighorn uplift. Late Paleocene paleocurrent data of S6 indicate westward flow, away from the Bighorn uplift. Sandstone samples show enrichment in feldspar and textural differences indicating exposure and erosion of the Precambrian core by late Paleocene.

ACKNOWLEDGEMENTS

I would like to thank my thesis advisor, Marc Hendrix for his support and patience. I could not have finished this project without his help and guidance. I would also like to thank my other committee members, Gray Thompson and Andrew Ware for the time and effort they contributed to this project. In addition, I would like to thank Don Winston for his suggestions and input on this project.

I would like to thank Neal Alexandroicz for his help in the field, and Michael Sperazza for his technical support in the sed lab.

The McDonough Grant provided funding for fieldwork and preparation of thin sections. This funding was much appreciated.

I would especially like to thank my sisters, Daisy and Wendy, and my parents. Without their help and support I would have flaked out and given up a long time ago. I hope they realize how much their support has meant to me.

TABLE OF CONTENTS

Abstract	ii
Acknowledgements	iii
Table of Contents	iv
List of Appendices and Plates	vi
List of Figures	vii
Introduction	1
Geologic Setting	2
Hypothesis	6
Methods of Study	
Field Sites	8
Measured Sections	8
Correlations	9
Section Descriptions and Interpretations	
Classification of Fluvial Geometries	
Type I Geometry	11
Type II Geometry	16
Type III Geometry	19
Descriptions of Individual Stratigraphic Units	
Cody Shale	22
Mesaverde Formation	26
Claggett Shale	33
Upper Mesaverde Formation	36
Teapot Sandstone Member	40
Meeteetse Formation	43
Lewis Shale	45
Lance Formation	47
Fort Union Formation	52

Sandstone Petrology	
Methods	55
Error	60
Results	
Stratigraphic Trends in Individual Sections	61
Basin Wide Trends	66
Mesaverde, Meeteetse and Lance formations	66
Fort Union Formation	69
Upper Fort Union Formation	69
Sequence Stratigraphic Framework	
Background	72
Sequences	74
Sequence S1	77
Sequence S2	77
Sequence S3	78
Sequence S4	80
Sequence S5	81
Sequence S6	81
Discussion	
Possible Controls on Sequence Architecture	83
Controls of Individual Sequences	
Sequences S1 and S2	85
Sequence S3	86
Sequence S4	87
Sequence S5	88
Sequence S6	91
Evidence for Uplift of the Ancestral Bighorn Range	91
Conclusions	94
Bibliography	100

APPENDICES

Appendix I: Trigonometric Thickness Corrections	96
Appendix II: Sandstone Point Count Data	97
Appendix III: Recalculated Modal Sandstone Compositions	98
Appendix IV: Precision Calculations for Modal Compositions	99

PLATES

Plate 1:	Stratigraphic sections of the Cody Shale and Lower Mesaverde Formation
Plate 2:	Stratigraphic Sections of the Mesaverde Formation
Plate 3:	Stratigraphic Sections of the Meeteetse and Lance Formations
Plate 4:	Stratigraphic Sections of the Fort Union Formation

LIST OF FIGURES

1. Map	3
2. General Stratigraphic Column	5
3. Type I Sandstone Sedimentary Structures	13
4. Type I Sandstone Stratigraphic Column	15
5. Type II Stratigraphic Column	17
6. Type II Outcrop	18
7. Type III Stratigraphic Column	20
8. Type III Outcrop	21
9. Cody Shale Stratigraphic Column	23
10. Cody shale Sedimentary Structures	24
11. Cody-Mesaverde Contact	27
12. Lower Mesaverde Stratigraphic Column	29
13. Mesaverde Isopach Map	31
14. Lower Mesaverde Isopach Map	32
15. Claggett Isopach Map	34
16. Greybull Sedimentary Structures	37
17. Greybull Mesaverde Stratigraphic Column	38
18. Teapot Sandstone	41
19. Teapot Paleocurrent Map	42
20. Meeteetse Formation at Little Buffalo Basin	44
21. Lewis Shale at Greybull	46
22. Middle Lance Formation at Little Sand Draw	49
23. Upper Lance Channel Scours at Little Buffalo Basin	50
24. Lance Paleocurrent Map	51
25. Upper Fort Union Paleocurrent Map	54
26. Ternary Diagram of All Samples	62
27. Ternary Diagrams of Little Sand Draw Samples	63
28. Ternary Diagrams of Greybull Samples	64
29. Ternary Diagrams of Little Buffalo Samples	65

30. Ternary Diagrams of Cretaceous Samples	67
31. Ternary Diagrams of Fort Union Samples and Upper Fort Union Samples	70
32. Non-marine Sequence model	75
33. Sequences S1-S6	76
34. S2-S3 Sequence Boundary	79
35. Outcrop of Middle Fort Union Formation at Little Buffalo Basin	90

INTRODUCTION

The purpose of this study is to analyze the evolution of the Bighorn basin of north-central Wyoming during its transition from an unbroken foreland basin setting in the Cretaceous Western Interior Seaway, to a structurally distinct basin partitioned by surrounding Laramide uplifts. To study this evolution, I adopted an integrated approach involving analysis of sequence stratigraphy, paleocurrent dispersal patterns, and sandstone provenance of the late Cretaceous Montana Group and the Paleocene Fort Union Formation.

Over the past several decades several new and powerful basin analysis techniques have been developed. Sequence stratigraphy has provided a powerful tool for dividing and correlating stratigraphic intervals as well as yielding insight into the underlying controls of sedimentation. Original sequence stratigraphic models were developed for marine and marginal marine settings, and sequence architecture was attributed to fluctuations of eustatic sea level (Posamentier et al 1988; Posamentier and Vail 1988; Van Wagoner et al 1988), but the degree to which eustatic control is the main influence in sequence development is currently a subject of intense debate (Miall, 1991). Over the past decade workers have attempted to apply sequence stratigraphic concepts to non-marine strata, and link sequence development to tectonic controls. Sandstone provenance has provided another tool to link basin evolution with tectonic control (Dickinson and Suczek, 1979), and further development of this field has allowed a better understanding of the sedimentary response to tectonic forces (Dickinson, 1986; Whipkey et al, 1991; Smosna

et al, 1999; Ridgeway et al, 1999). Recent studies have linked sequence stratigraphy with provenance (Miall, 2001) to give a clearer picture of basin evolution.

I have three main objectives in this study. First, I will attempt to link the sedimentary response of the basin with underlying allocyclic controls such as tectonics or eustatic sea level changes. Second, I seek to provide additional resolution to the paleogeography of the Bighorn basin, and third, I will attempt to constrain the timing of uplift of the ancestral Bighorn range to the east.

Geologic Setting

Located in north-central Wyoming and south-central Montana, the Bighorn basin is bounded by the Absaroka Range to the west, Beartooth uplift to the northwest, the Bighorn uplift to the east, and the Owl Creek and Washakie uplifts to the south-southwest (Figure 1). With the exception of the Absaroka volcanics, all of these uplifts are basement cored and of Late Cretaceous – Early Tertiary age. Prior to formation of these Laramide uplifts, the Bighorn basin area was part of the unbroken foreland basin of the Cretaceous Western Interior Seaway (Bown, 1980; Perry, 1992; Connor, 1992; Johnson et al, 1997). While the Elkhorn Mountains volcanics to the north were active during late Cretaceous time (Connor, 1992; Borrell, 1999), the Absaroka volcanics to the west are Eocene in age, postdating the time-span of this study (Bown, 1982).

Final retreat of the Western Interior Seaway and partitioning of the foreland basin by Laramide fault-block uplifts into distinct sub-basins such as the Wind River, Green River,

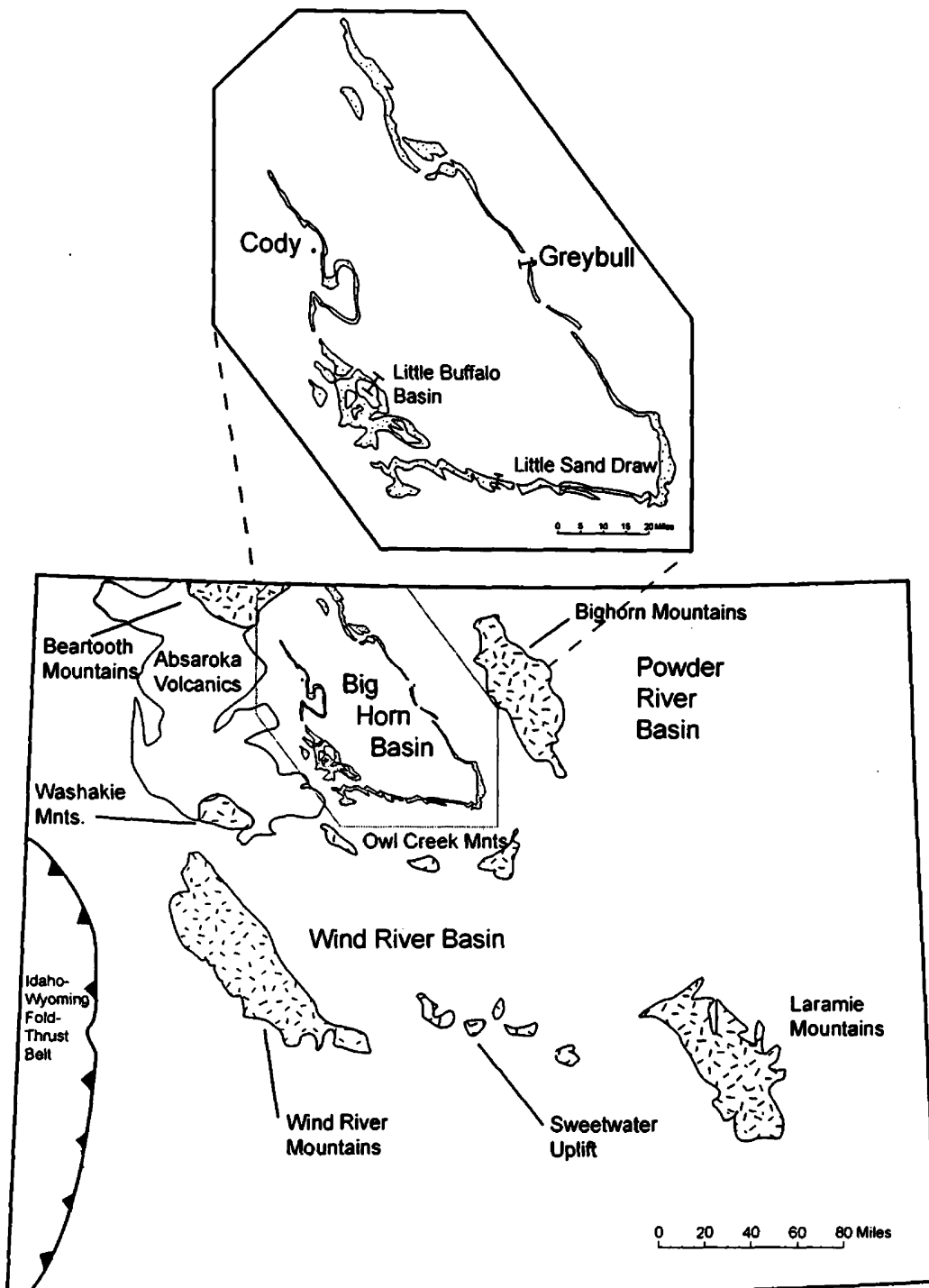


Figure 1. Location Map. Base map location of major basins and exposures of Precambrian crystalline rock in Wyoming. Stippled area in the Bighorn basin shows outcrops of Late Cretaceous strata. Expanded section shows locations of the Little Buffalo basin, Little Sand Draw, and Greybull measured sections. Modified from the geologic map of Wyoming (Love and Christiansen, 1985)

and Bighorn basins of Wyoming occurred during late Cretaceous and Paleocene time (Dickinson et al, 1988; Perry, 1992). The Campanian-Maastrichtian Montana Group and the Paleocene Fort Union Formation recorded these events in the Bighorn basin. The Montana Group of the Bighorn basin consists of the Cody Shale and the Mesaverde, Meeteetse, and Lance formations. The Mesaverde Formation is sub-divided into the informal lower Mesaverde member, the Claggett Shale, and the Teapot Sandstone. Also, the Lewis Shale intertongues with the Meeteetse Formation in the eastern part of the basin. The Fort Union Formation is not subdivided in the southern Bighorn basin (Figure 2).

A number of previous workers have established the broad stratigraphic framework of the Bighorn basin and provided some interpretations of the region's tectonic history. Original work was performed in this area by Hewett (1926), and a great deal of the geologic history as well as the biostratigraphic framework of the area was worked out by Gill and Coban (1973). Age constraints for non-marine strata of the Montana Group were provided by Belt et al (1997). The recent work of Keefer et al, (1998), Johnson et al (1998) and Roberts (1998) has provided more detailed lithologic descriptions of Cretaceous and Paleocene strata, as well as providing basin-wide correlations based on outcrop and subsurface data.

Several studies have investigated the timing of the Bighorn uplift, with estimates ranging from Cretaceous (Gries et al, 1992; Omar and Giegengack, 1997) to mid-Paleocene (Whipkey et al, 1991; Connor, 1992). Provenance studies based on petrofacies and

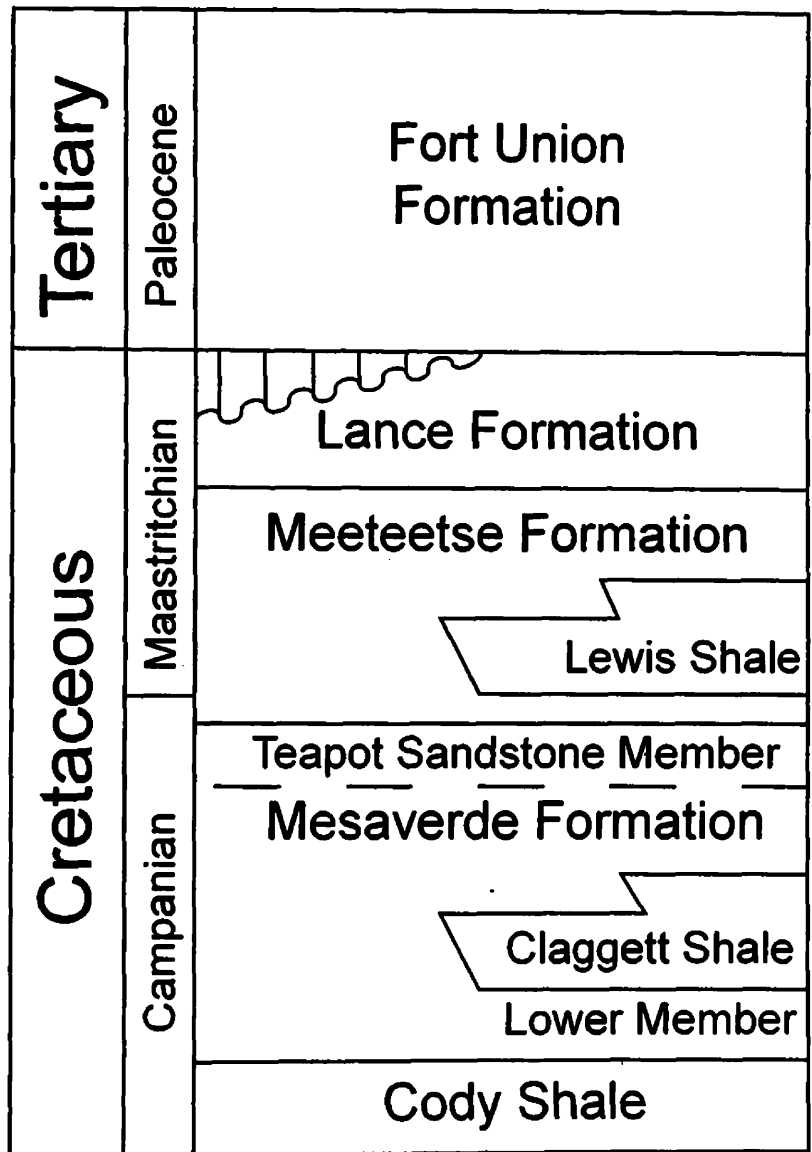


Figure 2. Generalized stratigraphic column for Upper Cretaceous and Lower Tertiary rocks of the Bighorn basin. Modified from Keefer et al (1998).

paleocurrent analysis have been performed in surrounding areas such as the Wind River basin (Courdin and Hubart, 1969), Green River basin (Schuster and Steidmann, 1986), and Powder River basin (Whipkey et al., 1991; Connor, 1992; Hansley and Brown, 1993), as well as the northern Bighorn basin (Yuretich and Hickey, 1984), but no such study has been performed in the southern Bighorn basin. Paleogeography and drainage patterns of the Bighorn basin have been a topic of prolonged debate (Seeland et al, 1998). Several studies have increased paleogeographic resolution in the northern part of the basin (Yuretich and Hickey, 1984; Yuretich and Hicks, 1986). In this study I will attempt to increase paleogeographic resolution of the southern Bighorn basin

Hypothesis

Late Cretaceous and Paleocene sedimentary rocks of the Bighorn basin should record partitioning of the foreland basin by basement-cored uplifts of that time. Partitioning and uplift may be reflected in several ways:

1. Sedimentary lithologies should reflect varying rates of subsidence, creation of accommodation space and sediment influx controlled by local tectonics.
2. Paleocurrent analysis should reflect the transition from an unbroken foreland basin to a structurally partitioned basin. Paleocurrent trends prior to uplift of the Bighorn Mountains should indicate eastward flow into the unified foreland basin. Paleocurrent trends after partitioning of the basin should indicate flow westward, away from the new highland, or deflection to the north or south around the Bighorn Range.

3. Sandstone petrology should indicate changing provenance as basement cored uplifts are exposed to erosion. In particular, initial uplift of the Bighorn range may be reflected in an unroofing sequence of the Mesozoic and Paleozoic sedimentary strata. Additional uplift should be indicated by exposure and erosion of the Precambrian basement core, consisting of Early Archean layered granitic and felsic gneiss and amphibolite (Whipkey et al, 1991).

METHODS OF STUDY

Field Sites

I selected three field sites in the southern Bighorn basin based on quality and consistency of outcrops. The three areas I chose for study were the Little Buffalo basin-Gooseberry Creek area southeast of the town of Meeteetse Wyoming, the Little Sand Draw area north of Thermopolis, and the Greybull site, along Dry Creek west of the town of Greybull, Wyoming (Figure 1). The Greybull site is proximal to the Bighorn uplift, and contains a clear signature of tectonic activity as represented by the angular unconformity at the Lance-Fort Union contact. The Little Sand Draw section contains the southernmost continuous exposures in the Bighorn basin and was chosen to provide some insight into drainage patterns at the southern end of the basin. The Little Buffalo basin area is the western-most field site, and should give a more complete picture of basin dynamics. I recorded the locations of measured sections with a Garmin GPS. These Locations are recorded on my detailed stratigraphic sections (Plates I-V).

Measured Sections

At each field site I measured and described stratigraphic sections at sub-meter resolution, collected paleocurrent data, and collected sandstone samples for petrologic analysis. While describing measured sections I recorded primary sedimentary structures, grain size trends of sandstone beds, and thickness and geometry of sandstone beds. I measured sections using a Jakobs staff for most well exposed sections, and using a rangefinder and Brunton compass to trigonometrically determine thicknesses of covered sections (Appendix I). Outcrops generally formed steep exposures on hogback ridges suitable to

measurement with Jakobs staff, alternating with long dip-slope covered sections measured with the rangefinder. Multiple measurements of an interval of the upper Fort Union Formation at Little Sand Draw resulted in thicknesses of 23.8 meters and 23.0 meters, giving a difference of approximately 3 - 4%. Measured thicknesses of formations in this study correspond well with thicknesses reported by Keefer et al. (1998).

I collected paleocurrent data using a Brunton compass to measure the strike and dip of planar sedimentary structures, and azimuth and plunge of linear sedimentary structures. Trough scour foresets were the most common paleocurrent indicator, and additional measurements were taken from parting lineation orientation, ripple crest axis orientation, and log cast long axis orientation. I could only measure trough axes in areas of exceptional exposure, so in general trough limbs were measured. I only measured those limb foresets with a three-dimensional exposure, and took special care to avoid measuring any paleocurrent indicator that seemed affected by soft sediment deformation. I corrected all measurements for structural dip as outlined by Miall (1990, p317).

Correlations

I used the Teapot sandstone as a basin-wide datum from for my stratigraphic columns. The Teapot Sandstone is easily identifiable in outcrop, and was recently correlated basin-wide (Keefer et al, 1998) using outcrop data and subsurface data. Correlations between sections in this study and identification of some members of the Montana Group (e.g. Claggett Shale, Lewis Shale) were aided largely by the recent work of Keefer et al.

(1998), Johnson et al (1998), and Roberts, (1998). I correlated the Paleocene Fort Union Formation based on fluvial geometries and the palynological data of Nichols (1998).

SECTION DESCRIPTIONS AND INTERPRETATIONS

Classification of Fluvial Geometries

The Montana Group contains several intervals of marine to marginal marine strata, but the majority of strata in all three sections examined is fluvial. I delineated three major styles of channel geometry and fluvial deposition based on sandstone/shale ratios, sandstone stacking patterns and geometry and sedimentary structures. These delineations are meant to provide a general framework to categorize intervals of fluvial deposition, and to relate these intervals to varying rates of accommodation space creation and sediment influx (A/S ratio). As such, these categories are somewhat generalized; variations are discussed for individual formations.

Type I Geometry

Multistory sandstone intervals are comprised of laterally extensive sheet sandstones from 10 meters to 80 meters thick, containing multiple upward fining intervals and internal scour surfaces with up to several meters of relief. These sandstones are commonly medium to coarse-grained, containing extrabasinal pebble or cobble lags as well as reworked clay intraclasts and iron concretions. Upward fining intervals contain basal trough cross beds of coarse to medium sand with rip-up clasts and woody debris. Trough scours decrease in size up section, and individual upward fining intervals may be capped by parallel laminations and climbing ripples in fine sand. A complete upward fining interval may be overlain by siltstone or lignite, but internal erosion surfaces commonly truncate these lithologies. Convolute bedding with oversteepened trough limbs is also common. Foresets with up to 5 meters of relief occur in some sandstone beds. Miall (1985) ascribes formation of large-scale foresets such as these to downstream migration

of major bedforms in deep channels. I interpret type I sandstones as braided river deposits where sediment supply was greater than accommodation space. Type I sandstone intervals in the Lance and Fort Union formations at Little Buffalo basin closely match Miall's (1977) "Donjek type" mixed gravel and sand braided deposit, whereas the Teapot Sandstone more closely matches Miall's (1977) "Bijou Creek type" sandy braided deposits. Figure 3 illustrates some structures of type I sandstones. Figure 4 shows the stratigraphic column of the type I interval of the Lance Formation at Little Buffalo basin.

In several of the major type I sandstones examined in this study, the most coarse-grained material occurs toward the top of the interval. Whereas upward fining trends generally overlie scour surfaces, an overall upward coarsening trend is common in the major multistory intervals. Typically each internal sequence is coarser grained than the underlying. Upward coarsening sequences in fluvial deposits may be caused by progradation of clastic material into the basin (Heller et al, 1988). In several locations the upper intervals of type I geometry have less evidence of amalgamation, with smaller scale, 10 to 15 meter sheet sandstones separated by mudstones and lignite. This decrease in amalgamation indicates an increase in the A/S ratio toward the top of the type I interval (Figure 4). Penderson and Steel (1999) noted a similar upward decrease in amalgamation in the upper Cretaceous Ericson sandstone, a fluvial sheet sandstone in the Green River basin of southern Wyoming correlative to the Teapot sandstone.



3a.

Figure 3: Type I sandstone elements. a) Laterally continuous multistory sheet sandstone in outcrop. b) woody debris and ripup clasts. c) internal scour surface with extrabasinal pebble lag. d) Convolute bedding. e) Climbing ripple foresets at top of internal fining intervals.



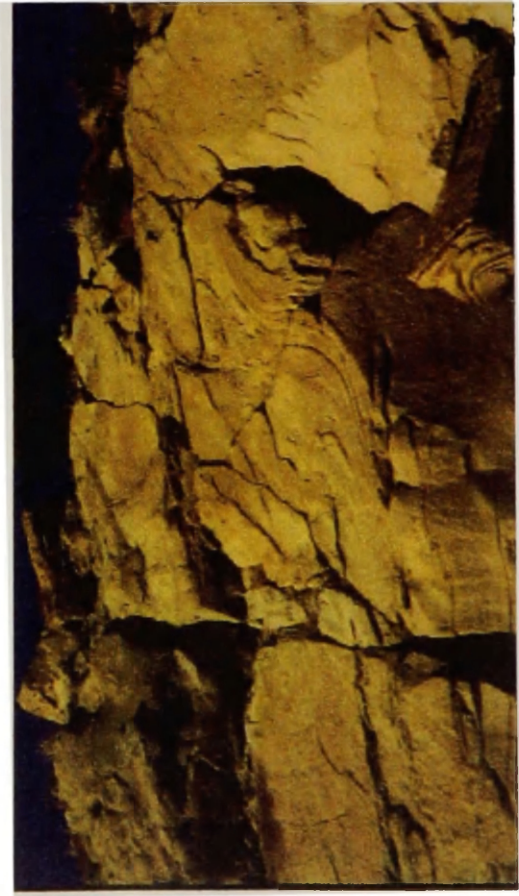
3c



3e



3b



3d

Little Buffalo Basin
Lance Formation

Location:
N 44 01.818'
W 108 42.554'

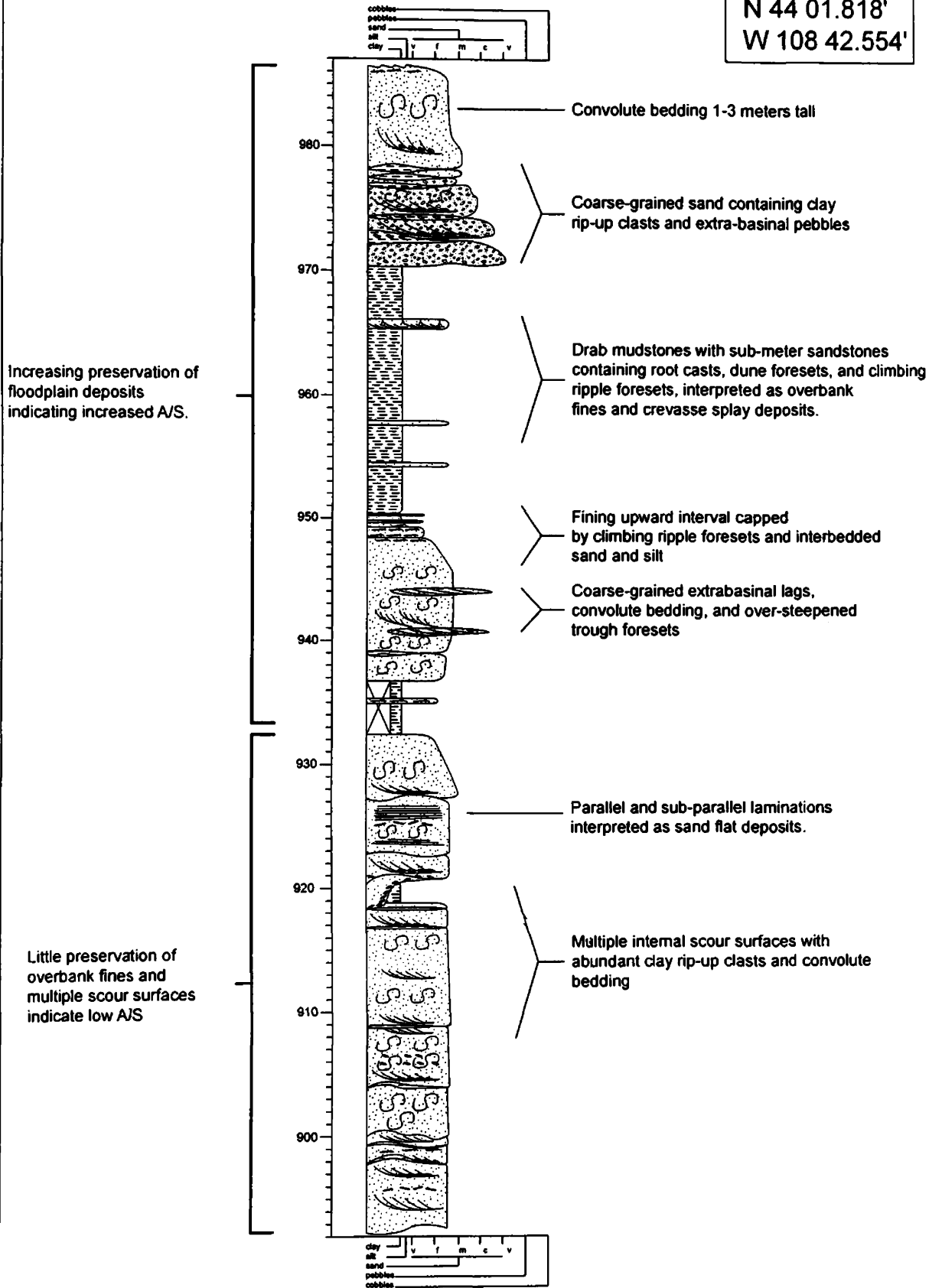


Figure 4. Detailed Stratigraphic section of the Lower Lance Formation at Little Buffalo Basin. This section illustrates the main characteristics of type I fluvial geometry.

Type II Geometry

Type II fluvial deposits consist of 3 to 8 meter thick fine to medium-grained sandstone beds that thin laterally over 50 to 200 meters (Figures 5 and 6). These sandstone beds are generally interbedded with variegated mudstone and lignite. In some instances sandstone beds are stacked in close succession, but channel amalgamation is not common. Both grain-size and sedimentary structures fine upward in sandstones: sandstone bodies contain basal trough scours, rip-up clasts, and convolute bedding, with ripple foresets, parallel laminations, and burrows toward the top. One of the main diagnostic features of type II intervals is the presence of well-developed lateral accretion surfaces in sandstone bodies. Rip-up clasts are less prevalent in type II sandstone beds than type I sandstone beds, and basal erosion surfaces generally have less than 1-meter relief. Sub-meter sheet sandstones in these intervals commonly contain climbing ripple foresets and parting lineations indicating rapid aggradational deposition, and are interpreted as crevasse splay deposits (Miall, 1985; Miall, 1996). Type II intervals match the facies model of meandering fluvial deposits (Cant, 1982), and I interpret Type II intervals as meandering river systems with an intermediate A/S ratio.

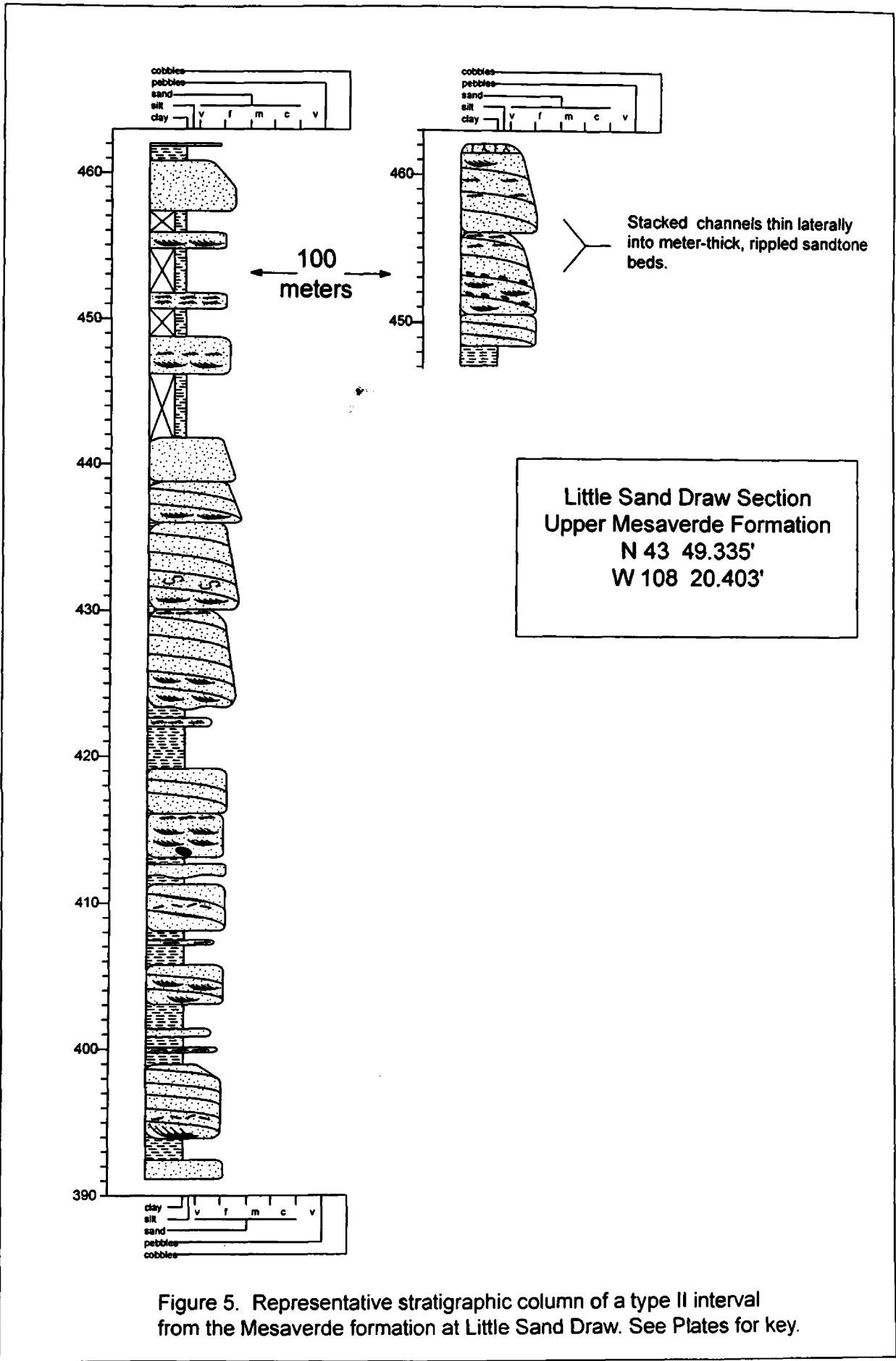


Figure 5. Representative stratigraphic column of a type II interval from the Mesaverde formation at Little Sand Draw. See Plates for key.

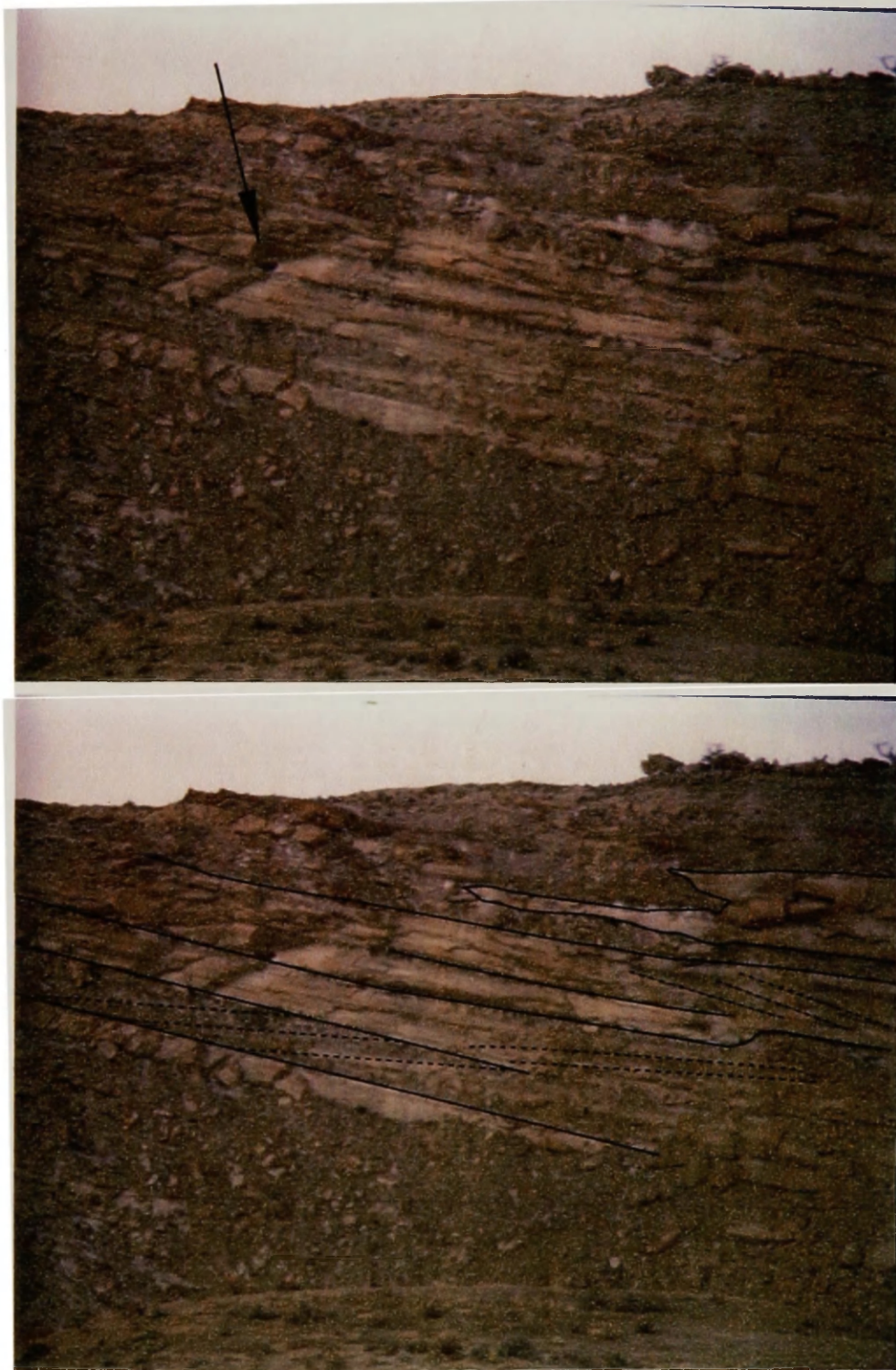


Figure 6. Type II Channel Geometry in the upper Mesaverde Formation at Little Sand Draw. Bedding planes dip to the right (solid lines). Lateral accretion surfaces cut across bedding planes (dashed lines). Note the Golden Eagle nest indicated by the arrow.

Type III Geometry

Type III geometry is typified by lenticular, isolated, channel-form sandstones overlain and underlain by mudstones and lignite (Figures 7 and 8). These sandstones are generally 1 to 5 meters thick, and 20 to 50 meters wide. Alternating centimeter to decimeter thick sandstone siltstone and mudstone directly underlie channel form type III channel sandstones. I have interpreted these as overbank floodplain deposits, consistent with the interpretations of Krauss (1999). Crevasse splay sandstone beds are also abundant. In some areas, multiple type III channels occur on the same stratigraphic horizon, sometimes connected by traceable sub-meter thick sandstone beds. This interconnected geometry is one of the diagnostic features of anastomosing fluvial systems, consistent with Krauss' (1999) interpretation of deposits in the Fort Union Formation of the northern Bighorn basin. The abundant overbank material and crevasse splay sandstones in Type III deposits indicates rapid rates of aggradation and a high A/S ratio (Zhang et al, 1995).

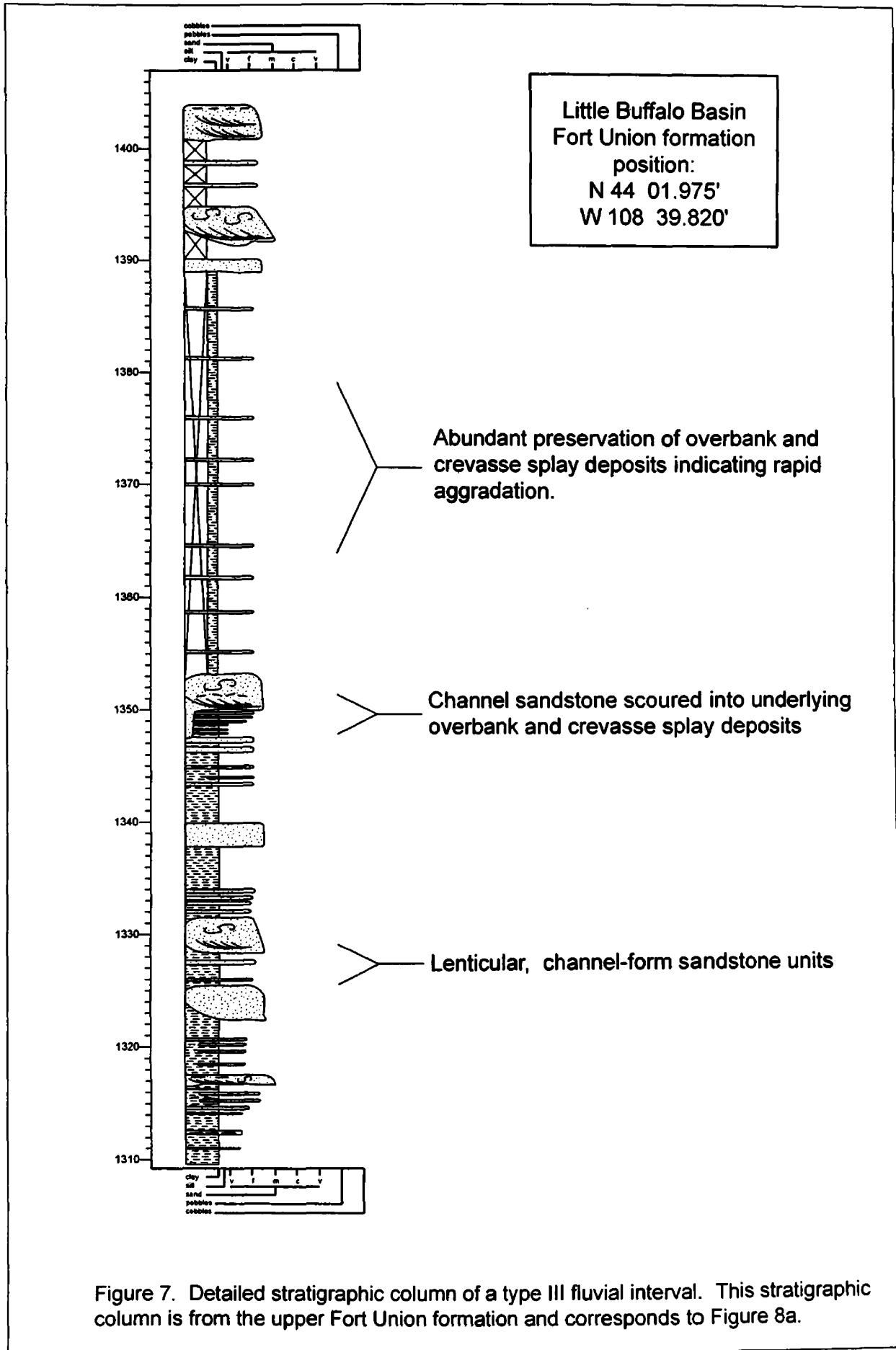


Figure 7. Detailed stratigraphic column of a type III fluvial interval. This stratigraphic column is from the upper Fort Union formation and corresponds to Figure 8a.



a



b

Figure 8: Type III Deposits. a) Oblique view of Upper Fort Union strata at Little Buffalo Basin showing abundant preservation of overbank deposits. b) Upper Fort Union strata with lenticular sandstones isolated in overbank fines.

Descriptions of Individual Stratigraphic Units

Cody Shale

I measured and described the upper 100 meters of the Cody shale at Little Buffalo basin and Little Sand Draw. I did not examine the Cody shale at Greybull due to posted property lines stating “No Trespassing or I will Shoot you in the Head.” The Cody Shale at Little Buffalo basin and Little Sand Draw consists of grey to black shale alternating with tabular sandstone that forms several upward coarsening, upward thickening sequences (Figure 9). The initial several meters of these sequences consist of fissile grey to black shale in the Little Sand Draw section and more drab shale in the Little Buffalo basin. Overlying these shale beds, tabular sandstone interbedded with shale grades from centimeter scale, very fine grained, sandstone to medium grained meter scale sandstone, with a maximum thickness of 2 meters. Lowermost sandstone beds at Little Sand Draw contain burrow marks, low angle truncations and ripple marks on upper bedding surfaces. By meter 10, well-developed HCS occurs, with low angle truncations and parallel laminations forming hummock and swale features (Figure 10a,b,c). I have interpreted this interval as a progradational marginal marine environment consistent with the descriptions of McCubbin (1982) and Wiemer (1988).

The Little Buffalo basin section contains similar upward coarsening, upward thickening packages, but sedimentary structures in sandstone beds at Little Buffalo basin indicate a more proximal environment of deposition. Whereas HCS is the most prevalent sedimentary structure in the Cody shale at Little Sand Draw, the Little Buffalo section

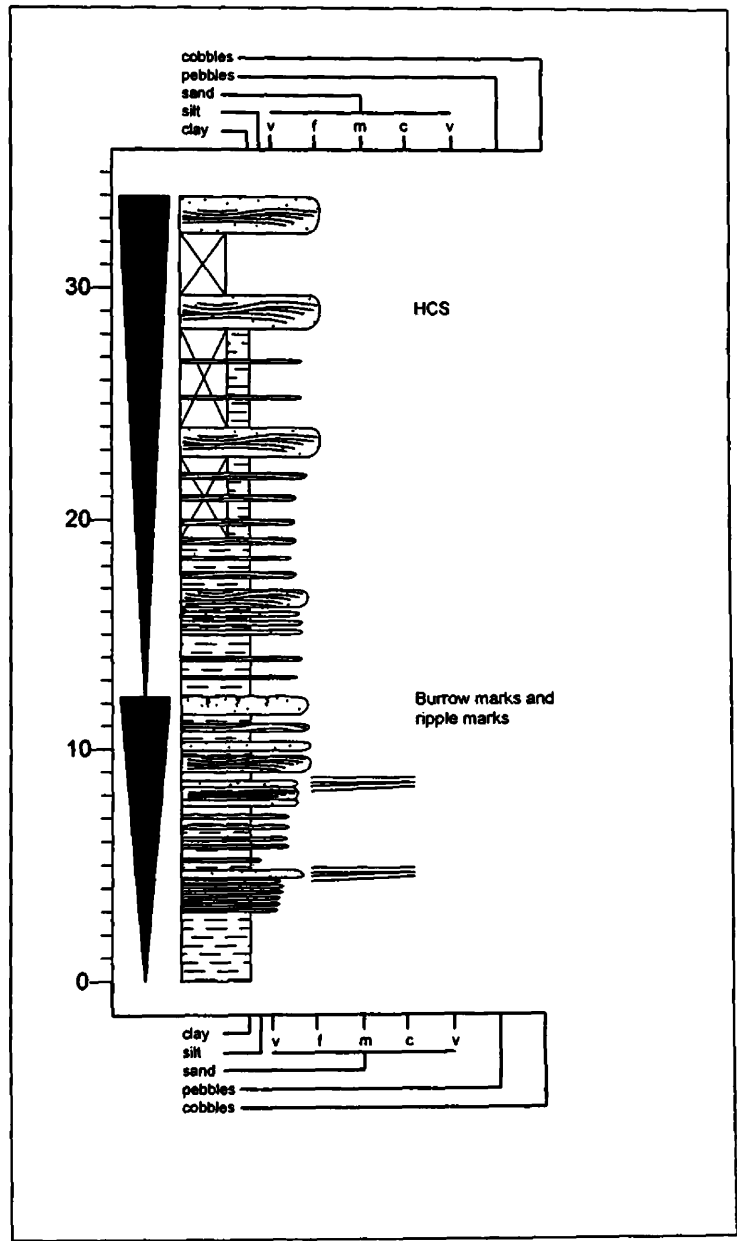


Figure 9: Coarsening upward, thickening upward sequences in the Cody Shale



a



b

Figure 10: Sedimentary structures of the Cody Shale: a) Upward thickening, upward coarsening interval. note the tabular nature of sandstone and shale beds b) Hummock and swale bedding with low angle truncations. c) ripple marks on bedding surfaces. d) Flute casts in float block at Little Buffalo basin.



c



d

Figure 10: Sedimentary structures of the Cody Shale: a) Tabular sand and shale with low angle truncations. b) Hummock and swale bedding with low angle truncations. c) ripple marks on bedding surfaces. d) Flute casts in float block at Little Buffalo Basin

contains little HCS. A 2-meter sandstone at meter 45 of the Little Buffalo basin section contains low angle truncations and marginally wavy bedding; these structures represent poorly formed HCS, but in general HCS is not present. Sandstone beds more commonly contain massive bedding, parallel laminations and climbing ripple foresets, with 3-dimensional, unidirectional ripples on upper bedding surfaces. Several sandstone beds (meters 30-50, Plate I) contain well-developed flute casts on their lower bedding surfaces (Figure 10d). These sedimentary structures suggest rapid deposition of sands by unidirectional traction transport. I have interpreted this interval to represent a progradational marine interval similar to Little Sand Draw, but more proximal to the source of clastic material.

A 10 to 13 meter tabular white fine to medium-grained sandstone at meter 100 in both sections marks the Cody – Mesaverde contact (Figure 11). This sandstone body contains parallel laminations and low angle truncations in the first two meters, overlain by steeper foresets with more obvious truncations, with foresets up to 2 meters in relief in the Little Buffalo section. The top 6 meters of this sandstone at Little Sand Draw contain shell fragments, parallel laminations and ripple foresets. This upward progression of sedimentary structures is indicative of a shoreface sand in a shallowing system (McCubbin, 1982) and is a continuation of the progradational Cody shale.

Mesaverde Formation

In the Little Buffalo basin the Mesaverde Formation consists of a single package of continental strata, whereas at Little Sand Draw the Mesaverde Formation consists of

Little Sand Draw Section
Cody Shale-Mesaverde fm.
Contact

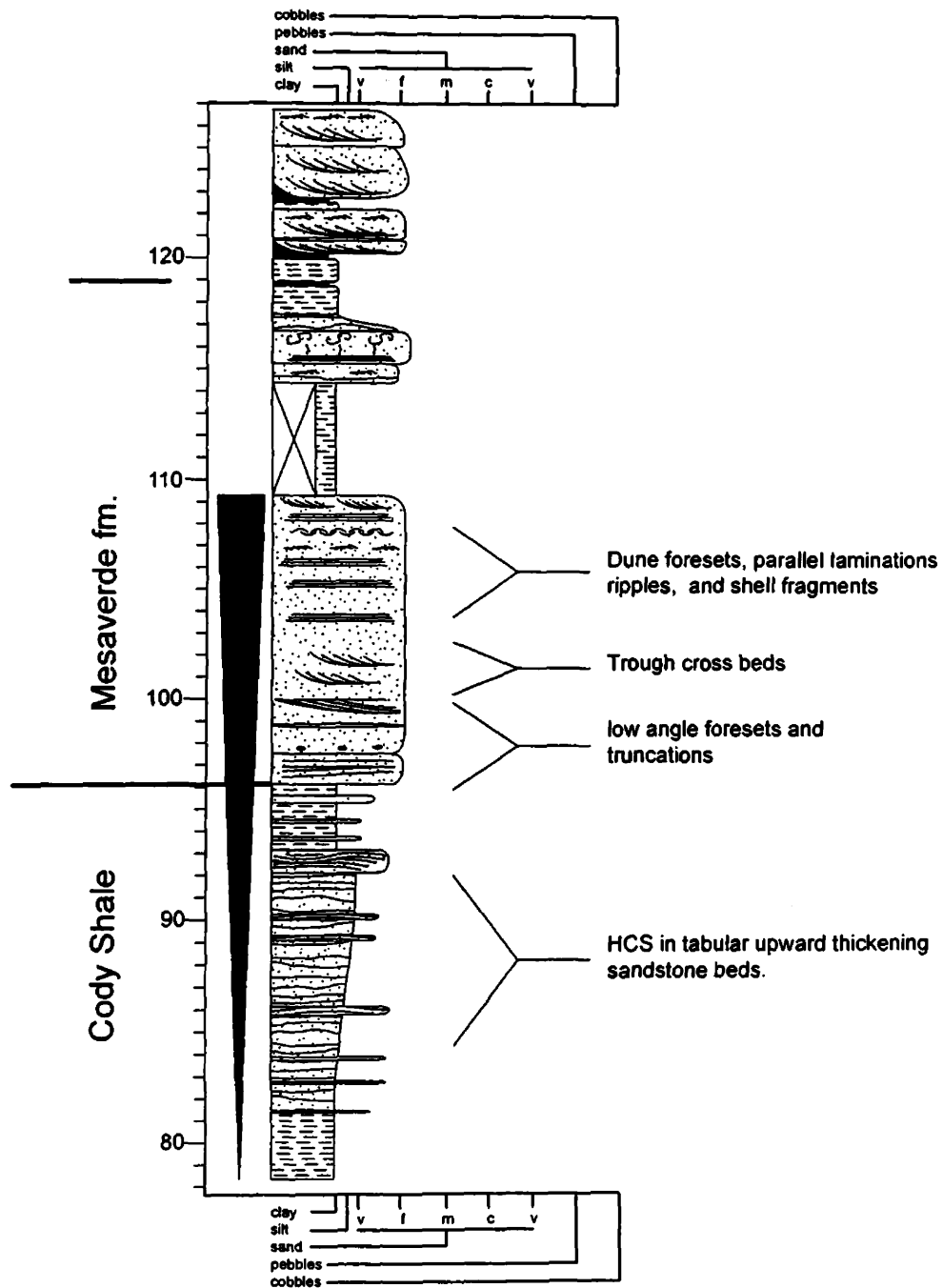


Figure 11: Stratigraphic column of the Cody Shale - Mesaverde Formation contact at Little Sand Draw. A 13 meter Shoreface sandstone marks the base of the Mesaverde Formation

informal upper and lower members of continental strata separated by an eastward thickening wedge of the marine Claggett shale (Keefer et al, 1998). The Lower Mesaverde at Little Sand Draw, and correlative strata at Little Buffalo basin (meters 110 to ~230 of both sections) consist of alternating sandstone, lignite, and mudstone (Figure 12). I interpret sandstone beds as channel fill and crevasse splay deposits; interbedded mudstone, siltstone, fine-grained sand and lignite represent overbank or interdistributary bay deposits. Channel sandstones form fining upward units containing basal trough cross beds with clay rip up clasts, woody debris, and climbing ripples toward the top of the sandstone (e.g. meters 120, 140 Sand Draw). Sandstones interpreted as crevasse splay deposits (e.g. meter 190 – 200 Sand Draw) sometimes contain massive bedding at the base, with dune and climbing ripple foresets toward the top.

I interpret this interval as a fluvial/deltaic environment based on facies models of Coleman and Prior (1982) and Cant (1982). The transition from the marine environment of the Cody shale to a fully terrestrial fluvial/deltaic environment indicates a basinward shift of the strand line and continued progradational deposition during a period of low A/S.

The type II-III fluvial/deltaic deposits of the Lower Mesaverde member are broken at Little Sand Draw by a ~30 meter type I fluvial sandstone (Figure 12) which may correspond to several tabular channel sandstones in the Little Buffalo basin. I interpret the type I sandstone to represent deposition during minimum A/S, and the overlying return of type II-III deposits to indicate an increase in A/S.

Little Buffalo Basin

Little Sand Draw

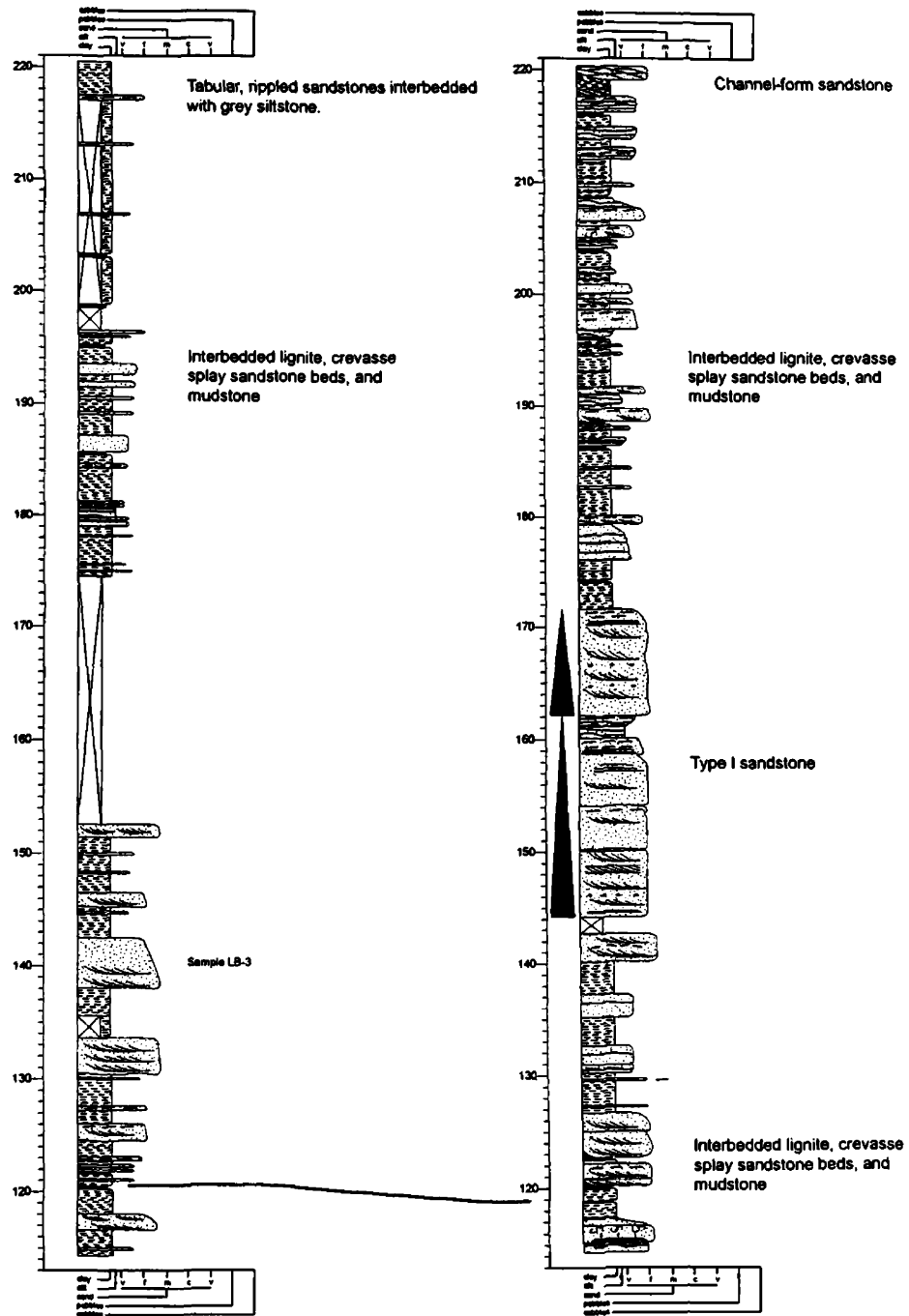


Figure 12: Stratigraphic columns of the lower Mesaverde formation at Little Buffalo Basin and Little Sand Draw

Isopach data (Keefer et al, 1998) of the Mesaverde Formation (Figure 13) shows two depositional thicks radiating from the Little Sand Draw area toward inferred strandline of the Western interior Seaway. These depositional thicks are similar to isopach thicks illustrated for delta lobe complexes of the Mississippi (Coleman and Prior, 1982), and may represent lobes of the interpreted fluvial/deltaic deposits of the Mesaverde Formation. Isopach data for the Lower Mesaverde member (Keefer et al, 1998) shows a general thinning of the member to the east, consistent with a wedge of continental strata encroaching into the Cody-Claggett shale in the more distal parts of the basin. Two thick tongues of the Lower Mesaverde Formation exist at Little Sand Draw and north of Greybull (Figure 14). These depositional thicks align with the delta lobes inferred from the Mesaverde isopach. Paleocurrent trends indicate flow toward these depositional thicks, consistent with the above interpretation.

Meter ~230 of the Little Sand Draw section marks the base of a tabular, 40 meter upward coarsening, upward thickening sandstone interval. This sandstone contains the same upward progression of sedimentary structures as shallow marine-shoreface sandstones described in the Cody Shale, and I interpret it as a shallow to marginal marine sandstone. This return to a shallow marine environment of deposition indicates a flooding surface at meter 230 and a continued increase in A/S ratio. This flooding surface represents the Claggett transgression. Ten meters of interbedded lignite and mudstone separate this shoreface sandstone from the main body of the Claggett shale.

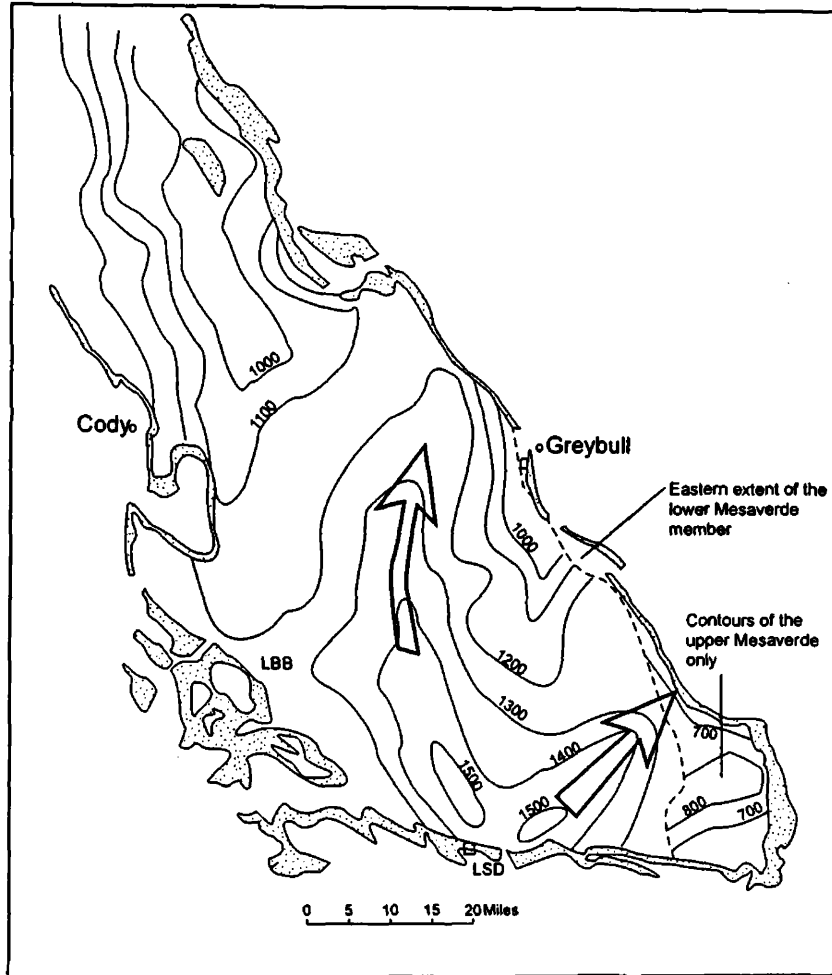


Figure 13. Isopach map of the Mesaverde Formation with interpreted drainage patterns of delta system. Isopach and outcrop location data modified from Keefer et al (1998). LBB = Little Buffalo basin, LSD = Little Sand Draw. Contour interval is in meters. Dashed line represents the eastern limit of the lower Mesaverde formation. Contours west of this line consist of the Lower Mesaverde Formation, Claggett Shale, and Upper Mesaverde. Contours east of this line consist of the Upper Mesaverde Formation only.

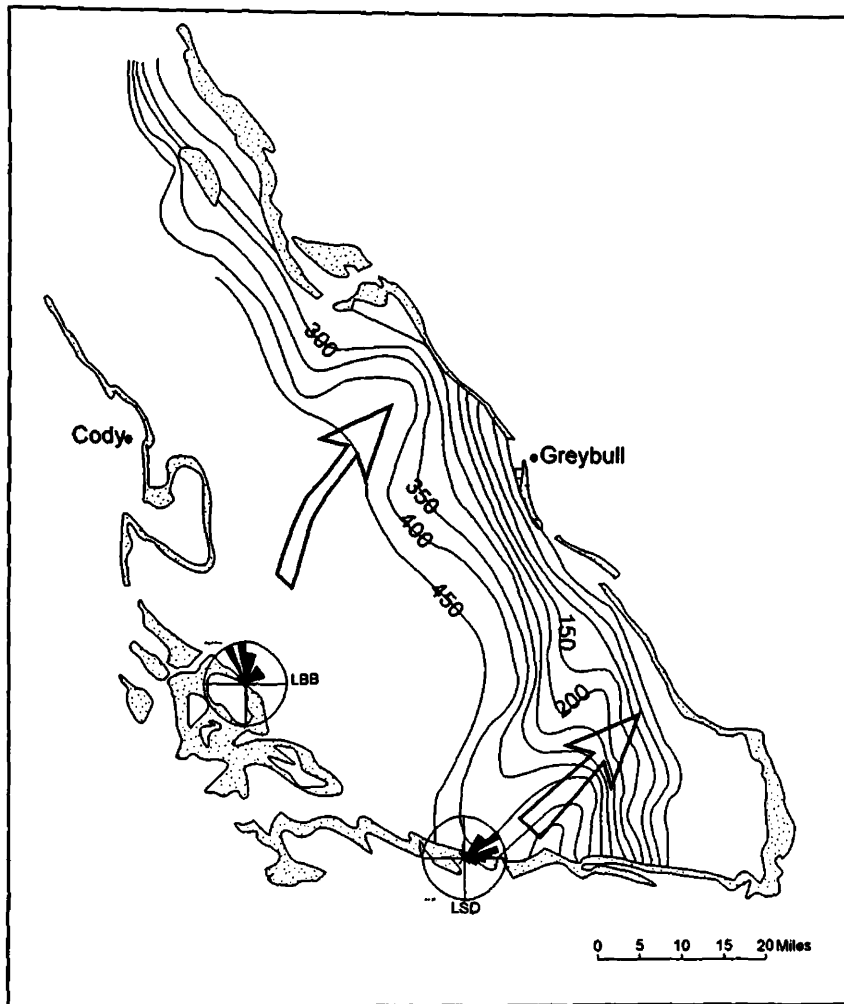


Figure 14. Isopach map of the Lower Mesaverde member with inferred drainage patterns of delta lobes from the Mesaverde Formation. Paleocurrent measurements align with the inferred delta lobes and with the depositional thicks in the Lower Mesaverde. Isopach data modified from Keifer et al (1998). Contour interval in meters.

Claggett Shale

Similar to the underlying Cody Shale, the Claggett Shale at Little Sand Draw forms an upward coarsening, upward thickening sequence of drab shale and tabular sandstone.

The Claggett shale contains several higher order sequences, and culminates in two 15-meter sandstones (Plate 2). This interval differs from the Cody Shale in several ways: sandstones of the Claggett shale contain parting lineations and climbing ripple foresets indicating traction transport, and gypsum layers suggesting restriction of flow. Also, the overlying sandstone shows possible tidal influence, containing tabular and trough foresets with well-developed organic lags, woody debris and rip up clasts, ball and pillow structures, scour surfaces, and possible herringbone structures.

An isopach map of the Claggett Shale indicates a relatively smooth NW-SE trending shoreline in the northern and central part of the basin (Keefer et al 1998). In contrast, in the southern area of the basin around Little Sand Draw, the Claggett shale shows two E-W trending depositional thicks separated by a relatively shallow area of Claggett deposition (Figure 15). These depositional thicks may represent distal areas of interdistributary bays associated with the inferred delta lobes of the Mesaverde Formation. Paleocurrent measurements from several major sandstone beds in this interval indicate variable flow directions to the northeast and southeast. Variable flow directions may be due to lobe switching events in the associated bay head. I interpret this interval of the Claggett as tidally influenced barrier sand deposits in a distal deltaic environment.

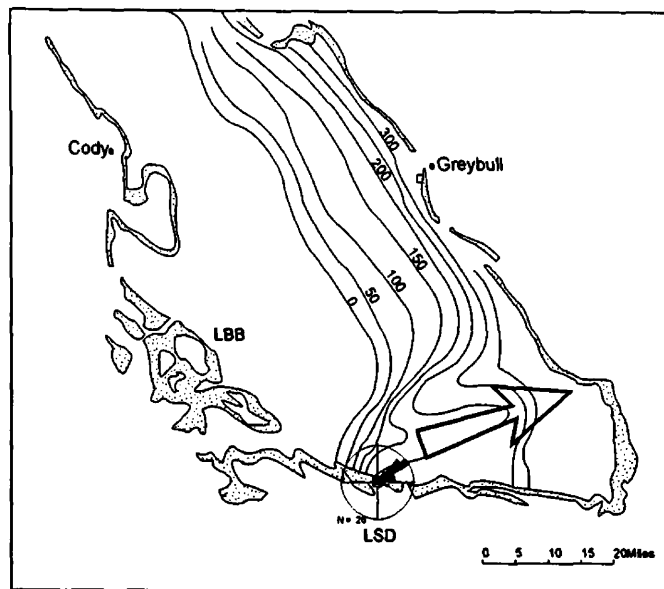


Figure 15a. Isopach map of the Claggett Shale. Stippled area represents outcrop area of the Mesaverde formation. A depositional thin of the Claggett corresponds roughly to the delta lobe inferred from the Lower Mesaverde and Mesaverde isopachs. Note that Paleocurrent trends of the Claggett Shale align with the inferred delta lobe. Also the smaller scale lobe north of Greybull is not evident in Claggett shale isopach contours. Outcrop locations and Isopach data modified from Keefer et al (1998).

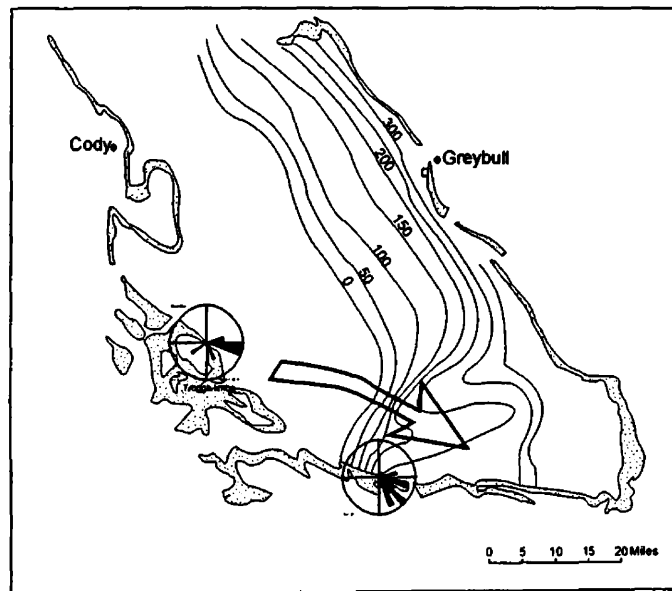


Figure 15b. Isopach map of the Claggett Shale with upper Mesaverde paleocurrent trends. Paleocurrent data plotted at Little Sand Draw is from the lenticular channel sandstone directly overlying Claggett deposits interpreted as an avulsion channel. Southwest trending flow is toward a depositional thick of the Claggett interpreted as an interdistributary bay. Reorientation of Little Buffalo paleocurrent trends from northward flow to eastward is consistent with a major reorientation of Delta lobes. Outcrop locations and Isopach data modified from Keefer et al (1998).

Although a covered interval (meter 240 - 310) of the Little Buffalo basin prevents exact comparison of sections, previous studies in the area (Johnson et al, 1998) documented continuous fluvial deposition at Oregon basin, approximately 15 miles north of Little Buffalo basin. Little Buffalo exposures resume at meter 305, where deposits consist of several tabular sandstone beds alternating with more lenticular channel sandstones, crevasse splay deposits, and overbank fines. A 50-meter interval roughly corresponding to the Claggett shale consists of generally isolated, lenticular sandstones similar to type III ribbon deposits (Plate II). I identified one tuff bed in this interval, supporting correlation with the Claggett shale, which is known to contain abundant bentonite beds (Johnson et al, 1998). The high A/S ratio indicated in this interval is consistent with the Claggett transgression observed at Little Sand Draw.

The base of the Greybull Section is approximately correlative with the top of the Claggett Shale. At its base, it consists of a 14 m fine-grained, tan sandstone similar to the shoreface sandstones in the Cody shale and Claggett Shale in the southern sections. This sandstone contains basal parallel laminations, long wavelength shallow truncations and minor hummock and swale relief for the first 5 m. Above, steeper foresets and truncations become visible, with some linear foresets traceable over 10 m. The top of the sandstone is red, iron stained and contains vertical burrows, symmetric ripples on bedding surfaces, and wood imprints (Plate II).

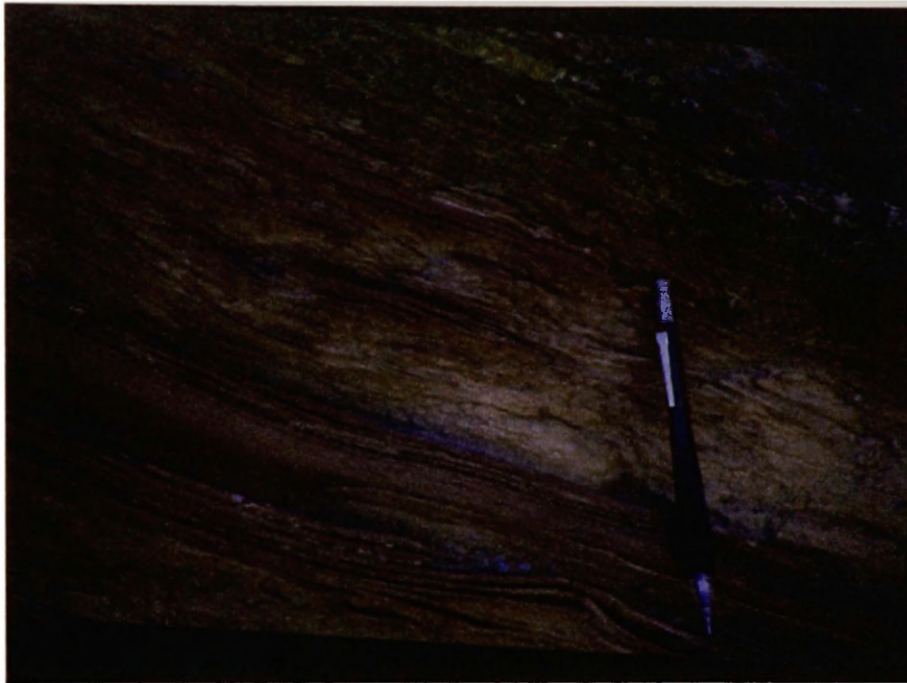
Deposits from meter 14 to meter 29 consist of alternating grey and purple organic rich mudstone, sub-meter lignite, and tabular sub-meter to 4-meter thick fine to very fine-

grained sandstone. This is a complex interval, with some clean, meter thick sandstone beds containing linear foresets, some dirty, interbedded sandstones and siltstones containing flaser bedding, and one sandstone body containing fragmented shell lags (Figure 16). Vertical burrows and bioturbation are apparent in many of these sandstone beds, as well as three-dimensional ripples and trace fossils on bedding surfaces. These features are typical of a tidally influenced marginal marine environment (Wiemer et al, 1982) and I have interpreted this interval as a tidal flat environment. The change in environment of deposition from shoreface to tidal flat suggests a progradational system. Also, the tidal flat environment is consistent with the depositional thin of the Mesaverde Formation at Greybull which may represent an interdistributary bay between the two inferred delta lobes of the Mesaverde Formation.

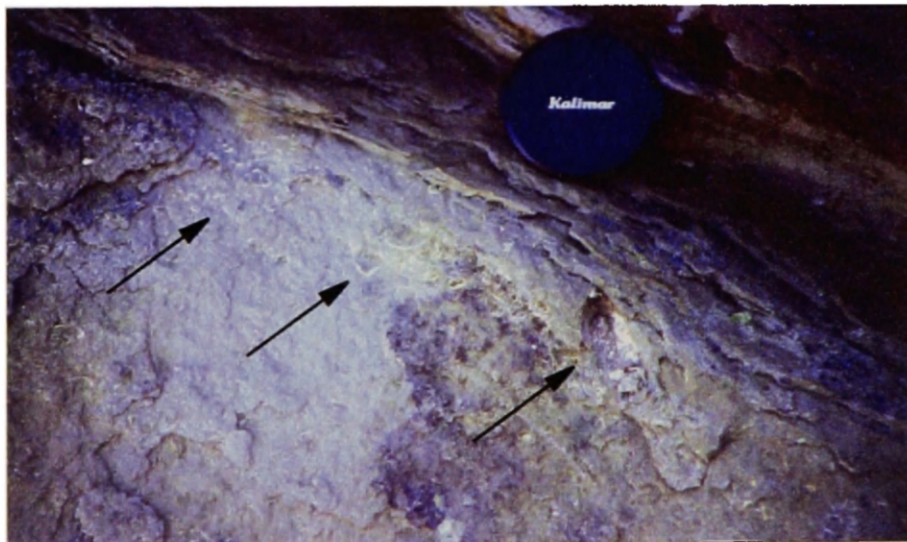
At Greybull, this interval is capped with a 4-meter fine-grained sandstone, with trough crossbeds and ripples. This sandstone grades up-section into silty sandstone that in turn is overlain by grey shale (Figure 17). As discussed in the next section, the top of this sandstone represents a flooding surface.

Upper Mesaverde

Overlying the Claggett Shale at Little Sand Draw, terrestrial deposition of the Mesaverde Formation resumes with a distinctive interval of type II sandstone deposits containing abundant lateral accretion surfaces. The type II sandstones of this interval become more closely stacked up section, with a corresponding decrease in preservation of overbank material suggesting a decrease in the A/S ratio (see Figures 6, 34). Johnson et al (1998)



a



b

Figure 16: sedimentary structures from tidal flat deposits at Greybull.
a) Flaser bedding b) shell fragments indicated by arrows.

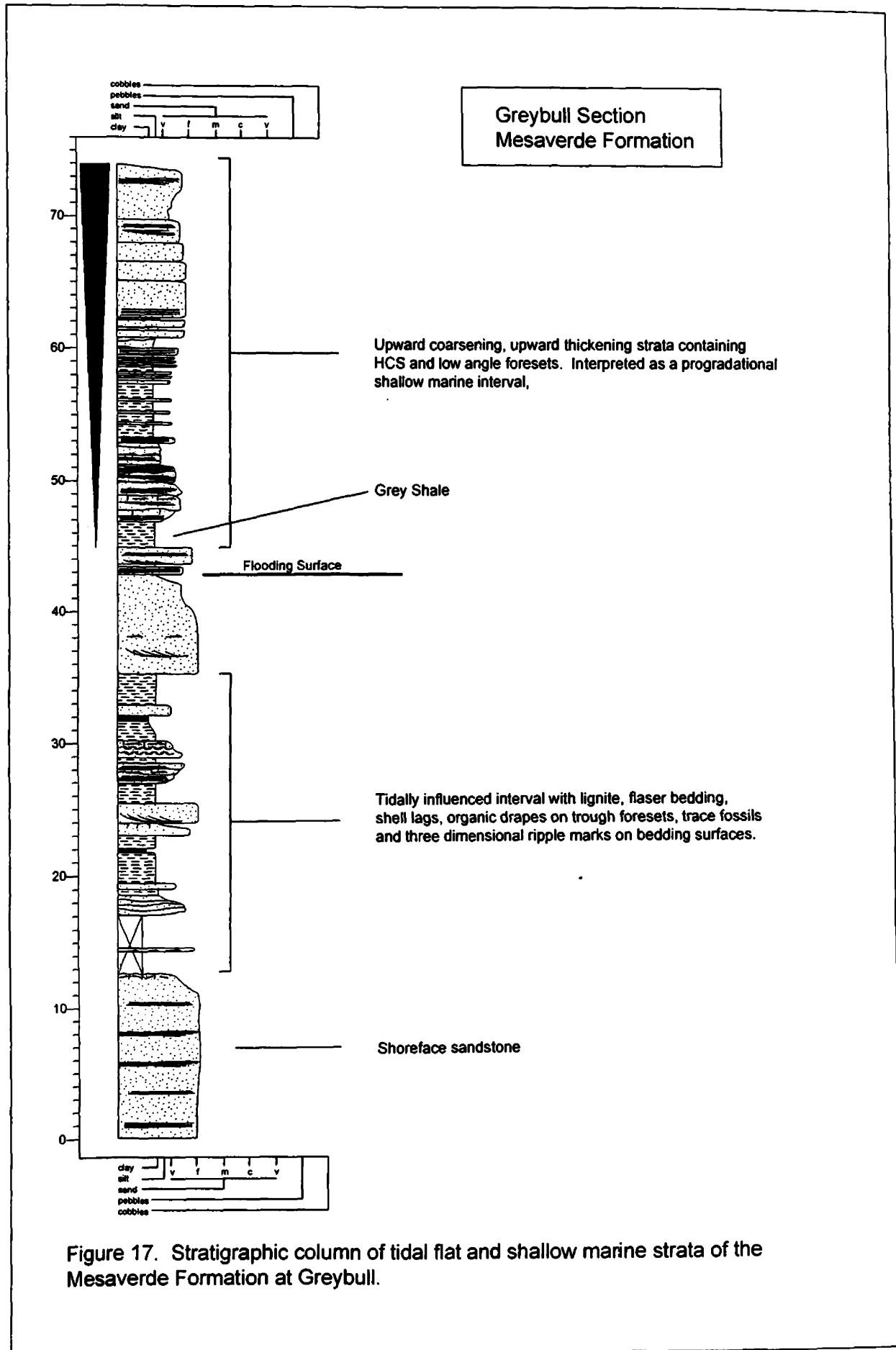


Figure 17. Stratigraphic column of tidal flat and shallow marine strata of the Mesaverde Formation at Greybull.

identified a sandstone bed in this interval which contains “flaser bedding couplets” interpreted as tidally influenced structures. I observed abundant clay drapes on lateral accretion surfaces in this interval, indicating alternating high and low flow regimes, and supporting the interpretation of a tidally influenced environment. I infer these channel sandstones to represent a tidally influenced deltaic system.

At the base of this type II sandstone dominated interval is a 15-meter lenticular sandstone (meter 370), which contrasts markedly from the surrounding rock. Thicker and more lenticular than surrounding sandstone bodies, this sandstone contains abundant rip-up clasts, woody debris, and log casts. This sandstone unit is laterally traceable for approximately 150 meters, but while it is laterally equivalent to type II meandering sandstone bodies, an erosive base suggests that it may not be time equivalent. This channel sandstone may represent a major avulsion event and associated reorganization of delta lobes. Trough foresets measured in this sandstone suggest flow to the southeast, and no longer parallel to the depositional thin of the Claggett (Figure 15b), but toward an inferred interdistributary bay, consistent with flows expected of an avulsion channel.

Upper Mesaverde strata in the Little Buffalo basin consist of a similar interval of sandstone units with obvious lateral accretion surfaces. This interval of the Little Buffalo basin does not conform to type II geometry as closely, but it is distinct from the underlying type III fluvial interval, containing more laterally continuous, more closely stacked sandstone. The increase in sand/shale of this interval suggests a decrease in A/S. Whereas measured sections at Little Buffalo basin and Little Sand Draw suggest a

decreasing A/S in the Upper Mesaverde, Johnson et al (1998) found a high amount of variability in this interval in the Grass Creek area. In multiple measured sections they documented areas of persistent channel sandstone accumulation laterally equivalent with overbank and crevasse splay deposits.

Upper Mesaverde strata at Greybull consist of an upward coarsening, upward thickening sandstone package overlying the tidal flat deposits. The base of this interval marks a flooding surface overlain by grey shale (Figure 17). I interpret the minor transgressive event indicated by the flooding surface as a minor advance of the retreating Claggett shale, which may correlate to the double shoreface sandstones marking the Claggett-Upper Mesaverde contact at Little Sand Draw. These beds fall on approximately the same stratigraphic interval, but the intrinsic autocyclic processes of tidal and marginal marine environments prevents exact correlation without more detailed study. Above this flooding surface interbedded fine sandstone and shale grade upward into a 6-meter very fine to fine-grained sandstone body. This interval is similar to the progradational shallow marine intervals of the underlying Cody shale and Claggett shale. The progradational interval at Greybull is consistent with decreasing A/S inferred for upper Mesaverde strata at Little Sand Draw and Little Buffalo basin.

Teapot Sandstone Member

The Teapot Sandstone member marks the top of the Mesaverde Formation (Figure 18). This is a type I sandstone body at both the Little Buffalo section and Sand Draw Section, with a thickness of 90 and 57 meters, respectively. At Greybull the Teapot sandstone is



Figure 18: Teapot sandstone at Little Sand Draw. Note the sharp contact between the type I Teapot Sandstone and underlying type II Mesaverde Formation strata. This contact is visible over the length of the outcrop, shows strong oxidation, and contains multiple burrow marks.

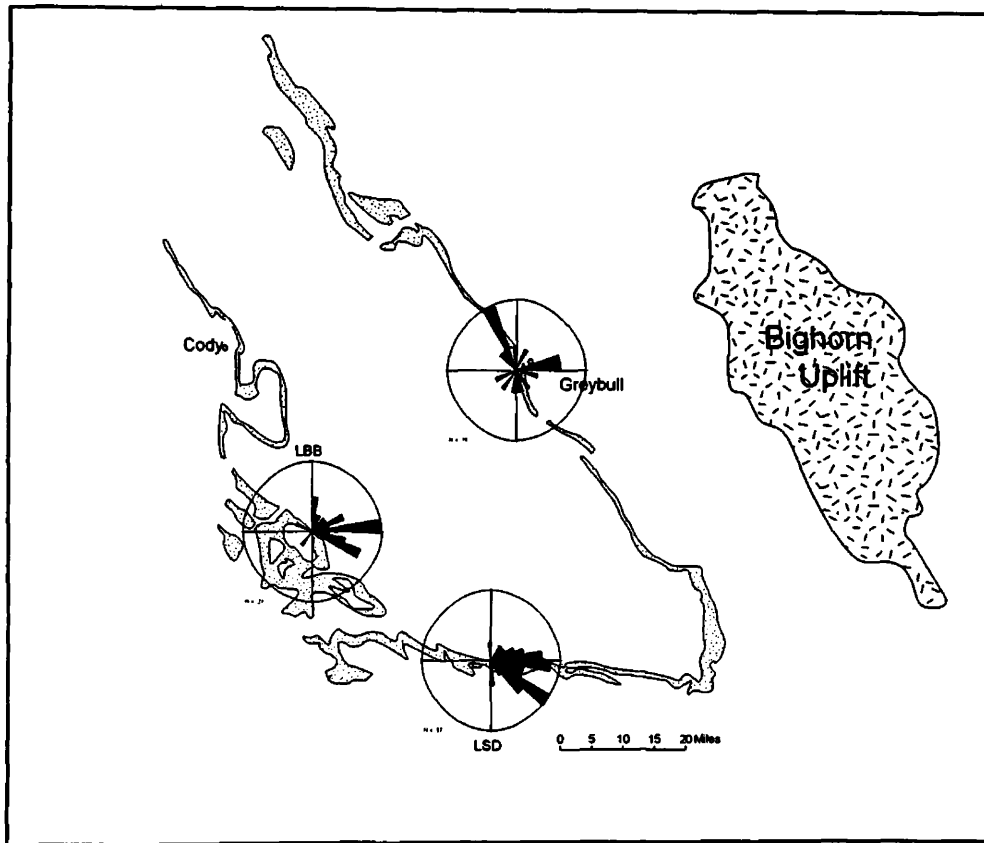


Figure 19. Paleocurrent trends of the Teapot sandstone indicate generally eastward flow. The northeastward flow direction indicated at Greybull is consistent with flow toward the contemporaneous Bearpaw Sea of Montana (Johnson et al, 1998). LBB = Little Buffalo basin, LSD = Little Sand Draw.

noticeably thinner (30 meters). The base of the Teapot sandstone at the Little Sand Draw section is marked by a 0.5-meter tabular sandstone with abundant rootcasts and disturbed bedding marks. With a deep reddish-purple color, this sandstone is visible over the length of the outcrop, and may represent a surface of non-deposition. This is consistent with the unconformity at the base of the Teapot sandstone identified by Gill and Coban (1973). Paleocurrent measurements indicate east – Southeast flow directions at Little Sand Draw and Little Buffalo basin, and northeast flow directions at Greybull, consistent with the measurements of Johnson et al, (1998). This paleoflow suggests uninterrupted flow eastward toward the Western Interior Seaway (Figure 19).

Meeteetse Formation

The Meeteetse Formation consists of white sandstone alternating with lignite and variegated grey, brown, and purple mudstone. The formation is easily identifiable in the field by distinct black and white banding (Figure 20). Mudstone in the Meeteetse is organic rich and commonly contains iron stains, ped structures and rootcasts. At Little Sand Draw type III fluvial geometry is well developed in the Meeteetse (Figure 8). In contrast, the Little Buffalo section contained several lenticular sandstone bodies, but did not show clear channel geometry. The preservation of coal beds at both sections indicates little reworking of floodplain material, and suggests a relatively high A/S ratio. This formation has been previously interpreted as a laterally continuous alluvial plain prograding eastward toward the retreating Cretaceous Interior Seaway.

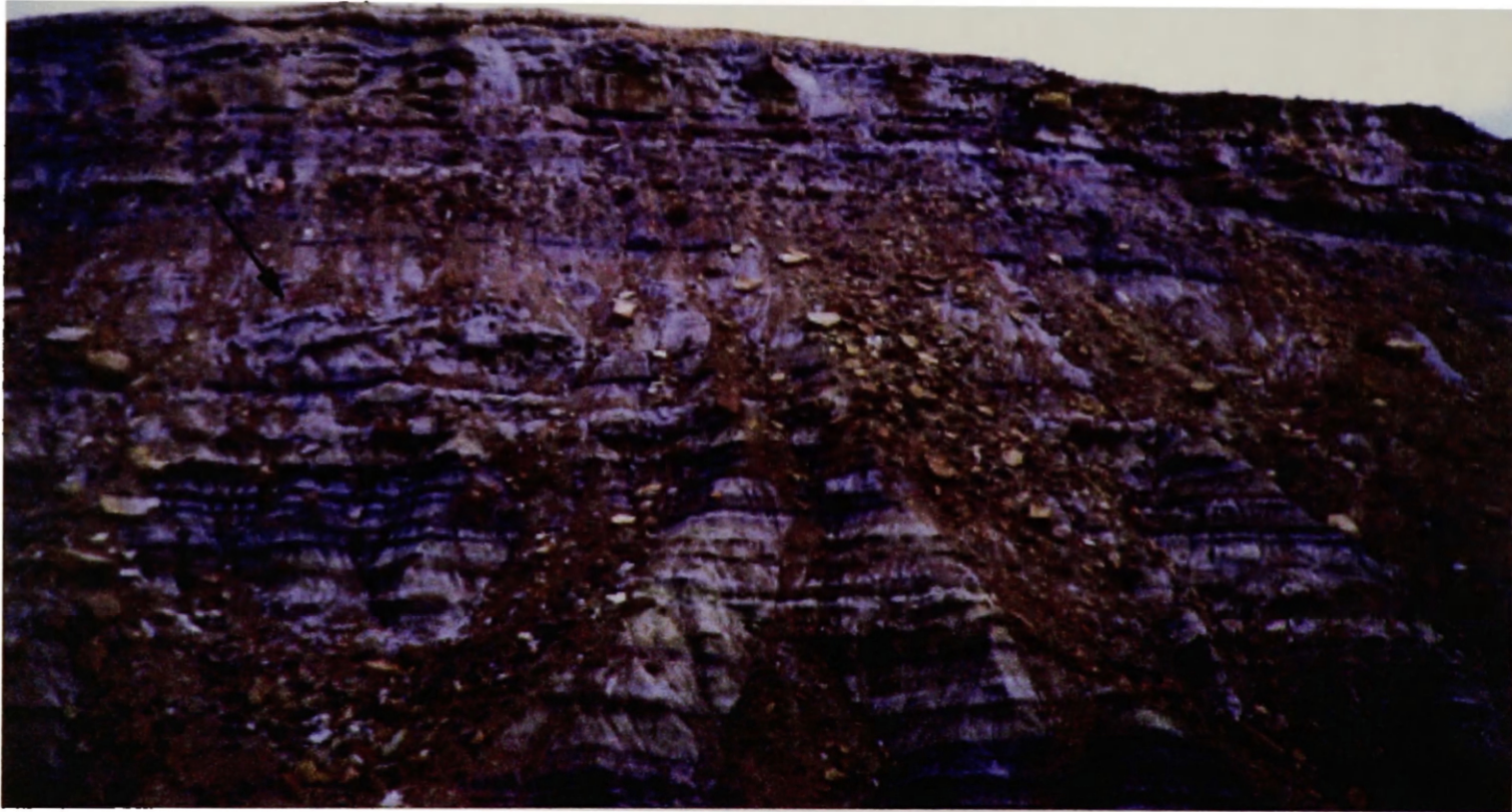


Figure 20: Meeteetse Formation at Little Buffalo Basin. Note the closer stacking of sandstone beds at the top of the ridge and lateral accretion surfaces indicated by the arrow. This outcrop is approximately 80 meters thick.

The uppermost portions of the Meeteetse Formation show an increase in sand/mudstone ratios, with more laterally continuous, closely stacked sandstones (Plate III). At Little Sand draw, this is a well-developed type II interval with abundant lateral accretion surfaces. At Little Buffalo basin, lateral accretion surfaces are less well developed, but channel sandstones show close stacking similar to other type II deposits, indicating a decrease in A/S ratio.

Meeteetse strata of the more distal Greybull site again show a marked contrast with the Little Buffalo and Sand Draw areas. At the Greybull site, the continental strata of the Meeteetse Formation are intertongued with the marine strata of the Lewis Shale (Keefer et al., 1998; Gill and Coban, 1973). Basal Meeteetse strata (meters 185-230) are similar to Meeteetse strata of the other sections to the southwest, consisting of interbedded sub-meter to 2 meter fine to medium grained sandstone, siltstone, mudstone, and lignite. Sandstone bodies are similar to crevasse splay deposits observed elsewhere in this interval with massive bedding, parallel laminations, and climbing ripples, plus numerous well developed burrows and rootcasts.

Lewis Shale

Meter 230 marks the transgressive flooding surface of the Lewis Shale at Greybull, with a transition from mudstone and sandstone of the Meeteetse Formation to black fissile shale (Figure 21). The Lewis Shale consists of an upward coarsening, upward thickening interval similar to the progradational Cody and Claggett shales; black, fissile shale is overlain by interbedded centimeter to decimeter thick tabular sandstone and shale and is

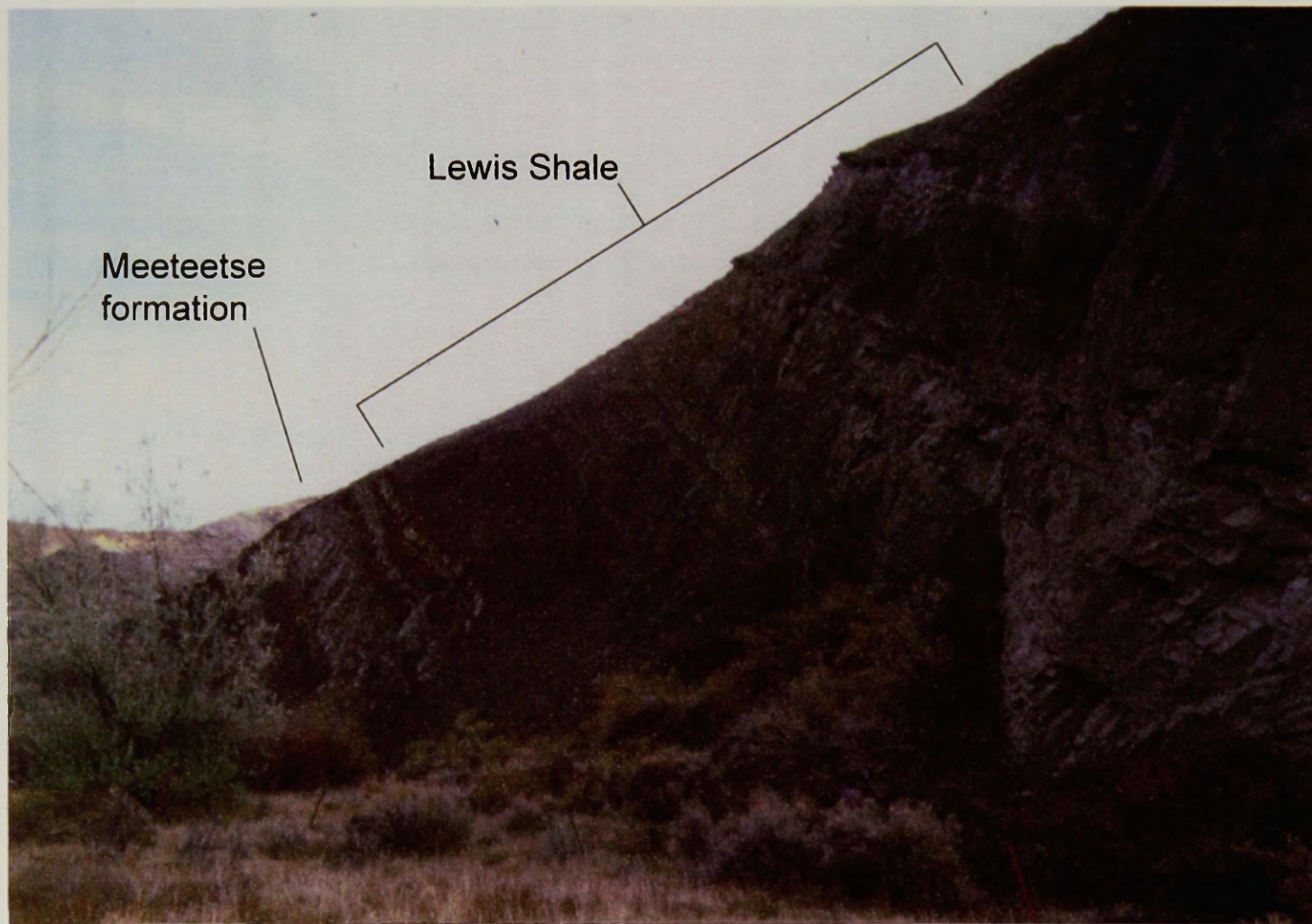


Figure 21. Contact of Meeteetse Formation and Lewis Shale at Greybull. Note the upward coarsening, upward thickening trend of the Lewis Shale.

capped by 16 meters of shaley sandstone. Sandstone beds contain climbing ripple foresets, minor soft sediment slump folding and possible ball and pillow structures. The presence of the marine Lewis Shale indicates that relative sea level was still a controlling factor on sedimentation during deposition of the Meeteetse Formation. Also, the transgression of marine strata on underlying continental strata indicates an increase in A/S, consistent with the type III interval of Meeteetse strata observed at Little Sand Draw.

Lance Formation

The basal Lance Formation contrasts sharply with the underlying Meeteetse Formation. At Little Buffalo basin the Lance Formation consists of a 65-meter type I sandstone, forming a series of prominent hogback ridges. This sandstone contains multiple internal scour surfaces, lateral accretion surfaces in the first 10 meters, and large-scale soft sediment deformation and trough cross beds. Rip up clasts are common, and the upper sandstone beds contain extra-basinal angular chert pebbles. Webb (2000) identified this outcrop of the Lance as an incised valley fill system, and Belt et al (1997) identified the presence of a regional unconformity at the Lance-Meeteetse contact. Paleocurrent data from this sandstone indicate southeastward flow.

The first 30 meters of the Lance are the most strongly amalgamated. Overlying this interval, overbank fines are preserved, separating individual type I sandstone bodies. Increased preservation of overbank fines towards the top of the type I interval indicates an increase in accommodation space. A type I sandstone marks the base of the Lance at

Little Sand Draw, but it is not as thick as the type I interval at Little Buffalo basin, and the contact with the underlying Meeteetse Formation is more gradational.

Similar to the Teapot-Meeteetse contact, type III strata overlie the basal type I interval of the Lance. The type III interval at Little Sand Draw contains numerous isolated channels on the same horizon, possibly indicating anastomosing systems (Figure 22). Uppermost Lance strata consist of type II deposits. There is a 94 meter covered section in the middle of the Lance Formation at Little Buffalo basin, but the uppermost Lance shows a noticeable transition from lenticular, isolated type III ribbon sandstones to Type II geometry just below the Fort Union Formation. This is not a typical Type II interval, in that lateral accretion surfaces are not visible, and channel sandstones show several meters of basal scour (Figure 23). Channel sandstones in this interval show a similar thickness/width ratio to other type II intervals, and there is an increasing sandstone/mudstone ratio compared to the underlying type III interval, indicating a decrease in A/S ratio.

Exposures of the Lance Formation at Greybull did not permit detailed assessment of channel geometry. In general, the Lance Formation at Greybull seemed to contain evenly spaced sandstone beds and overbank fines suggesting a more constant A/S ratio throughout deposition. Paleocurrent trends in basal Lance deposits at Little Buffalo basin and Little Sand Draw indicate flow to the east. Paleocurrent trends in the uppermost Lance at Greybull indicate flow to the northwest (Figure 24)



Figure 22. Middle Lance strata at Little Sand Draw. The type III channel sandstone on the left is laterally traceably to channel sandstones forming prominent ships prow structures in the distance. Note the closer stacking of channel sandstone beds in the overlying Fort Union in the upper left.



Figure 23: Scour surfaces and stacked channels in the upper Lance Formation at Little Buffalo basin.

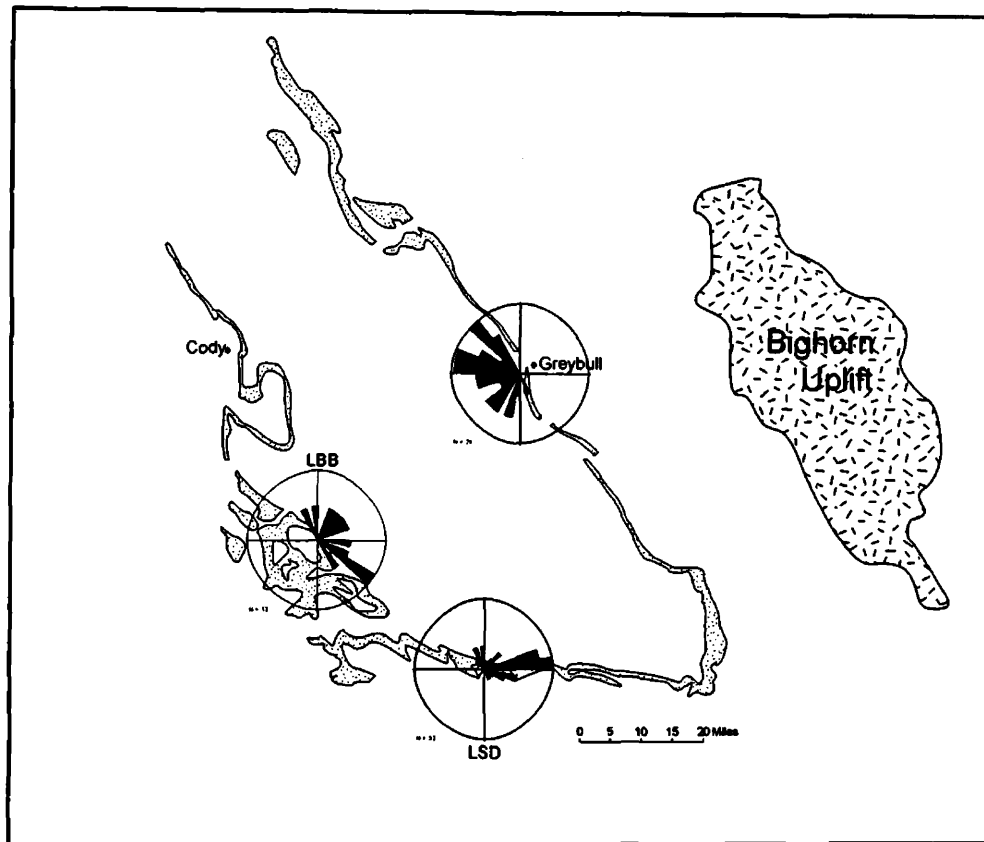


Figure 24. Paleocurrent map of the Lance Formation. Paleocurrent trends on the western side of the basin indicate eastward flow into the basin. Paleocurrent trends on the eastern side of the basin suggest northwestward flow sub-parallel to the basin axis and away from the incipient Bighorn uplift. Measurements at Little Buffalo Basin and Little Sand Draw are from lower Lance strata, whereas measurements at Greybull are from earliest Paleocene Lance strata. Outcrop data modified from Love and Christiansen (1985).

Fort Union Formation

The Fort Union Formation is very similar to the underlying Lance Formation. At Little Buffalo basin, the base of the Fort Union is marked by a multistory sandstone, indicating a marked decrease in A/S from the underlying Lance Formation. A covered section occurs above the multistory sandstone, but resumed exposure on the next hogback reveals type III deposits surrounding an isolated multistory channel complex. Above this hogback, exposures were poor and did not permit measurement of the entire Formation. The multistory interval is not as amalgamated at Little Sand Draw, but there is a marked increase in sandstone to shale ratio and numerous smaller scale multistory sandstones (Figure 22). Sandstones at the base of the Fort Union Formation at Little Sand Draw contain clast supported roundstone extrabasinal conglomerate lags, and coarse-grained lags continue through the first 100 meters of the formation. After the first 100 meters of the formation channels appear to become less closely stacked, indicating increased A/S. This change in stacking patterns was also noted by Roberts (1998) at a nearby site.

The Fort Union Formation at Greybull is cut by an angular unconformity that has removed all but the Upper Paleocene strata of the Fort Union Formation. Deposits directly overlying the unconformity show close stacking and abundant scour surfaces. Overlying this interval, there is a sharp increase in overbank fines, and sandstone beds form interconnected type III lenticular geometry. The upper Paleocene Fort Union Formation at Little Sand Draw shows a similar progression, with a 20-meter multistory sandstone overlain by mudstone-dominated strata. Geometry of the fine-grained interval

is not visible in this outcrop, due to badland-style erosion, but the dominance of overbank material indicates high A/S.

Paleocurrent trends in the upper Fort Union Formation indicate continued flow to the east at Little Buffalo basin, but at Little Sand Draw paleoflow trends indicate flow to the southeast, and Greybull flows trend to the west (Figure 25), indicating topographic definition of the Bighorn basin.

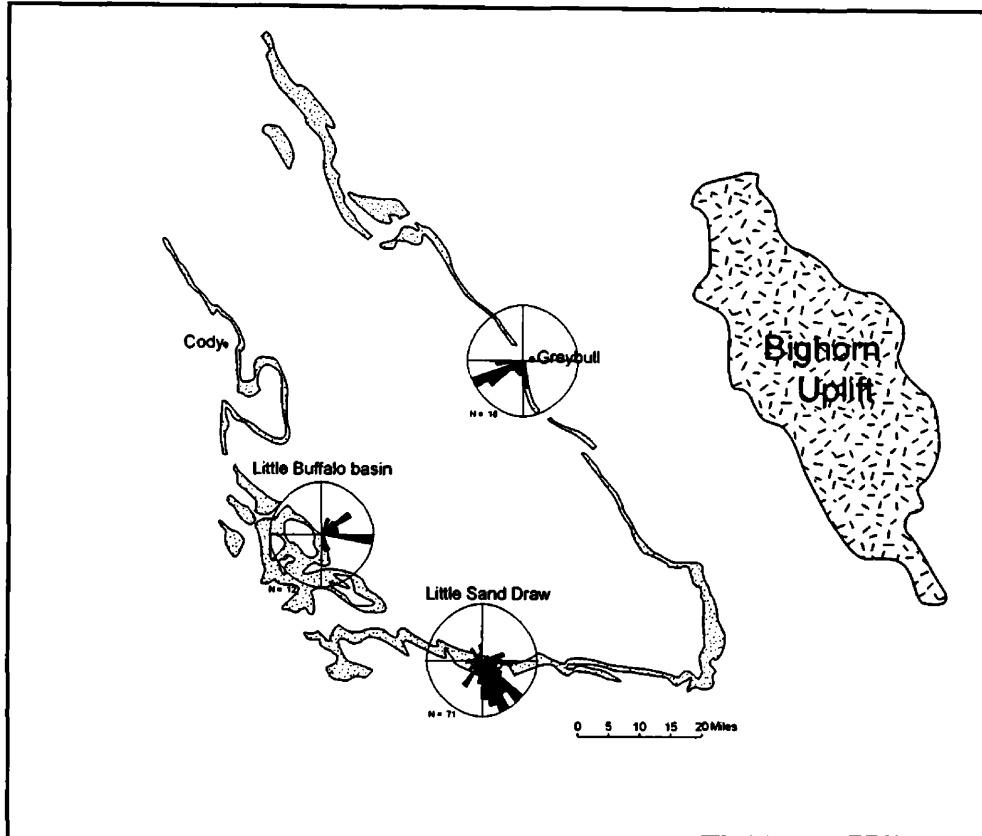


Figure 25. Paleocurrent Map of the upper Fort Union Formation. Little Buffalo basin paleocurrent measurements from middle Paleocene strata indicate continued eastwards flow into the Bighorn Basin. Greybull Paleocurrent measurements from late Paleocene strata (S6) indicate westward flow away from the Bighorn Uplift. Little Sand Draw paleocurrent measurements from Late Paleocene strata (S6) indicate southeastward flow directions. The southeastern Paleoflow trend at Little Sand Draw aligns parallel to the basin axis.

SANDSTONE PETROLOGY

Methods

I collected sandstone samples from outcrops in each field site throughout the entire length of each measured section . Instead of collecting samples at regular intervals, I collected samples from the thickest sandstone beds of a given interval that seemed the least altered. I avoided iron-enriched or calcified areas, assuming that these areas would contain more replacement and alteration. I tried to collect medium grained samples for point counting whenever possible, in order to avoid compositional differences due to grain size. I also collected several samples from extrabasinal pebble lags of the Teapot sandstone and the Lance and Fort Union formations for qualitative pebble study. Thin sections were cut and prepared by Spectrum Petrographics (Salem, Oregon). All thin sections were impregnated with blue epoxy, and one half of each slide was stained for plagioclase and potassium feldspar.

I primarily counted slides using a modified Gazzi-Dickinson method. I examined slides for diagenetic alteration before counting, and did not count slides containing abundant diagenetic calcium carbonate, oversized pores or obvious dissolution or replacement of original detrital grains.

Point Count Categories

Monocrystalline quartz: Monocrystalline quartz with straight to strongly undulose extinction was the most common framework grain type in all slides. Quartz grains contained inclusions of mica flakes, tourmaline, and zircon as well as some unidentified

minerals. A given grain was counted as monocrystalline quartz if the crosshairs fell on a quartz crystal larger than 0.0625 mm.

Polycrystalline quartz: I counted a detrital grain as polycrystalline quartz if the grain consisted of pure quartz with individual quartz crystals smaller than 0.0625mm in diameter, and. If other minerals were present in the grain it was counted as a lithic fragment. Polycrystalline quartz showed straight to undulose extinction with several textures. Sheared, undulose quartz and polygonized, serrated quartz indicated minor metamorphic input.

Chert: Several types of chert were identifiable in thin-section. I identified a few grains of radiolarian chert, but this was not a common constituent. I identified clean, inclusion free chert, with small blebs of crystalline quartz that had indistinct boundaries. I distinguished this chert from metasedimentary siltstone fragments by the less distinct boundaries quartz blebs compared with the well-defined quartz grains in siltstone fragments. Some chert was cloudier and took some plagioclase stain. I distinguished this chert from lithic volcanics on the basis of lower internal relief, lack of feldspar lathes, and local presence of dolomite rhombs. I counted all chert, including chalcedony, in one category.

Feldspar: I counted feldspar grains in two categories: plagioclase, and potassium feldspar. Potassium feldspars consisted mainly of orthoclase and microcline, identified by green stain (sodium cobaltinitrite). Plagioclase was identified by pink stain (Barium chloride +

rhodizonate). In some slides feldspars had been partially removed or altered. I counted these grains as the original framework mineral when possible.

Muscovite, chlorite, and biotite: I identified muscovite, chlorite, and biotite by their diagnostic platy, layered structure and bird's eye extinction under crossed polars. I distinguished these minerals from each other on the basis of color. Muscovite was generally colorless, biotite was dark brown and pleochroic, and chlorite showed green to clear or pink to clear pleochroism.

Metasedimentary grains: The two common types of metasedimentary grains I identified were siltstone clasts consisting of quartz grains in a microcrystalline cherty matrix, and siltstone grains consisting of quartz in a sericite matrix.

Metamorphic grains: I identified uncommon schist, slate, and gneiss grains, and counted all in one category. Metamorphic grains were differentiated from polycrystalline quartz by the presence of minerals other than quartz in the grain (usually muscovite or sericite).

Lithic volcanic grains: I identified cloudy, dirty grains of microcrystalline quartz as lithic volcanic clasts. I differentiated these grains from cloudy chert by a higher internal relief under plain light, the presence of plagioclase laths, and indistinct internal boundaries under crossed polars.

Lithic plutonic grains: I identified plutonic fragments by the presence of quartz and feldspar, and sometimes muscovite, in the same grain. Using the Gazzi-Dickinson method, I generally counted these grains as the constituent mineral that the crosshairs landed on. If the crosshairs landed on a finely crystalline area of the grain (<0.0625mm) I counted it as lithic plutonic. I observed some coarse granitic fragments in slides from the upper Fort Union Formation, but most of the grains lower in the sections counted as lithic plutonic fragments were fairly fine-grained, suggesting a volcanic origin.

Intraclasts: I counted intra-basinal silt-clay clasts separate from other siltstone clasts. Extrabasinal siltstone clasts showed strong lithification and induration, whereas intrabasinal clasts had poorly defined or deformed boundaries. Intrabasinal clasts generally formed pseudomatrix (Dickinson, 1970), with grain boundaries and sedimentary fabric deformed around extrabasinal clasts.

Matrix: There was little cement or matrix in most of these samples. The most common interstitial component were accordion-like booklets probably representing a clay mineral. This material was not positively identified, and was instead grouped in the matrix category.

Carbonate: I did not identify extra-basinal limestone or dolomite clasts in any sample. I identified diagenetic calcium carbonate by diagnostic high relief in plain light and high interference colors under crossed polars. Most of the diagenetic carbonate I observed had partially replaced framework feldspar grains. If I could still identify the original grain, I

counted it as such. If too much replacement had occurred in a given slide, I did not count it.

Other categories: A small percentage of clasts in each slide were too altered to identify. I counted these as either unidentified grains or lithic unidentified grains. I grouped accessory minerals such as zircon, garnet, tourmaline, and green hornblende as well as unidentified accessory minerals in one category. Porosity was easily identified by blue epoxy, but was not included in count totals, so that 500 grains were counted per slide regardless of variations in porosity.

Lithic Populations

I tried to count several lithic grain types in addition to the above categories. The additional grain types I identified were 1) two distinct populations of siltstone fragments, 2) reworked quartz grains identified by well rounded or half round grains with quartz overgrowths isolated in angular sands and 3) granitic fragments. Unfortunately, the small percentage of lithics present in these sandstones (other than chert) made quantifications of these populations difficult. Standard deviations were of the same order of magnitude as percentages for lithic volcanic fragments and lithic sedimentary fragments identified using the Gazzi-Dickinson method. Also, in some slides unidentified lithics were as abundant as identifiable lithic populations. Therefore, in the following discussion I will focus on normalized Q-F-Lt and Q-P-K compositions. Presence or absence of lithic fragments will be discussed only qualitatively.

Error

I counted 500 grains per slide, not including porosity. I performed multiple counts on several slides prior to counting the majority of slides, in order to calibrate my counting methods and assess the precision of my results. I counted slides GB-13 and UFU-3 periodically throughout the counting process in order to determine the standard deviation inherent in my counts. Four counts of slide GB-13 produced standard deviations of ± 3 percent quartz, ± 1 percent feldspar, and ± 2.5 percent total lithics for normalized Qm-F-Lt. Standard deviations of normalized Qm-P-K are ± 2 percent Qm, ± 1.5 percent plagioclase, and ± 1 percent potassium feldspar. Standard deviations for 5 counts of slide UFU-3 are ± 2.7 percent quartz, ± 3.7 percent feldspar and ± 3.4 percent total lithics for normalized Qm-F-Lt. And ± 4.1 percent quartz, ± 3.4 percent plagioclase, and ± 1.5 percent potassium feldspar for normalized Qm-P-K. I used the larger of the two values between GB-13 and UFU-3 as the internal error value for each category. Error bars in all ternary diagrams are the sum of standard deviations of the given group plus the internal error determined above. Both UFU-13 and Gb-13 are fairly dirty, feldspar rich samples. Recounting of GB-12, which is a clean quartz sandstone, yielded standard deviations below 1 for all categories, therefore the internal error reported here is probably a conservative figure. In order to simplify my results, I have not reported errors with the following results; error is indicated by error bars on ternary diagrams. Appendices II-IV show raw point count data, recalculated modal compositions, and error calculations.

Results

General sandstone compositions from all samples counted range from 40% to 90% monocrystalline quartz, 0 to 35 % feldspar, and 5% to 30% lithic fragments, including chert. Keighin (1998) reported generally higher lithic percentages in the Montana Group of the southern Bighorn basin, but it is unclear what point count method was used in this study. If the Gazzi-Dickinson method was not used, higher percentage of lithics would be expected (Dickinson, 1985). Modal compositions of my data agree well with compositions reported by Connor (1992) for the southern Bighorn and Powder River basins. Compositions fall into the recycled orogen province of Dickinson and Suczek (1979), consistent with a foreland basin tectonic setting (Figure 26). Whereas all samples fall into the recycled orogen province of Dickinson and Suczek (1979), several statistically significant stratigraphic trends in each section and areal trends across the basin provide insight into evolution of the basin

Stratigraphic trends in individual sections

All three sections show a general increase in feldspar content up section. Little Sand Draw samples have an average composition of $Qm_{67} F_6 Lt_{26}$ in the Mesaverde, Lance, and lower Fort Union formations, and $Qm_{58} F_{24} Lt_{18}$ in the upper Fort Union Formation (Figure 27). Greybull samples have an average composition of $Qm_{56} F_{17} Lt_{27}$ in the Mesaverde, Meeteetse, and Lance. Uppermost Lance samples show a sharp decrease in Lithic grains and feldspar grains, with an average composition of $Qm_{87} F_0 Lt_{13}$, and Upper fort Union samples have an average composition of $Qm_{51} F_{31} Lt_1$, similar to upper Fort Union samples at Little Sand Draw (Figure 28). In contrast, Little Buffalo

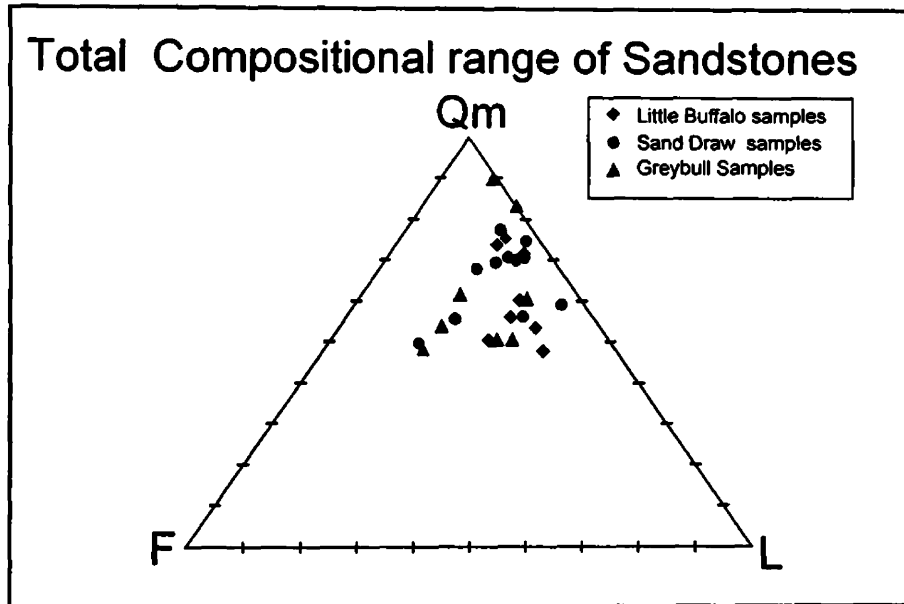


Figure 26: Ternary plot of all samples counted. Samples fall in the Recycled Orogen province of Dickinson and Suczek (1979).

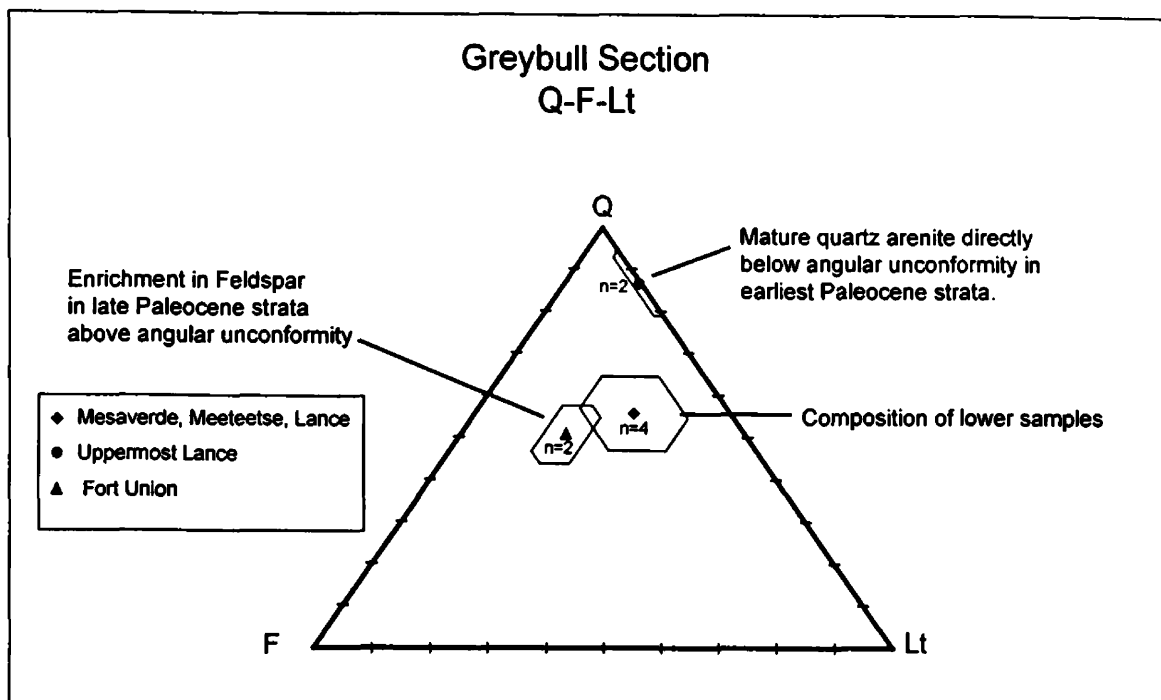


Figure 28a: Quartz-feldspar-total lithic ternary plot of Greybull samples. Points represent mean values of samples from specified formations. Error bars represent standard deviation of the samples plus internal error. Number of samples is indicated for each average value.

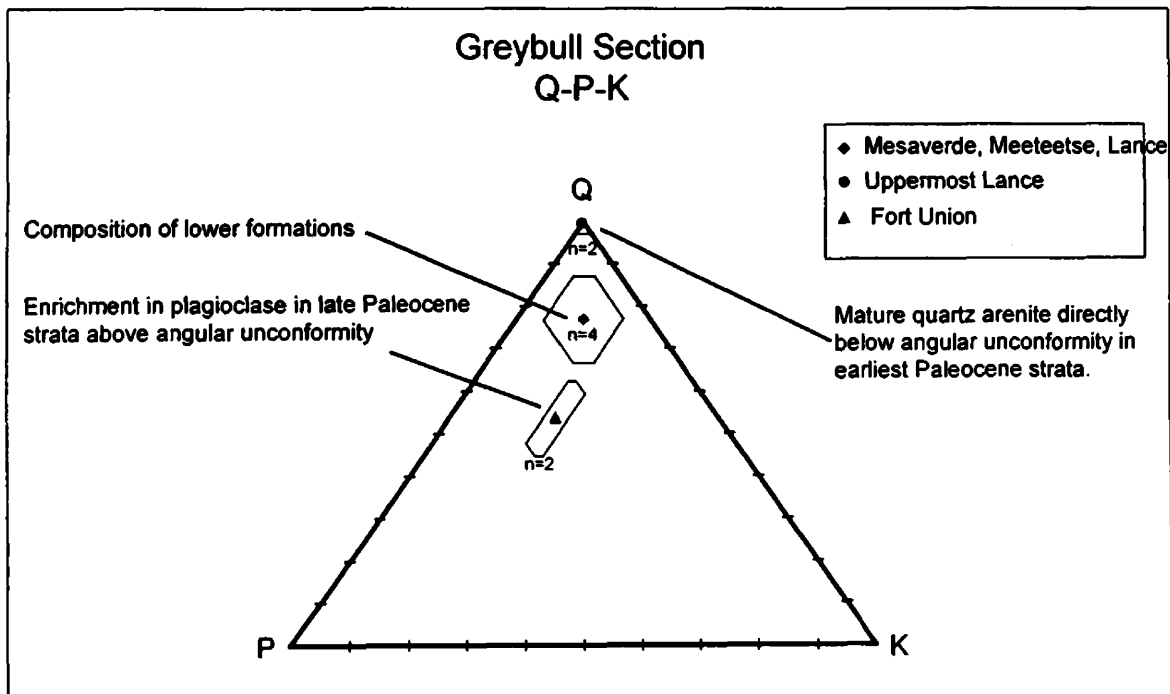


Figure 28b. Quartz-plagioclase-potassium feldspar ternary plot for the Greybull section. Points represent mean values of samples from a given interval. Error bars represent standard deviation of the samples plus internal error. Number of samples is indicated for average value.

basin samples contain consistently higher percentages of potassium feldspar, and in fact show an increase in potassium feldspar and lithic grains up section. Little Buffalo basin samples have an average composition of $Qm_{68} F_7 Lt_{25}$ in the Mesaverde Formation, and $Qm_{54} F_{14} Lt_{32}$ in the overlying Lance and Fort Union Formations (Figure 29). This differentiation between Cretaceous - lower Paleocene samples and upper Paleocene samples at Greybull and Little Sand Draw suggests sedimentary input from a new source by late Paleocene time. The lack of a similar trend in Little Buffalo Basin samples suggests input from different source terrains between the western and eastern areas of the basin. Comparison of these trends across the basin gives a clearer picture of this differentiation.

Basin Wide Trends

Mesaverde, Meeteetse and Lance Formations

Samples from the Mesaverde and Lance formations have similar average compositions $Qm_{67} F_6 Lt_{26}$ and at Little Sand Draw and $Qm_{68} F_7 Lt_{25}$ at Little Buffalo basin respectively. Little Sand Draw samples of the lower Fort Union Formation have a very similar composition as the underlying Lance and Mesaverde, and are included in the average. In contrast, Greybull samples of the Montana Group contain a greater percentage of feldspar, with an average composition of $Qm_{56} F_{17} Lt_{27}$ (Figure 30a). These trends are evident in ternary plots, and while error bars of Little Sand Draw and Greybull samples overlap, error bars of Little Buffalo and Greybull samples do not overlap, suggesting different clastic input in the northern and southern parts of the basin. Comparison of Quartz-Plagioclase-Potassium feldspar modal compositions shows

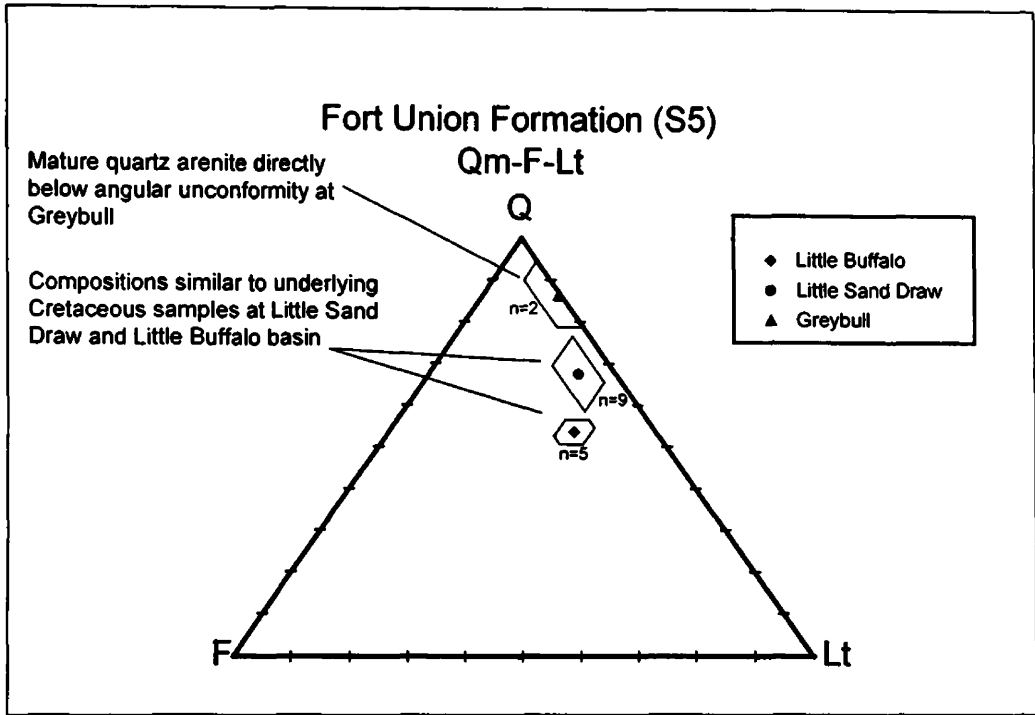
average compositions of $Q_{m92} P_1 K_7$ at Little Sand Draw, and $Q_{m89} P_2 K_8$ at Little Buffalo basin, compared to $Q_{m76} P_{12} K_{12}$ further north at Greybull. Standard deviations indicate that Greybull compositions are distinct from Little Sand Draw and Little Buffalo basin compositions (Figure 30b). Taken together, these compositions indicate that sands in the southern part of the basin are more quartz rich, Whereas the northern part of the study area contains more feldspar; feldspar in the southern part of the basin consists of potassium feldspar, whereas at Greybull there is an even percentage of plagioclase and K-spar. Connor (1992) noted this same trend in the Lance Formation of the Powder River basin, and attributed the greater plagioclase content of the northern basin to volcanoclastic input from the Elkhorn Mountains Volcanics. Large detrital biotite plates (sample GB-4) are consistent with input from a volcanic source. Sandstone composition from the southern part of the basin is similar to that reported by Borrell (2000) for the Eagle Sandstone of the Crazy Mountains basin. Borrell interpreted these sandstones to have a reworked sedimentary source. Sandstone of the Lower Judith River Formation in the Crazy Mountains basin has an average composition similar to the composition of Greybull samples from the Montana Group. Borrell interpreted this sandstone to have a primary reworked sedimentary source area with minor input from volcanics. Also, Upper Judith River sandstone contains a greater percentage of plagioclase than potassium feldspar, similar to the composition noted at Greybull. Gill and Coban (1973) also attributed several regressions in the Montana Group of the Williston basin to choking of systems by volcanoclastic input. While my sandstone compositions at Greybull are consistent with this inferred volcanic input, more detailed study is needed to positively link petrological trends of the Bighorn Basin with volcanic activity to the north

Fort Union Formation

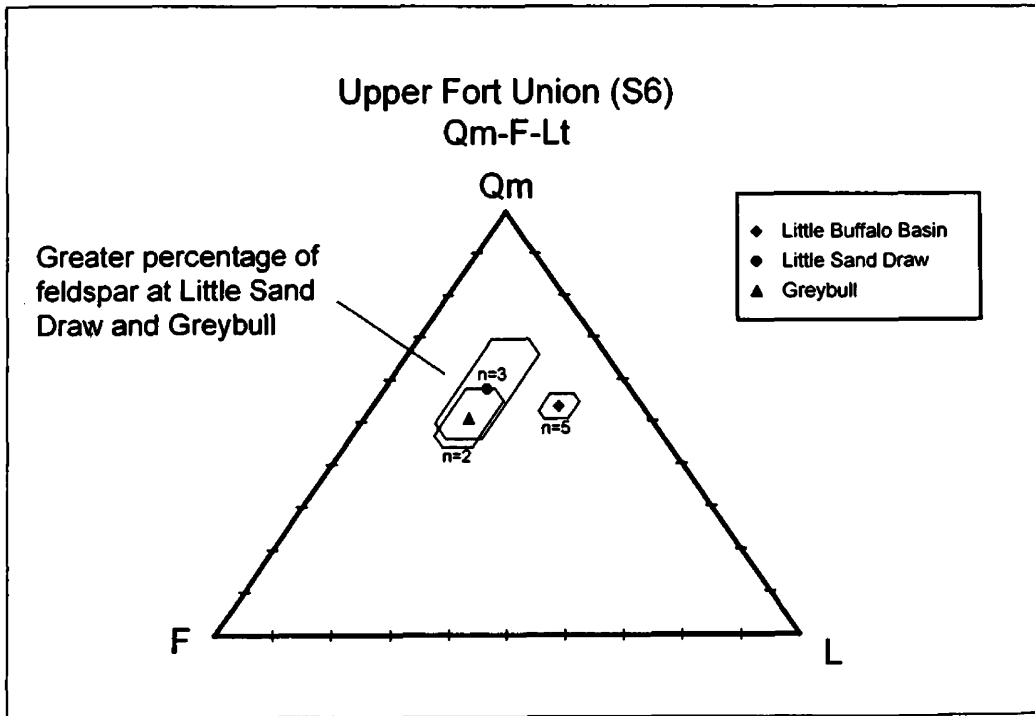
Fort Union samples at Little Sand Draw have the same average composition as underlying strata (average Qm₆₇ F₆ Lt₂₆). In contrast, composition of Fort Union samples at Little Buffalo basin show an increase in lithic grains, (average Qm₅₄ F₁₄ Lt₃₂), whereas composition of uppermost Lance samples at Greybull show a sharp decrease in lithics and feldspar (average Qm₈₇ F₀ Lt₁₃) (Figure 31a). I have compared Lance compositions to Fort Union compositions here because palynological dates have placed the uppermost Lance at Greybull in the early Paleocene (Nichols, 1998). The compositionally distinct Greybull samples do not contain oversized pores, calcium carbonate replacement, or any other signs of diagenetic altering. Texturally, the sandstone in these samples is better rounded and sorted than both underlying sandstone of the Greybull section and Fort Union sandstone to the south. Increased maturity of this sandstone could be due to greater weathering, or could indicate a second cycle source terrain. The increase in lithic grains at Little Buffalo basin is consistent with the presence of quartzite-chert conglomerates in the Fort Union around Little Buffalo basin and Grass Creek basin (Krauss, 1985; Roberts et al 1991; Seeland, 1998).

Upper Fort Union Formation

Overlying the angular unconformity at Greybull, the Fort Union Formation shows a sharp increase in feldspar content (average Qm₅₁ F₃₁ Lt₁). The upper Paleocene Fort Union Formation at Little Sand Draw shows a similar feldspar enrichment, with an average of Qm₅₈ F₂₄ Lt₁₈ (Figure 31b). Qualitative examination of these samples reveals presence of granitic fragments and reworked quartz grains with quartz overgrowths.



a



b

Figure 31: Basin-wide compositions of the Fort Union formation. a) Qm-F-Lt of the lower Fort Union formation b) Qm-F-Lt plot of the upper Fort Union Formation.

A textural inversion observed in some samples, with well-rounded, reworked quartz grains observed next to immature, angular granitic fragments and feldspar grains implies a bimodal source terrain, with input from first cycle plutonic rock as well as second cycle sedimentary rock (Folk, 1980). Also, glauconite is an accessory grain in the upper Fort Union samples. Glauconite is generally interpreted to form only in shallow marine systems, and to be unstable in terrestrial environments. Thus, the presence of glauconite suggests a proximal source area of reworked marine strata (Folk, 1980; Whipkey et al., 1991).

I could not sample the entire Fort union Formation at Little Buffalo basin due to poor exposures of the Formation, but previous studies (Krauss, 1985) documented quartzite conglomerates in the Fort Union and Eocene Willwood Formation in the area, suggesting a continuous, single source.

SEQUENCE STRATIGRAPHIC FRAMEWORK

Background

Sequence stratigraphy has been one of the major developments in sedimentary geology over the past several decades, providing a powerful tool for dividing and correlating sedimentary strata as well as predicting the spatial distribution of depositional facies. The original concepts of global eustatic sea level, transgressions, and regressions were developed by Suess (1885), and the original idea of the sequence was developed by Sloss (1962). Much of the development of sequence stratigraphy was carried out by Exxon researchers such as Posamentier et al (1988), Posamentier and Vail (1988), and Van Wagoner et al (1988). These original sequence stratigraphic models were developed for marine to marginal marine settings, and the development of sequences was attributed mainly to the control of eustatic sea level changes.

Application of these models to non-marine environments is still a relatively new area of research, and still an area of considerable debate (Shanely and McCabe, 1994). Non-marine models are still being tested and revised. In addition, sequence stratigraphic work in tectonically active areas must take into account tectonically induced subsidence and source area uplift as well as changes in the rate of sediment supply (Miall, 1991; Krystinik and DeJarnett, 1995).

Many recent workers in the Western interior seaway have placed more emphasis on tectonic controls of relative sea level and accommodation (Penderson and Steel, 1999; Willis, 2000; Yoshida et al, 2000; Cataneau and Elango, 2000, Miall, 2001). At the same

time, in less tectonically active parts of the foreland, eustatic control of sequences has been inferred (Rogers, 1998; Roberts, 1999). Shanely and McCabe(1994) have also noted that “ the Pendulum may have swung too far” towards allocyclic control on deposition, with not enough emphasis placed on autocyclic processes. As stated by Shanely and McCabe (1994) “When well practiced, sequence stratigraphy attempts to explain the formation of sequences and sequence boundaries through an understanding of all controls on sedimentation.”

Several models of non-marine sequence stratigraphy have been developed (Posamentier and Vail, 1988; Wright and Marriott, 1993; Shanely and McCabe, 1994; Zhang et al, 1995). Marine sequences consist of changing environments of deposition controlled by varying rates of accommodation and sedimentation, whereas non-marine models occur entirely in continental strata, and are composed of various styles of fluvial geometries. The model of Zhang et al (1995) matches the stratal stacking patterns I observed in the fluvial deposits of the Lance, Fort Union, and parts of the Meeteetse most closely. Whereas the more traditional models for marginal marine settings fit the lower Mesaverde Formation and Cody Shale. In addition, intertonguing of the Claggett and Lewis shales with continental strata of the Mesaverde and Meeteetse formations allows comparison between traditional and non-marine models.

The non-marine sequence model of Zhang et al. (1995) consists of low stand deposits, transgressive deposits, and highstand deposits, all bounded by unconformities (sequence boundaries). These systems tracts are couched in terms of low stand, transgressive, and

high stand tracts, but these terms do not imply a eustatic sea level control, instead representing varying rates of creation of accommodation and sediment supply (A/S), whether driven by eustatic or tectonic forces. Low stand systems tract (LST) consist of amalgamated, braided river sheet sands corresponding to periods of low A/S ratio, and the type I intervals defined in this study. Transgressive systems tract (TST) consists of lenticular channel form sandstones isolated by overbank fines interpreted by Zhang et al (1995) as anastomosing systems. TST deposits have a high A/S ratio and correspond closely to the type III lenticular intervals defined in this study. The highstand systems tract (HST) of Zhang et al (1995) consist of meandering fluvial strata deposited during periods of decreasing A/S ratio, and are analogous to the type II meandering intervals I identified in this study. Figure 32 shows an idealized cross section of a sequence.

Sequences

On the basis of the non-marine model of Zhang et al (1995), as well as more traditional marginal marine models (Posamentier and Vail, 1988) I have divided the formations of this study into 6 sequences, S1 – S6 (Figure 33). Age constraints for these sequences were based on ammonite zones (Gill and Coban, 1973), palynological zones (Nichols, 1998), and isotopic age dates (Hicks et al, 1995; Belt et al, 1997). These age constraints indicate that the identified sequences correspond to 3rd order sequences, with an average duration in the range of 2 – 10 million years (Miall, 1990). Several of the sequence boundaries identified here correspond to sequence boundaries identified by Wiemer (1988) and the alloformation boundaries identified by Hicks and Tauxe (1992).

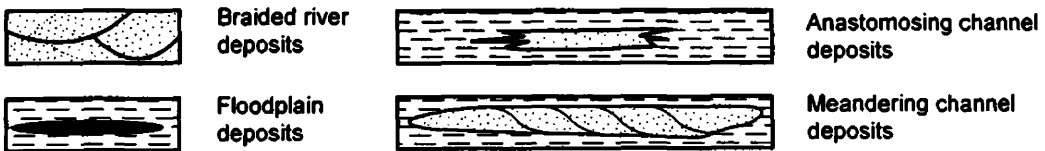
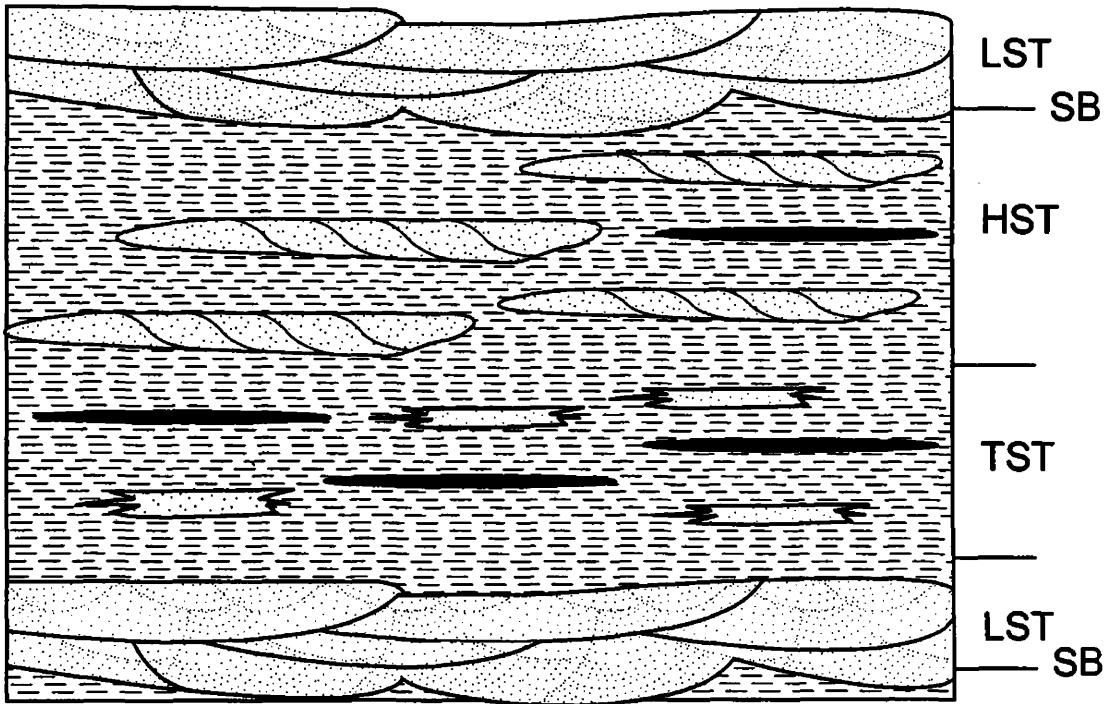


Figure 32: Cross sectional view of the non-marine model of Zhang et al (1995).

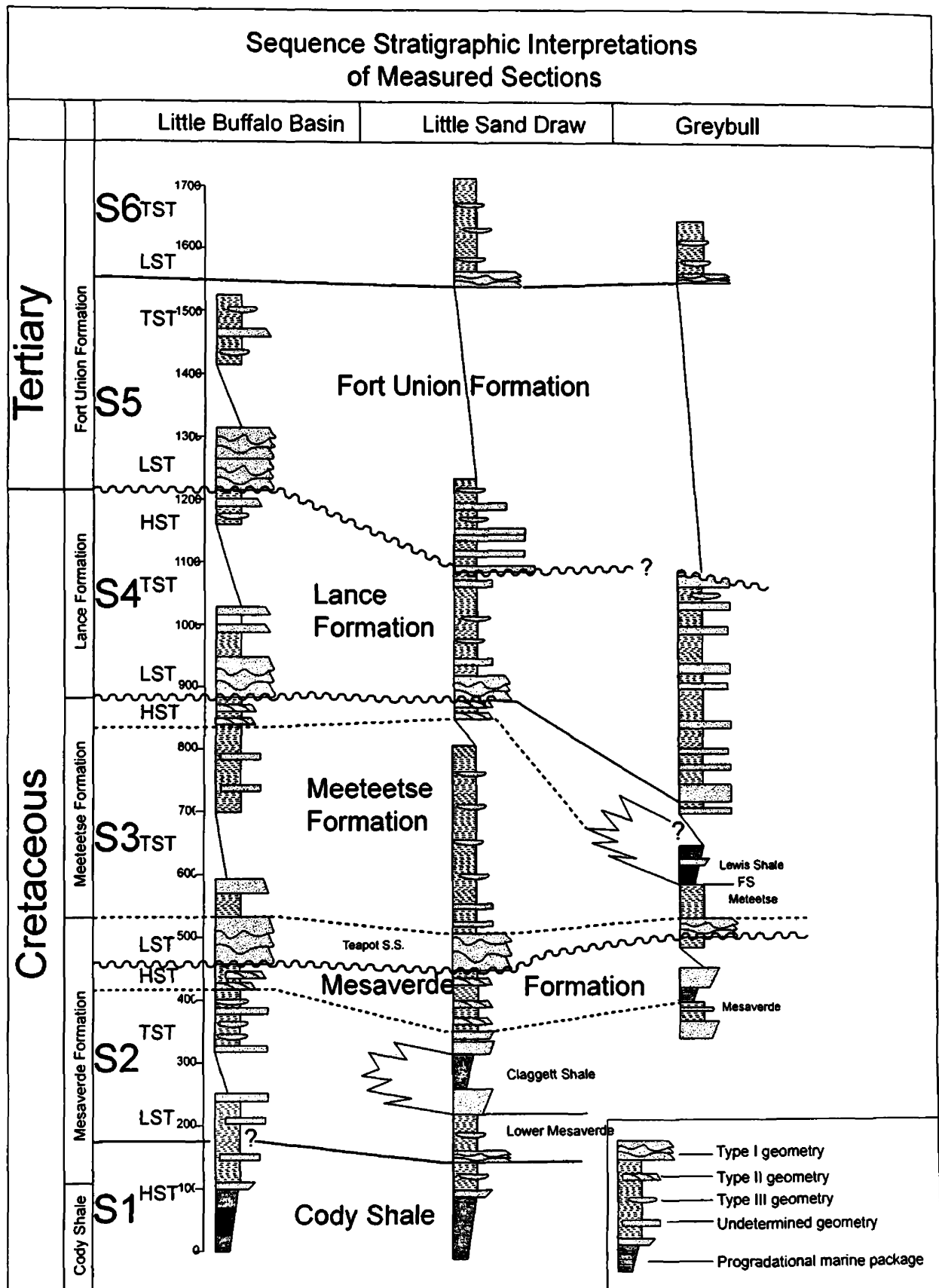


Figure 33. Sequence architecture of measured sections. Condensed stratigraphic columns were generated from detailed measured sections. Sequence architecture is based on the model of Zhang et al (1997).

Sequence 1

The Cody Shale and lower Mesaverde Formation form sequence 1, which I interpret as HST deposits. These units form a progradational package indicating a decrease in creation of accommodation, and a concomitant basinward shift of the shoreline. The Cody Shale contains ammonites *scaphites hippocrepis* (Gill and Coban, 1973) placing it in the early Campanian. I have placed the S1 - S2 sequence boundary at the base of the type I sheet sandstone in the lower Mesaverde member at the Little Sand Draw (Figure 12). The HST and sequence boundary identified here corresponds closely to the general description of sequence boundaries of the Cretaceous Western Interior Seaway provided by Weimer (1988). I did not identify this sequence boundary at Little Buffalo basin, but several tabular sandstone beds which occur at approximately the same stratigraphic level may represent the sequence boundary.

Sequence 2

I interpret the multistory sandstone in the Lower Mesaverde as the LST of sequence 2, consistent with the models of Posamentier and Vail (1988). I have interpreted the type II-III fluvial deposits of the Lower Mesaverde and the lower half of the Claggett Shale at Little Sand Draw as TST deposits. The Claggett shale contains several flooding surfaces and progradational packages. I have placed the maximum flooding surface (MFS) of S2 at meter 280 in the Claggett Shale. This flooding surface is overlain by the thickest interval of shale deposition observed in the Claggett, suggesting the most distal environment and therefore maximum flooding. I have interpreted the type III interval from meter ~300 to ~350 of Little Buffalo basin as the upper part of the TST. The

Claggett Shale falls in the ammonite zone of *bacculites* sp. (Gill and Coban, 1973), and also contains the Ardmore bentonite, (Keefer et al, 1998), which has an Ar-Ar date of 80.7 +/- 5 Ma (Hicks et al, 1995). I interpret upper Mesaverde tidal deltaic strata at Little Sand Draw and meandering fluvial strata Little Buffalo basin as HST of sequence 2. Deltaic channel sands at Little Sand Draw show closer stacking up-section, consistent with the decreasing A/S of HST (Figure 34).

The lowest measured interval of the Greybull section fall in the HST of sequence 2. This interval contains two progradational packages separated by a minor flooding surface. The progradational intervals are consistent with decreasing A/S ratio of the HST, whereas the flooding surface may correspond to the double shoreface sandstone beds at Little Sand Draw. I place the S2-S3 sequence boundary at the base of the Teapot sandstone. The base of the Teapot shows evidence of subarial exposure and hiatus, with strong oxidation, disturbed bedding, and abundant root casts. As discussed below, this boundary was interpreted by Gill and Coban (1973) as a regional unconformity truncating progressively older strata to the west.

Sequence 3

I have grouped the Teapot sandstone and Meeteetse Formation together in sequence 3. At Sand Draw and Little Buffalo basin, I identified systems tracts based on the non-marine sequence model of Zhang et al. (1995). The type I Teapot sandstone represents LST, the type III ribbon geometry of the lower Meeteetse represents TST, and the upper Meeteetse type II meandering interval represents HST. I identified systems tracts at the more distal

Architecture of the S2-S3 sequence boundary

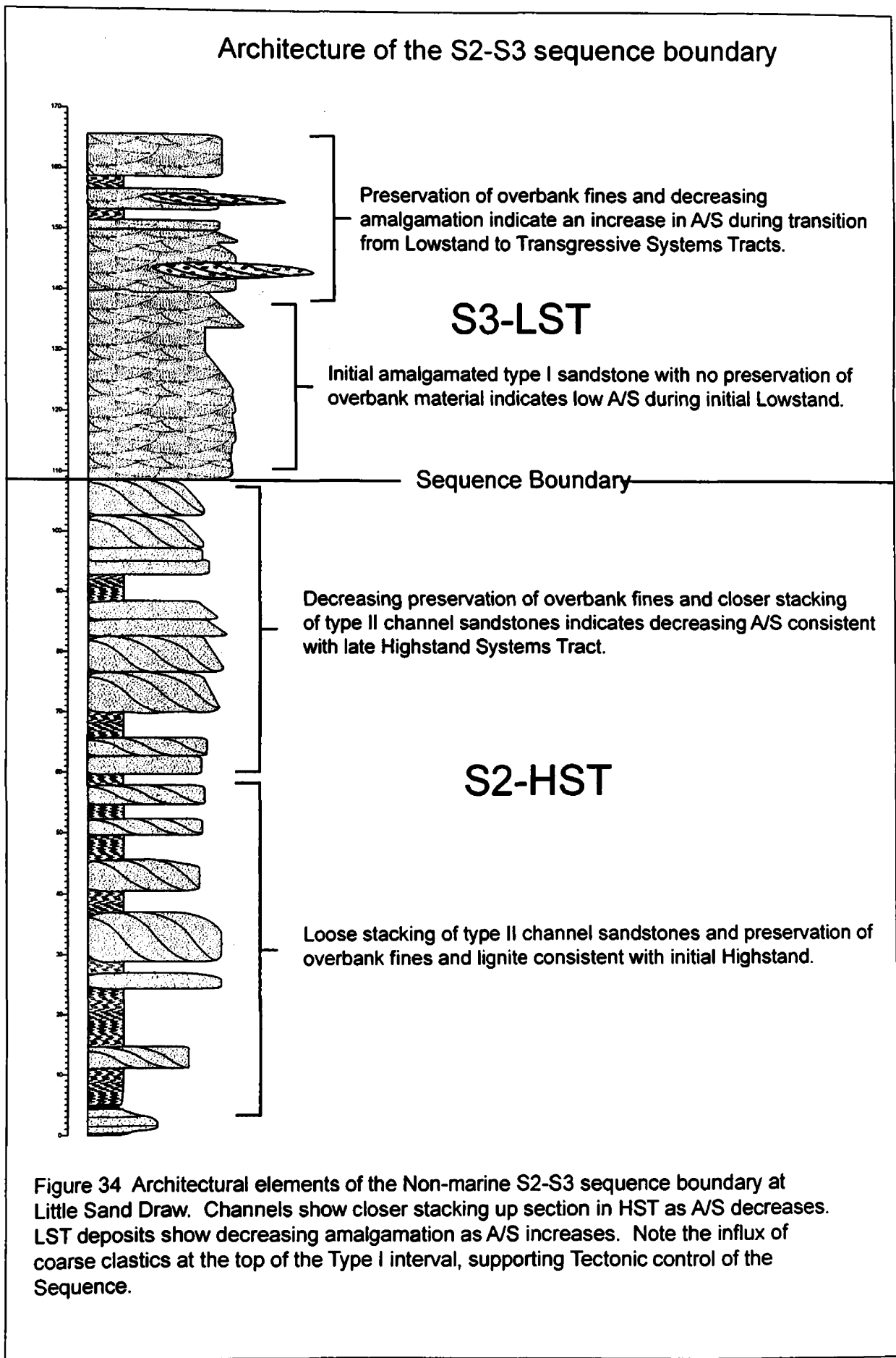


Figure 34 Architectural elements of the Non-marine S2-S3 sequence boundary at Little Sand Draw. Channels show closer stacking up section in HST as A/S decreases. LST deposits show decreasing amalgamation as A/S increases. Note the influx of coarse clastics at the top of the Type I interval, supporting Tectonic control of the Sequence.

Greybull section based on the standard marginal marine sequence model (Posamentier and Vail, 1988). The Teapot sandstone represents LST, mudstone dominated continental Meeteetse strata represent TST, and the Lewis Shale represents HST, with the SMF at the Meeteetse-Lewis boundary. The Lewis Shale falls in the Ammonite zone of *baculites jenseni*, placing it in the latest Campanian. Also, an ash bed in the Meeteetse Formation of north-central Wyoming was dated at 74.9 (Love, 1973, K40/Ar40 date). Comparison of the non-marine and marine strata of sequence 3 between sections gives strong support for the model of Zhang et al. (1995). I have placed the S3-S4 boundary at the base of the Lance Formation, consistent with the alloformation boundary of Hicks (1992). As discussed below, Belt and Hicks (1997) identified this boundary as a regional unconformity truncating strata progressively to the west.

Sequence 4

Sequence 4 consists of the Lance Formation. At both Little Buffalo basin and Little Sand Draw the Lance contains basal multistory sandstone interpreted as LST deposits.

Overlying LST deposits, type III ribbon strata that I interpret as TST grade up-section into type II meandering strata that I interpret as HST. The Lance Formation at Greybull contains more evenly spaced channel sandstone units and overbank fines and less distinct sandstone geometries, suggesting a more even rate of accommodation and sedimentation throughout deposition. I have placed the S4-S5 boundary at the base of the Fort Union Formation. Hewett (1926) documented an unconformity at the Lance-Fort Union contact, and the transition from type II geometry in the uppermost Lance to type I

multistory sandstone beds in the lower Fort Union is consistent with the sequence boundary of Zhang et al (1995).

Sequence 5

I have placed the lower and middle Fort Union Formation in S5. Exposures of this sequence are less complete than underlying sequences. At Little Buffalo basin, the major multistory sandstone at gooseberry creek represents LST, and is overlain by a type II-III lenticular interval I interpret as TST deposits. Upper strata of the Fort Union were not exposed at Little Buffalo basin. At Little Sand Draw I have interpreted the closely stacked, smaller scale type I sandstone interval as LST. Less amalgamation and more lenticular geometry of type I sandstone beds suggest a higher A/S ratio here than at Little Buffalo basin, but there is still a noticeable decrease in A/S compared to the underlying Lance Formation (Figure 22). This interval grades up section into smaller, more lenticular, less amalgamated sandstones indicating an increase in A/S. I have interpreted this as initial TST deposits. Incomplete exposures of the middle Fort Union Formation at Little Sand Draw did not allow complete characterization of S5. Also, truncation of the Fort Union Formation at Greybull by the angular unconformity has removed S5.

Sequence 6

Observed only at Greybull and Little Sand Draw, sequence 6 consists of the upper Paleocene interval of the Fort Union Formation. At Little Sand Draw a 20-meter type I sandstone forms the LST of the sequence. Overlying this sandstone, strata change markedly to mudstone and siltstone. Badland style weathering did not allow

characterization of geometry, but the predominance of overbank fines suggests an increased A/S ratio. I have interpreted this interval as TST deposits. At Greybull, sequence 6 directly overlies the angular unconformity forming the contact of the Lance and Fort Union. The base of this interval is marked by closely stacked channel sands with scour surfaces with 1-2 meters relief, indicating a relatively low rate of A/S and is classified as the LST. Overlying this, the sandstone/shale ratio decreases markedly, indicating increased A/S ratio, and several horizons of interconnected type III sandstone horizons are visible, suggesting anastomosing systems and interpreted as TST. Correlation of S6 is based on the palynological data of Nichols (1998).

DISCUSSION

Possible controls on Sequence Architecture

Tectonic activity, eustatic sea level fluctuations, and autocyclic processes such as delta lobe switching are the three primary controls on the rates of accommodation space production and sedimentation considered here. The Absaroka thrust sheet to the west was active throughout deposition of Cretaceous sequences (Jordan, 1981; Wiltschko and Dorr, 1983) and basement-cored uplifts were actively deforming during deposition of the late Cretaceous and Paleocene sequences (Dickinson, 1988, Perry 1992). Eustatic sea level curves show several transgressions and regressions during the time of this study (Haq et al, 1988), and previous studies have attributed Campanian transgressive-regressive cycles to eustatic fluctuations (Hicks, 1992). Also, autocyclic processes are an inherent part of Fluvial/deltaic systems and must be taken into account when interpreting stratal stacking patterns.

The documented tectonic activity of the Absaroka thrust sheet of the time should have an influence on sedimentation in the Montana Group of the Bighorn basin, but actual correlation with thrusting events is difficult due to poor age constraints on thrust events (Jordan, 1981). Also, there is a danger of circular reasoning, since timing of thrust events is commonly determined through dating of synorogenic deposits in proximal basins (Wiltschko and Dorr, 1983). Further complicating this type of correlation is the recent work of Heller et al (1988). Traditional models linking thrust events with foreland basin sedimentation have correlated thrust events with an influx of coarse clastic material into

the basin, whereas periods of tectonic quiescence are associated with lower energy, finer grained environments of deposition.

The major sheet sandstones of the Bighorn basin such as the Teapot sandstone have traditionally been attributed to tectonic rejuvenation to the west (Hewett, 1926, Gill and Coban, 1973). In contrast, Heller et al (1988) modeled the opposite relation between tectonics and foreland deposition. They have linked initial thrusting events with rapid subsidence caused by tectonic loading. This subsidence would result in a high rate of creation of accommodation space, and would trap coarse clastics close to the thrust sheet, where subsidence is most pronounced. As thrusting ceases, subsidence rates would decrease, yielding lower rates of accommodation: coarse clastics would tend to prograde out from the thrust sheet into the more distal parts of the foreland. Erosion of the thrust highland would remove tectonic load, resulting in isostatic rebound and low rates of accommodation. In a non-marine setting this would result in deposition of amalgamated, stacked sheet sandstones (Zhang et al, 1995). Heller et al (1988) argue that proximal to the thrust sheet the traditional model of synorogenic sedimentation would hold, whereas in more distal areas of the basin the exact opposite patterns of sedimentation should be expected. Heller et al (1988) also use the terms proximal and distal only qualitatively, making it difficult to determine which model is appropriate.

Linking eustatic sea level fluctuations to stratigraphic sequences seems more straightforward, but sequences deposited in tectonically active areas will contain tectonic as well as eustatic signatures. The effects of relative sea level change can be clearly seen

in marine to marginal marine sequences, but eustatic control of 3rd order sequences is much more difficult to prove. Relative sea level is a combination of the rates of change of eustatic sea level, subsidence, uplift, and sedimentation. Therefore eustatic control is not required (Shanley and McCabe, 1994). Miall (1990) has shown that chronostratigraphic errors associated with eustatic curves are the same order of magnitude as the span of third order sequences, possibly leading to miscorrelation by several sequence boundaries. Furthermore, global eustatic curves are based on correlation of unconformities across numerous basins, and it may be an exercise in circular reasoning to align sequence boundaries with eustatic curves based on these same unconformities.

Controls of individual sequences

Sequences S1 and S2

Sequences S1 and S2 contain marine strata and are clearly subject to changes in relative sea level, but as discussed above this does not imply eustatic control. Based on ammonite zones of the Cody Shale and Claggett Shale, as well as the documented presence of the Ardmore bentonite in the Claggett Shale in the Bighorn basin (Keefer et. al., 1998) the S1-S2 boundary appears to correspond to the widespread 80 Ma sequence boundary. Several studies to the north in Montana (Rodgers, 1998; Roberts, 1999) have inferred eustatic control of sequence architecture for strata of the 80-ma event. Also, studies of the basal Claggett Shale unconformity corresponding to the S1-S2 sequence boundary identified in this study, indicate that it represents a greater time gap to the south and east, toward more distal parts of the basin (Hicks et al. 1995). This was interpreted by Hicks

et al to indicate sea level control as opposed to tectonic control. The global sea chart of Haq et al (1988) indicates a major regression at 80 Ma and several minor transgressive-regressive events from 75 to 80 ma, which may correspond to the S1-S2 boundary and the progradational parasequences within the Claggett Shale and Mesaverde Formation. Conversely, the interpreted tidally influenced fluvial/deltaic system would be subject to autocyclic processes likely to produce cyclic sedimentation patterns. Whereas the S1-S2 sequence boundary seems to represent at least a regional, if not necessarily global sea level change, the fluctuating paleocurrent trends of the Claggett Shale at Little Sand Draw supports autocyclic control of parasequences.

Sequence 3

Gill and Coban, (1973) interpreted the base of the Teapot Sandstone as a regional unconformity truncating progressively older strata of the underlying Mesaverde Formation to the West. This interpretation was based on the progressive truncation of ammonite zones underlying the Teapot Sandstone. Several studies have disputed the presence of the Teapot unconformity (Johnson et al, 1998), but these studies have traced marker beds over relatively short outcrop distances, whereas the Teapot unconformity documented by Gill and Coban (1973) was found over a distance of 250 miles through the Bighorn and Powder River basins. No obvious angular relationship has been documented on the Teapot unconformity: the minor angular contact of the Teapot unconformity identified by Gill and Coban would not necessarily be identifiable by tracing marker beds. Progressive truncation of strata to the west suggests tectonic uplift to the west.

Krystinik and DeJarnett (1995) noted that the Bearpaw transgression of Montana corresponded with synchronous subareal exposure in the Bighorn basin as represented by the Teapot-Ericson unconformity. They argued that regional tectonic forces were the primary control of sequence architecture in Wyoming during deposition of the Teapot Sandstone. In southern Wyoming, seismic lines show clear evidence of structural uplift and truncation below the correlative Ericson Sandstone (Krystinik and DeJarnett, 1995), supporting tectonic control of the S2-S3 sequence boundary in the Bighorn basin. The eastward thinning trend and the coarsening upward profile of the Teapot Sandstone are consistent with a prograding clastic wedge caused by tectonic rejuvenation of a source area to the west. The latest Campanian age of *baculites jenseni* in the Lewis shale (Gill and Coban, 1973; Obradovitch, 1993) of S3 places the underlying Teapot sandstone in the Middle to Early Campanian. Hicks (1992) attributed the Teapot sandstone to forebulge uplift during active thrusting to the west. Wiltschko and Dorr (1983) identify a thrust event of the Absaroka thrust sheet at 78 Ma, but lacking age constraints on the S2-S3 boundary, correlation is not possible.

Sequence 4

The Lance-Meeteetse contact has been documented as a regional unconformity similar to the Teapot unconformity. This unconformity has a larger hiatus toward the west, and becomes angular at the correlative Harebell-Meeteetse contact north of Jackson Hole, Wyoming indicating tectonic control (Belt et al, 1997). A provenance shift in Lance and Fort Union strata at Greybull further supports tectonic control of the Lance Formation.

Belt et al (1997) dated the lower Lance Formation near Little Buffalo basin at 67.9 Ma, and underlying Meeteetse Formation sediments at 70.4 Ma based on isotopic and geomagnetic data. This time period closely postdates to the main movement of the Absaroka thrust sheet at 70.5 Ma (Wiltschko and Dorr, 1983), suggesting tectonic control of the sequence. Previous studies also indicate structural definition of the area during deposition of the Lance Formation. Gillespie and Fox (1991) attributed aerial variations in fluvial geometries of the Lance Formation in the Wind River basin to varying rates of subsidence during initial structural definition of the basin

Sequence 5

Conglomerate intervals of the Fort Union Formation have been attributed to uplift of the Washakie range (Roberts et al, 1991; Seeland 1998), the Basin Creek Range (Krauss, 1985) and the Sevier thrust belt (Hicks, 1992). Wiltschko and Dorr (1983) dated final movement of the Absaroka thrust sheet at 65 Ma, corresponding reasonably well with the early Mastication-Paleocene S4-S5 sequence boundary. Conversely, an angular relation between the Cretaceous Harebell conglomerate and the Cretaceous-Paleocene Pinion conglomerate has been attributed to uplift of the Washakie range (Love, 1973). I did not identify any provenance change associated with the S4-S5 boundary, suggesting that uplift of the Washakie range was not extensive enough to expose Precambrian core material to erosion during deposition of S5. Roberts et al (1991) interpreted matrix supported conglomerates in the Fort Union near Grass Greek as debris flow deposits. This interpretation suggests influence of the Washakie Uplift on S5, since it is more

proximal than the Absaroka thrust sheet. Tectonic control of S5 seems evident, but it is not possible to attribute control to any single uplift with the available data. Evidence suggests numerous coeval uplifts, which probably all had some influence on sedimentation in S5.

Upper Fort Union strata of S5 at Little Buffalo basin conform closely to the recent interpretations of Krauss (1999) in the northern bighorn basin. She described the type III ribbon deposits of the Fort Union Formation (S5-S6) as anastomosing river deposits formed as a result of major avulsion events, giving a wholly autocyclic explanation for variations in fluvial stacking patterns. Figure 35 shows the upper Fort Union outcrop at Little Buffalo basin with major sandstone beds highlighted. Sandstone stacking patterns in this interval reveal a multistory channel system surrounded by isolated lenticular sandstones consistent with the anastomosing avulsion deposits described by Krauss (1999). This outcrop clearly shows autocyclic control of geometry on outcrop scale, with a multistory channel sandstone surrounded by laterally equivalent type III ribbon deposits. As explained by Zhang et al (1997), an increasing rate of accommodation will result in rapid aggradation and lowered gradients, favoring formation of low energy anastomosing river systems. Rapid aggradation of anastomosing channels will result in avulsion and channel abandonment. Whereas autocyclic processes control the fine scale geometry of the interval, allocyclic forces probably drove the transition from the underlying 110-meter multistory interval to the overlying type III interval.

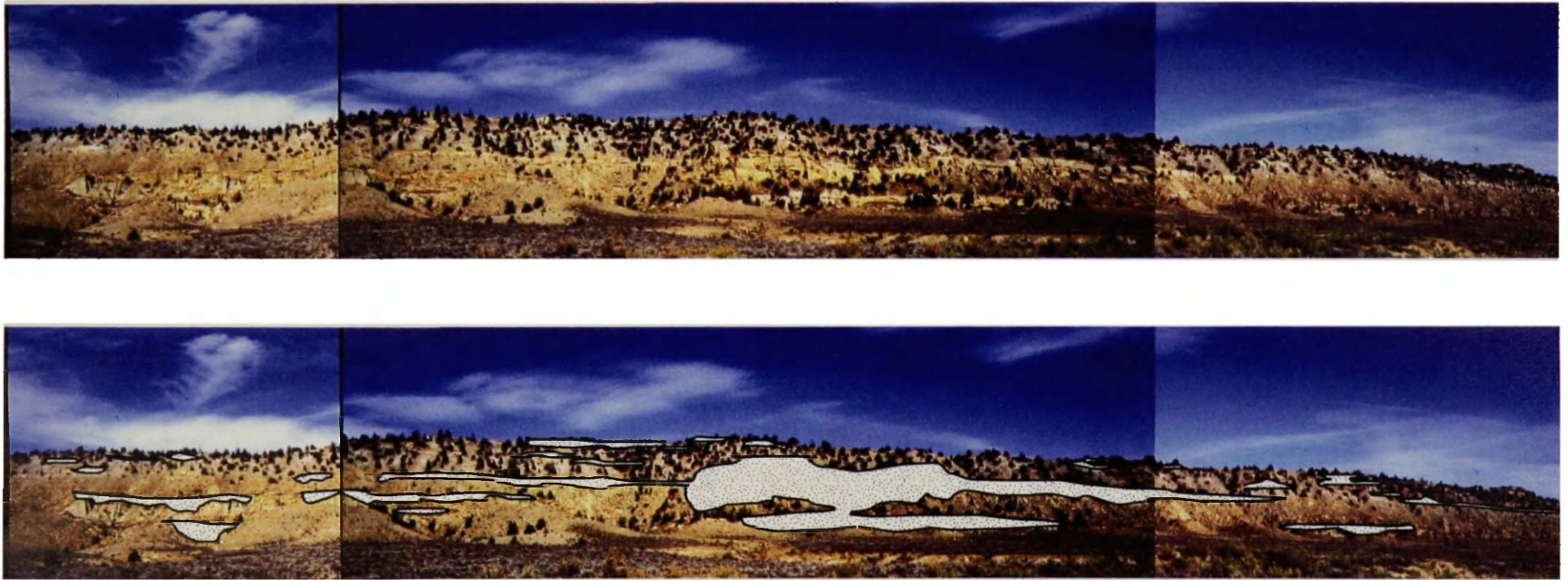


Figure 35: Trace of sandstone beds in the middle Fort Union Formation at Little Buffalo Basin. This ridge illustrates the lateral variability of fluvial deposits, with a multistory channel complex surrounded by type III lenticular geometry. See the Huckleberry Ridge sections on Plate 4 for detailed stratigraphic sections of this outcrop.

Sequence 6

Sequence 6 shows clear evidence of tectonic control in the form of the angular unconformity that forms the S5-S6 sequence boundary at Greybull. Further evidence of tectonic control is given in provenance data and paleocurrent trends discussed below.

Evidence for uplift of the Ancestral Bighorn Range

Whipkey et al. (1991) found petrologic evidence of exposure and erosion of the Precambrian core of the Bighorn range by late Paleocene. Hoy and Ridgeway (1998) inferred that initial uplift began earlier. They estimate an average of 6.46 km of uplift and 4.6 km of shortening along the eastern front of the range by the end of Lebo Shale deposition in the mid-Paleocene. They attribute deposition of the Lebo Shale member of the Fort Union Formation in the Powder River basin to erosion and redeposition of the soft, poorly lithified Mesozoic cover of the Bighorns. Hansley and Brown have inferred initial uplift of the Bighorns in earliest Paleocene, citing petrological evidence of an unroofing sequence in the Tullock Member of the Fort Union Formation of the Powder River basin. Deposits of the uppermost Lance Formation in the Bighorn basin may represent a similar unroofing event.

As mentioned above, the Greybull at the S5-S6 boundary clearly indicates tectonic uplift. Paleocurrent data directly underlying the angular unconformity indicate flow to the north-northwest along the basin axis, suggesting that the Bighorn basin had already been structurally defined by this time (Figure 24). Sandstone in this interval consists of well-rounded, texturally and compositionally mature quartz arenites, suggesting either long transport distances or a second cycle sedimentary source terrain. Given the paleocurrent

trend at Greybull away from the present day location of the Bighorn Range, the preferred interpretation here is a second-cycle source area. Strata directly underlying the angular unconformity at Greybull have been placed with the Cretaceous Lance Formation, but recent palynological data (Nichols, 1998) have indicated an earliest Paleocene age. The overlying sequence 6 has been dated as late Paleocene, constraining formation of the unconformity to Paleocene. The angular unconformity may be an extension of the Sheep Mountain anticline, a secondary structural uplift associated with the Bighorn uplift and located to the northeast. The main west-dipping fault of the central Bighorn uplift runs along the eastern front of the range (Hoy and Ridgeway, 1998), and initiation of uplift along main faults to the east may predate formation of the Sheep Mountain anticline. Based on paleocurrent and petrologic trends observed at Greybull, I interpret the uppermost Lance strata to record initial uplift, unroofing and redeposition the Mesozoic strata overlying the incipient Bighorn uplift.

Provenance and paleocurrent data from sequence 6 suggest further uplift of the Bighorn range. Sequence 6 consists of the Late Paleocene Fort Union Formation at Greybull and Little Sand Draw. Paleocurrent trends for this sequence indicate flow to the west at Greybull. A marked increase in feldspar content (Figure 28), as well as the presence of granitic fragments suggests a plutonic source. I interpret these trends to reflect uplift and exposure of the Precambrian core of the Bighorns to the east. On the western side of the basin, previous studies (Krauss, 1985) documented continued eastward flow and deposition of quartzite conglomerates into the Eocene, indicating continued erosion of reworked sedimentary strata. Paleocurrent trends at Little Sand Draw indicate flow to the

southeast, and sandstone compositions are similarly enriched in feldspar and granitic fragments as observed at Greybull (Figure 27, 31). The presence of glauconite and reworked quartz grains at Little Sand Draw reflect a second cycle source of marine strata. I interpret these trends to represent deflection of drainages to the south around the Bighorn Uplift. Provenance trends reflect clastic input from valleys draining the western slope of the Bighorn range and eroding the Precambrian core and Paleozoic sedimentary strata.

Drainage patterns of the southern Bighorn basin have been the source of continuous discussion. A southern drainage out of the Bighorn basin during Paleocene time was suggested by Love (1988), Bown (1980) and Lillegraven and Ostrech (1988).

Conversely, in a recent paleogeographic study, Seeland (1998) proposed drainage to the north out of the basin based on the smoothed vector mean paleocurrent data of several workers. Seeland noted however, that paleocurrent data obtained by him and S.B. Roberts (Seeland, 1998, p. 146) indicated a southeastern flow. It is unclear from his discussion whether these data were included in the vector calculation, but south trending vectors are not illustrated in his unsmoothed data set.

The unconformity documented at Greybull and on the western side of the basin at Hamilton dome (Hewett, 1926) should be taken into account when considering paleodrainage patterns. The angular relationship of the unconformity at Greybull indicates presence of at least a local paleohigh in the area, and truncation of up to 500 meters of strata to the west (Hewett, 1926) may indicate an east-west topographic high across the central part of the basin. Deposition appears to be continuous in the southern

part of the basin (Johnson et al, 1998), and rapid subsidence in the northern Wind River basin formed Lake Waltman during this time (Flemmings and Nelson, 1991). Inferred uplift to the north and concomitant subsidence to the south is consistent with a southern drainage of the Bighorn basin during Late Paleocene.

CONCLUSIONS

Based on lithofacies trends of measured stratigraphic columns I have identified six sequences in the upper Cretaceous and Paleocene strata of the Bighorn basin.

Comparison of non-marine sequences with laterally equivalent marine sequences supports the non-marine model of Zhang et al. (1995). Furthermore, agreement between sequences S4 – S6 and the geometry predicted by the model of sequences Zhang et al (1995) gives a clear example of tectonically driven sequence architecture with no evidence of sea level influences. Based on lithofacies, provenance, and paleocurrent trends of these sequences, in conjunction with recently improved age constraints on sequence boundaries I conclude the following:

- 1) Sequences S1 and S2 record relative sea level control. The S1-S2 sequence boundary is widely recognized in the Cordilleran foreland basin and represents a regional relative sea level change. Allocyclic forces may influence parasequences within the Claggett Shale of S2, but paleocurrent trends suggest autocyclic control. Provenance and paleocurrent data indicate eastward flow into the basin from a sedimentary source, with minor volcanic input in the northern part of the basin

- 2) Sequences S3 - S5 were controlled by tectonic events to the west of the Bighorn basin. The S2-S3 boundary shows characteristics of tectonic control, but cannot be correlated to a specific tectonic event. The S3-S4 sequence boundary corresponds closely to major movement of the Absaroka thrust sheet at 70.5 Ma whereas S5 is likely controlled by uplift of the Washakie Range. S4 and S5 show an increase in lithic fragments at Little Buffalo basin, consistent with the quartzite conglomerate lags present in the Lance and Fort Union formations.

- 3) S5 and S6 provide evidence of the Bighorn Uplift. Paleocurrent and provenance data of S5 indicate flow along the Bighorn basin axis at Greybull, and initial unroofing of the bighorn uplift by early Paleocene. Paleocurrent and provenance data of S6 indicate exposure and erosion of the Precambrian core and diversion of drainage systems by late Paleocene.

Formation	Section	Tape #	Tape L (m)	Tp Azim	Slp ang	Slp dir	Bd Strk	Bd Dip	Dip Dir	True Thck Same. Dir.	True Thck Opp. Dir.
Cody	LSD	4-6	116	47	3	ne	125	14	ne	21.5	33.3
Meeteetse	LSD	4-50a	22	145	8	se	120	24	ne	0.9	6.5
Meeteetse	LSD	4-50(total)	540	32	2	ne	120	24	ne	202.1	236.5
Meeteetse	LSD	4-51	46	75	22	ne	120	22	ne	4.7	27.3
Meeteetse	LSD	4-52	38	0	0	na	119	22	ne	12.5	12.5
Meeteetse	LSD	4-56	40	12	5	ne	119	22	ne	11.0	17.5
Meeteetse	LSD	4-58	24	12	20	ne	119	22	ne	0.5	15.7
Meeteetse	LSD	4-61a	480	46	5	ne	119	22	ne	132.5	210.0
Meeteetse	LSD	4-61b	318	25	4	sw	119	22	ne	98.0	139.1
Meeteetse	LSD	5-12	24	17	2	sw	120	20	ne	7.2	8.8
Lance	LSD	2-45a	17.6	2	0	na	120	22	ne	5.8	5.8
Lance	LSD	2-45b	18	21	22	ne	120	22	ne	0.1	12.4
Lance	LSD	2-46a	25	92	1	e	121	22	ne	4.1	4.9
Lance	LSD	2-46b	17.3	75	0	na	121	22	ne	4.7	4.7
Lance	LSD	2-61a	25	19	20	ne	121	20	ne	0.2	15.9
Lance	LSD	2-61b	25	32	0	na	121	20	ne	8.5	8.5
Lance	LSD	2-61c	18	35	12	ne	123	22	ne	3.1	10.1
Lance	LSD	2-61d	31	27	6	ne	123	22	ne	8.5	14.5
Lance	LSD	2-62a	24	30	0	na	123	22	ne	9.0	9.0
Lance	LSD	2-62b	25	20	5	ne	123	22	ne	7.1	11.1
Lance	LSD	2-62c	24	23	0	na	123	22	ne	8.9	8.9
Lance	LSD	2-63	15	3	10	e	117	22	ne	2.6	7.5
Lance	LSD	2-64a	25	31	15	ne	115	22	ne	3.0	15.0
Lance	LSD	2-64b	25	351	0	na	115	22	ne	7.8	7.8
Lance	LSD	2-64c	29	348	0	na	115	22	ne	8.7	8.7
Cody	LBB	1-55a	412	15	3	ne	160	15	ne	40.3	81.9
Mesaverde	LBB	1-55b	560	150	5	se	160	15	ne	22.1	72.2
Mesaverde	LBB	1-56	570	292	1	se	160	12	ne	78.3	97.8
Mesaverde	LBB	1-68	21.5	155	0	na	170	22	ne	2.1	2.1
Meeteetse	LBB	5-17a	336	132	2	se	165	12	ne	26.5	49.5
Meeteetse	LBB	5-17b	475	136	4	se	165	12	ne	15.3	80.1
Meeteetse	LBB	5-17c	516	144	3	se	165	12	ne	12.0	64.8
Lance	LBB	5-1	470	74	11	ne	165	12		8.2	183.6
Lance	LBB	5-14a	780	149	2	ne	165	12	ne	18.0	71.3
Lance	LBB	5-14b	560	154	0	na	165	12	ne	22.2	22.2
Lance	LBB	5-15	188	68	8	ne	165	12	ne	12.8	64.0
Lance	LBB	5-16	750	115	2	se	165	12	ne	93.7	144.9
Fort Union	LBB	1-36a	500	45	2	ne	125	10	ne	68.3	102.6
Fort Union	LBB	1-36b	194	74	5	sw	125	10	ne	9.4	42.7
Fort Union	LBB	1-37	50	65	12	sw	125	10	ne	2.9	17.6
Fort Union	LBB	1-41	50	80	14	w	125	10	ne	6.0	17.9
Meeteetse	LBB	2-42	11.5	199	19	sw	126	16	ne	0.7	6.5
Meeteetse	LBB	2-43	28	170	16	se	126	16	ne	2.3	12.6
Meeteetse	LBB	2-28a	25	72	0	na	0	13	e	5.3	5.3
Meeteetse	LBB	2-28b	25	69	0	na	0	13	e	5.2	5.2
Meeteetse	LBB	2-28c	25.5	75	6	ne	0	13	e	2.9	8.1
Meeteetse	GB	3-28	100	102	0	na	170	33.6	w	51.3	51.3
Meeteetse	GB	3-40	68	190	20	n	160	35	sw	0.7	37.4
Meeteetse	GB	3-41	26	270	30	e	170	32	sw	0.7	22.8
Meeteetse	GB	3-43	24	240	4	sw	160	35	sw	12.1	14.9
Meeteetse	GB	3-45a	34	211	0	na	170	32	w	11.8	11.8
Meeteetse	GB	2-45b	34	270	30	e	170	32	w	1.0	29.8

Appendix I. Trigonometric thickness corrections of measured covered intervals. Chart tabulates tape length, tape azimuth, tape plunge, plunge direction, bedding strike, bedding dip, and dip direction. Corrected thickness depends on whether plunge and dip are in the same, or opposite directions.

Sample#	Formation (Location)	Q m	Q p	Cht.	K	P	Lv	Lslt	Lmsed	Lm	Lunid	bt	ms	chl	heav.	Co3	Matr.	Por	Lp	Unid T	Total
SD-2	Mesaverde (LSD)	248	12	23	35	3	6	24	23	1	7	1	1	0	0	38	70	59	0	8	559
LB-2	Mesaverde (LBB)	323	22	23	8	6	25	6	3	0	9	0	0	0	0	18	53	102	1	3	602
LB-3	Mesaverde (LBB)	253	14	25	19	9	8	1	8	2	5	0	3	0	0	85	60	77	2	6	577
GB-3	Mesaverde (GB)	203	7	53	45	24	15	25	39	8	8	8	0	0	1	0	52	90	5	7	590
GB-1	Mesaverde (GB)	261	16	63	16	25	15	16	23	0	13	0	0	0	0	0	34	111	4	14	611
GB-4	Teapot (GB)	238	9	75	51	42	20	1	21	2	12	1	0	0	1	0	14	153	3	10	653
SD-3	Teapot (LSD)	208	11	26	19	1	9	69	20	1	3	1	2	0	0	0	126	33	0	4	533
SD-4	Teapot (LSD)	239	11	86	16	0	0	15	44	1	7	0	2	0	0	0	77	69	0	2	569
SD-25	Teapot (LSD)	217	16	50	22	0	11	28	16	13	8	1	0	19	0	1	89	44	4	5	544
LB-7	Teapot (LBB)	279	22	31	16	1	16	42	15	3	6	2	5	1	3	0	46	62	5	7	562
LB-10	Meeteetse (LBB)	290	10	39	23	4	35	6	6	1	6	1	2	0	2	0	52	98	0	23	598
LSD-3	Lance (LSD)	308	13	47	17	4	14	4	25	0	9	1	1	0	2	0	42	132	0	13	632
LSD-1	Lance (LSD)	307	19	37	21	12	9	6	18	3	7	3	6	0	0	0	37	134	7	7	633
LSD-6	Lance (LSD)	301	14	35	16	6	7	9	0	8	2	3	1	0	0	7	82	80	3	6	580
RSL-20	Lance (LBB)	192	15	71	46	6	34	5	26	9	3	1	3	0	2	11	61	94	6	9	594
GB-12	Lance (GB)	433	9	29	0	4	1	2	6	0	0	0	1	0	0	0	13	123	0	2	623
GB-9	Lance (GB)	345	8	52	0	0	0	21	10	0	0	0	3	0	0	1	58	98	0	2	598
GB-5	Lance (GB)	261	4	39	32	57	8	4	19	2	3	4	2	2	1	0	52	97	4	6	597
LSD2-2	Fort Union (LSD)	235	15	69	28	23	14	5	21	4	9	4	0	0	2	7	53	139	10	1	639
LSD-8	Fort Union (LSD)	356	12	72	12	0	6	0	15	1	3	0	1	3	0	0	17	121	1	1	621
UFU-2	Fort Union (LSD)	394	25	39	2	0	14	0	14	0	4	0	0	0	0	0	6	148	1	1	648
UFU-20	Fort Union (LSD)	228	7	54	52	49	5	10	5	3	7	5	2	0	0	2	57	107	7	7	607
UFU-21	Fort Union (LSD)	248	10	26	27	27	4	12	8	7	9	6	2	8	1	7	83	32	7	8	532
UFU-3	Fort Union (LSD)	206	9	40	55	86	12	4	2	0	4	4	0	1	0	7	63	58	2	5	558
RS-5	Fort Union (LBB)	210	9	73	30	15	6	24	44	2	4	3	1	0	3	9	59	71	3	5	571
RS-7	Fort Union (LBB)	205	9	49	59	27	13	22	35	1	7	3	3	1	2	1	60	78	0	3	578
RS-6	Fort Union (LBB)	243	14	67	37	7	4	27	26	0	5	0	1	0	0	6	55	81	2	6	581
RS-4	Fort Union (LBB)	231	12	52	37	23	31	5	13	5	7	8	2	2	2	3	49	100	13	5	600
GB-11	Fort Union (GB)	207	6	54	51	96	6	19	8	0	2	3	3	2	1	0	28	107	8	6	607
GB-13	Fort Union (GB)	215	10	37	44	68	8	18	14	0	4	9	2	0	2	3	55	80	2	9	580

Appendix II. Sandstone point count data. Qm = monocrystalline quartz, Qp = polycrystalline quartz, Cht = chert, K = potassium feldspar, P = plagioclase feldspar, Lv = lithic volcanic grains, Lslt = siltstone intraclasts, Lmsed = metasedimentary grains, Lm = metamorphic grains, Unid L = unidentified lithic grains, ms = muscovite, bt = biotite, chl = chlorite, heav. = accessory minerals, CO3 = Carbonate grains (diagenetic), Matr. = Matrix, Por = porosity, Lp = lithic plutonic grains, Unid = unidentified non-lithic grains. See sandstone petrology methods section for descriptions of categories.

Recalculated Modal Compositions of Sandstone Samples								
Sample#	Formation (Location)	QM	F	LT		QM	P	K
SD-2	Mesaverde (LSD)	69.3	10.6	20.1		86.7	1.0	12.2
LB-2	Mesaverde (LBB)	77.1	3.3	19.6		95.8	1.8	2.4
LB-3	Mesaverde (LBB)	73.8	8.2	18.1		90.0	3.2	6.8
GB-3	Mesaverde (GB)	50.5	17.2	32.3		74.6	8.8	16.5
GB-1	Mesaverde (GB)	60.4	9.5	30.1		86.4	8.3	5.3
GB-4	Teapot (GB)	50.6	19.8	29.6		71.9	12.7	15.4
SD-3	Teapot (LSD)	69.8	6.7	23.5		91.2	0.4	8.3
SD-4	Teapot (LSD)	59.2	4.0	36.9		93.7	0.0	6.3
SD-25	Teapot (LSD)	61.5	6.2	32.3		90.8	0.0	9.2
LB-7	Teapot (LBB)	71.7	4.4	23.9		94.3	0.3	5.4
LB-10	Meeteetse (LBB)	70.0	6.5	23.4		91.5	1.3	7.3
LSD-3	Lance (LSD)	70.5	4.8	24.7		93.6	1.2	5.2
LSD-1	Lance (LSD)	70.7	7.6	21.7		90.3	3.5	6.2
LSD-6	Lance (LSD)	77.4	5.7	17.0		93.2	1.9	5.0
RSL-20	Lance (LBB)	47.8	12.9	39.3		78.7	2.5	18.9
GB-12	Lance (GB)	89.8	0.8	9.3		99.1	0.9	0.0
GB-9	Lance (GB)	83.1	0.0	16.9		100.0	0.0	0.0
GB-5	Lance (GB)	61.4	20.9	17.6		74.6	16.3	9.1
LSD2-2	Fort Union (LSD)	56.2	12.2	31.6		82.2	8.0	9.8
LSD-8	Fort Union (LSD)	74.6	2.5	22.9		96.7	0.0	3.3
UFU-2	Fort Union (LSD)	80.1	0.4	19.5		99.5	0.0	0.5
UFU-20	Fort Union (LSD)	55.6	24.6	19.8		69.3	14.9	15.8
UFU-21	Fort Union (LSD)	67.8	14.8	17.5		82.1	8.9	8.9
UFU-3	Fort Union (LSD)	49.8	34.1	16.2		59.4	24.8	15.9
RS-5	Fort Union (LBB)	53.4	11.5	35.1		82.4	5.9	11.8
RS-7	Fort Union (LBB)	50.7	21.3	28.0		70.4	9.3	20.3
RS-6	Fort Union (LBB)	60.3	10.9	28.8		84.7	2.4	12.9
RS-4	Fort Union (LBB)	56.2	14.6	29.2		79.4	7.9	12.7
GB-11	Fort Union (GB)	48.1	34.2	17.7		58.5	27.1	14.4
GB-13	Fort Union (GB)	53.8	28.0	18.3		65.7	20.8	13.5

Appendix III. Recalculated Modal compositions of sandstone samples. Formulae for calculating modal compositions from raw data are listed below. See appendix I for definitions of abbreviations.

Qm-F-Lt:	
%Qm	$\%Qm = Qm / (Qm + Qp + Cht + P + K + Lv + Lmsed + Lm + Lp + Lunid) * 100$
%F	$\%F = P + K / (Qm + Qp + Cht + P + K + Lv + Lmsed + Lm + Lp + Lunid) * 100$
%Lt	$\%Lt = (Qp + Cht + Lv + Lmsed + Lm + Lp + Lunid) / (Qm + Qp + Cht + P + K + Lv + Lmsed + Lm + Lp + Lunid) * 100$
Qm-P-K:	
%Qm	$\%Qm = Qm / (Qm + P + K) * 100$
%P	$\%P = P / (Qm + P + K) * 100$
%K	$\%K = K / (Qm + P + K) * 100$

Standard Deviations of Multiple Counts												
Sample#		QM	F	LT		QP	LV	LSM		QM	P	K
GB-12		89.8	0.8	9.3		84.4	2.2	13.3		99.1	0.9	0.0
GB-12		90.8	0.0	9.2		74.1	11.1	14.8		100.0	0.0	0.0
Standard Deviations		0.7	0.6	0.1		7.3	6.3	1.0		0.6	0.6	0.0
LB-2		77.1	3.3	19.6		61.6	34.2	4.1		95.8	1.8	2.4
LB-2		75.4	5.7	18.9		66.2	9.5	24.3		92.9	2.5	4.5
Standard Deviations		1.2	1.7	0.5		3.2	17.5	14.3		2.1	0.5	1.5
GB-13		48.5	28.8	22.7		46.3	29.6	24.1		62.7	23.4	13.9
GB-13		51.1	28.2	20.7		51.9	36.4	11.7		64.4	21.1	14.5
GB-13		55.3	27.1	17.6		54.0	38.1	7.9		67.1	20.7	12.1
GB-13		53.8	28.0	18.3		68.1	11.6	20.3		65.7	20.8	13.5
Standard Deviations		3.0	0.7	2.3		9.3	12.1	7.5		1.9	1.3	1.0
UFU-3		45.6	22.5	31.9		53.4	12.1	34.5		66.9	16.5	16.5
UFU-3		46.4	28.4	25.1		60.0	18.0	22.0		62.0	19.6	18.4
UFU-3		51.6	18.7	29.7		57.7	12.5	29.8		73.4	11.4	15.2
UFU-3		48.5	25.3	26.1		82.3	12.9	4.8		65.7	19.7	14.6
UFU-3		51.0	25.4	23.6		69.6	15.2	15.2		66.8	17.8	15.4
Standard Deviations		2.7	3.7	3.4		11.5	2.5	11.8		4.1	3.4	1.5

Appendix IV. Standard deviations of multiple counts. Standard deviations of quartzose samples (GB-12, LB-2) are generally less than 2%. Standard deviations of more feldspar-lithic rich samples (GB-13, UFU-3) are higher, up to 4%. The maximum values from GB-13 and UFU-3 were used to calculate error bars on ternary plots. Because of the high values of standard deviations of Qp-Lv-Ls compositions tabulated above, lithic content was discussed only qualitatively.

BIBLIOGRAPHY

Belt, E. S., Hicks, J. F., and Murphy, D. A., 1997, A pre-Lancian regional unconformity and its relationship to Hell Creek paleogeography in southeastern Montana. *Contributions to Geology*, University of Wyoming, v. 31, no. 2, p. 1-26.

Borrell, J.K., 1999, Sedimentary record of Upper Cretaceous through Tertiary tectonism, northeastern Crazy Mountains basin, central Montana. Unpublished masters thesis, University of Montana, Missoula.

Bown, T.M., 1980, Summary of latest Cretaceous and Cenozoic sedimentary, tectonic, and erosional events, Bighorn basin, Wyoming. *Papers on Paleontology*, 24, p. 25-32.

Burns, B. A., Heller, P. L., Marzo, M., and Paola, C., 1997, Fluvial response in a sequence stratigraphic framework: Example from the Monserrat fan delta, Spain. *Journal of Sedimentary Research*, v. 67, n. 2, p. 311-32.

Cant, D. J., 1982, Fluvial Facies Models and their application. In: Scholle, P. A and Spearing, D., eds., Sandstone Depositional Environments, AAPG Memoir 31.

Coleman J. M., and Prior, D.B., 1982, Deltaic environments of deposition. In: Scholle, P.A and Spearing, D., eds., Sandstone Depositional Environments, AAPG Memoir 31.

Connor, C. W., 1992 "The Lance Formation – petrography and stratigraphy, Powder River basin and nearby basins, Wyoming and Montana. U.S.G.S. Bulletin 1917-I.

Courdin, J. L., and Hubert, J. F., 1969 Sedimentology and mineralogical differentiation of sandstones in the Fort Union Formation (Paleocene). Wind River basin, Wyoming. In: 2nd Symposium on Tertiary rocks of Wyoming; Wyoming Geol. Assoc., 21st Field Conf., 1969, Guidebook.

Dickinson, W. R., Suczek, C. A., 1979, Plate tectonics and sandstone composition. *The American Association of Petroleum Geologists Bulletin*, v. 63, n. 12, p. 2164 – 2182.

Dickinson, W. R., 1970, Interpreting detrital modes of greywacke and arkose. *Journal of Sedimentary Petrology*, v. 40; 2, pp. 695-707.

Dickinson, W. R., 1985 Interpreting provenance relations from detrital modes of sandstones. In: Zuffa G.G., ed., Provenance of Arenites. p. 331-336.

Dickinson, W. R., Lawton, T. F., and Inman, K. F., 1986, Sandstone detrital modes, central foreland region: Stratigraphic record of Cretaceous-Paleogene tectonic evolution. *Journal of Sedimentary Petrology*, v. 56, p. 276-293.

Dickinson, W. R., Klute, M. A., Hays, M. J., Janecke, S. U., Lundin, E. R., McKittrick, M. A., and Olivares, M. D., 1988, Paleogeographic and paleotectonic settings of Laramide sedimentary basins in the Central Rocky Mountain region. *Geological Society of America Bulletin*, v. 100, p. 1023-1039.

Flemmings, P. B. and Nelson, S. N., 1991, Paleogeographic evolution of the Latest Cretaceous and Paleocene Wind River basin. *The Mountain Geologist*, v.28, no. 2/3, p. 37-52.

Folk, R. L., 1980, Petrology of sedimentary rocks. Hemphill Publishing Co., Austin, Texas, 78703.

Gill, J. R., and Coban, W. A., 1973, Stratigraphy and Geologic History of the Montana Group and Equivalent rocks, Montana, Wyoming, and North and South Dakota. U.S. Geological Survey Professional Paper 776, 37 p.

Gillepsie, J. M. and Fox, J. E., 1991, Tectonically influenced sedimentation in the Lance Formation, eastern Wind River basin, Wyoming. *The Mountain Geologist*, v.28, no. 2/3, p. 53-66.

Gries, R., Dolson, J. C., and Reynolds, R. G. H., 1992, Structural and stratigraphic evolution and hydrocarbon distribution, Rocky Mountain Foreland. In: Macqueen, R.W., and Leckie, D.A., eds., Foreland basins and Fold Belts, AAPG Memoir 55, p. 395-425.

Hansley, P. L., and Brown, J. L., 1993, Provenance of the Tullock Member of the Fort Union Formation, Powder River basin, Wyoming and Montana: Evidence for Early Paleocene Laramide Uplift. *The Mountain Geologist*, v. 30, no. 1, p.25-35.

Haq, B. U., Hardenbol, T., and Vail, P. R., 1988, Mesozoic and Cenozoic chronostratigraphy and cycles of sea level change. In: Wilgus C. K, Hastings, B. S., Kendall, C. G. St. C., Posamentier, H. W., Ross, C. A., Van Wagoner, J. C., eds., Sea-Level Changes – an Integrated Approach, SEPM Special Publication No. 42.

Heller, P. L., Angevine, C. L., and Winslow, N. S., 1988, Two-Phase stratigraphic model of foreland basin sequences. *Geology*, v. 16 p. 501-504.

Hewett, D. F., 1926, Geology and oil and gas resources of the Oregon basin, Meeteetse, and Grass Creek quadrangles, Wyoming. U.S. Geological Survey Professional Paper 145, 111p.

Hicks, J. F., Obradovich, J. D., and Tauxe, L., 1995, A new calibration for the Late Cretaceous time scale: the $^{40}\text{Ar}/^{39}\text{Ar}$ isotopic age of the C33r/C33n geomagnetic reversal from the Judith River Formation (Upper Cretaceous), Elk basin, Wyoming, USA. *Journal of Geology*, v. 103, p. 243-256.

Hicks, J. F., and Tauxe, L., The Sequence stratigraphy of the Latest Cretaceous sediments of northern Wyoming: The interplay between tectonic and eustatic controls on foreland basin sedimentation. *GSA Abstracts with Programs*, 1992, p. A110.

Hoy, R. G., and Ridgeway, K. D., 1998, Structural and Sedimentological development of Footwall growth synclines along an intraforeland uplift, east-central Bighorn Mountains, Wyoming. *GSA Bulletin*, v. 110, n. 2 p. 284.

Jordan, T. E., 1981, Thrust loads and foreland basin evolution, Cretaceous, western United States. *AAPG Bulletin*, v. 65, n. 12, p. 2506-2520

Johnson, R. C., Keefer, W. R., Keighin, C. W., and Finn, T. M., 1997, Deposition of the upper Cretaceous Lance Formation in central Wyoming. *AAPG Bulletin*, 81, 7, p. 1226.

Johnson, R. C., Keefer, W. R., Keighin, C. W., and Finn, T. M., 1998 Detailed outcrop studies of the upper part of the upper Cretaceous Cody Shale, Mesaverde, Meeteetse, and Lance formations. In: Keefer, W.R. and Goolsby, J.E., eds., Cretaceous and Lower Tertiary rocks of the Bighorn basin, Wyoming and Montana., 49th Guidebook of the Wyoming Geological Association, 1998.

Keefer, W. R., Finn, T. M., Johnson, R. C., and Keighin, C. W., 1998, Regional stratigraphy and correlation of Cretaceous and Paleocene rocks. In: Keefer, W.R. and Goolsby, J.E., eds., Cretaceous and Lower Tertiary rocks of the Bighorn basin, Wyoming and Montana., 49th Guidebook of the Wyoming Geological Association, 1998.

Keighin, C. W., 1998, Petrography of selected upper Cretaceous sandstones. In: Keefer, W.R. and Goolsby, J.E., eds., Cretaceous and Lower Tertiary rocks of the Bighorn basin, Wyoming and Montana., 49th Guidebook of the Wyoming Geological Association, 1998.

Krauss, M. J., 1985, Early Tertiary quartzite conglomerates of the Bighorn basin and their significance for paleogeographic reconstruction of Northwest Wyoming. " In: Flores, R.M. and Kaplan, S.S., eds.,

Cenozoic Paleogeography of West-Central United States. The Rocky Mountain section, Society of Economic Paleontologists and Mineralogists, Denver, Colorado, 1985.

Krauss, M. J., and Wells, T. M., 1999, Facies and facies architecture of Paleocene floodplain deposits, Fort Union Formation, Bighorn basin, Wyoming. *The Mountain Geologist*, v. 36, no. 2, p. 57-70.

Kval, E. P. and Vondra, C. F., 1993 Effects of relative sea level changes and local tectonics on a Lower Cretaceous fluvial to transitional marine sequence, Bighorn basin, Wyoming, USA. In: Alluvial Sedimentation, Special publication number 17 of the international association of sedimentologists, Blackwell Scientific Publications, Oxford, Great Britain.

Lillegraven, J. A., and Ostrech, L. M., Jr., 1988, Evolution of Wyoming's early Cenozoic topography and drainage patterns. *Journal of Vertebrate Paleontology*, v. 7, n. 3, p.19

Love, J. D., 1973, Harebell Formation (Upper Cretaceous) and Pinyon Conglomerate (Uppermost Cretaceous and Paleocene), northwestern Wyoming. U.S.G.S. Professional Paper n. 734-A, 54 p.

Love J. D., and Christiansen, A. C., 1985, Geologic Map of Wyoming. U.S.G.S, Reston, Va., United States.

Love J. D., 1988, Geology of the Bighorn basin, northern Wyoming and southern Montana. In: Sloss, L. L., ed., The Geology of North America, v. d-2, Geological Society of America, p. 201-204.

McCubbin, D. G., 1982, Barrier island and strand plain facies. In: Scholle, P.A and Spearing, D., eds., Sandstone Depositional Environments, AAPG Memoir 31.

Miall, A. D., 1977, A review of the braided river depositional environment. *Earth Science Reviews*. v. 13, p. 1-62.

Miall, A. D., 1985, Architectural-element analysis: A new method of facies analysis applied to fluvial deposits. *Earth Science Reviews*, v. 22 (1985), p. 261-308.

Miall, A. D., 1991, Stratigraphic sequences and their chronostratigraphic correlation. *Journal of Sedimentary Petrology*, v. 61, 4, p. 497-505.

Miall, A. D., 1990, Principals of sedimentary basin analysis. Springer-Verlag New York Inc., New York.

Miall, A. D., 1996, The geology of fluvial deposits: Sedimentary facies, basin analysis, and petroleum exploration. Springer-Verlag New York Inc., New York.

Miall, A. D., 2001, The Castlegate Sandstone of the Book Cliffs, Utah; sequence stratigraphy, paleogeography, and tectonic controls. *Journal of Sedimentary Research*, v. 71, n. 4, p. 534 – 548.

Nichols, D. J., 1998, Palynological Age Determinations of Selected Outcrop Samples from the Lance and Fort Union Formations in the Bighorn basin, Montana and Wyoming. In: Keefer, W.R. and Goolsby, J.E., eds., Cretaceous and Lower Tertiary Rocks of the Bighorn basin, Wyoming and Montana, 49th Guidebook of the Wyoming Geological Association, 1998.

Obradovich, J. D., 1993, A Cretaceous time scale, In: Caldwell, W. G. E., and Kauffman, E. G., eds., The Evolution of the Western Interior basin. Geological Association of Canada Special Publication 39, p. 379-396.

Omar, G. I., and Giegengack, R., 1997, Exumation and deformation history of the Bighorn Mountains, Wyoming, from fission track analysis of basement apatites. Abstracts with Programs, Geological Society of America Annual Meeting, p. 279.

Penderson, P. K., and Steel, R., 1999, Sequence stratigraphy and alluvial architecture of the upper Cretaceous Ericson Sandstone, Glades-Clay basin area, Wyoming/Utah border. *The Mountain Geologist*, v. 36, n. 2, p. 71 – 84.

Perry, W. J., Nichols, D. J., Dyman, T. S., and Haley, C. J., 1992, Sequential Laramide deformation of the Rocky Mountain Foreland of southwestern Montana, Wyoming, and north-central Colorado. *U.S.G.S. Bulletin* 2012C, pp. C1-C14.

Posamentier, H. W., Jervey, M. T., and Vail, P. R., 1988, Eustatic controls on clastic deposition I – Conceptual framework. In: Wilgus C. K, Hastings, B. S., Kendall, C. G. St. C., Posamentier, H. W., Ross, C. A., Van Wagoner, J. C., eds., Sea-Level Changes – an Integrated Approach, SEPM Special Publication No. 42.

Posamentier, H. W., and Vail, P. R., 1988, Eustatic controls on clastic deposition II – Sequence and systems tract models. In: Wilgus C. K, Hastings, B. S., Kendall, C. G. St. C., Posamentier, H. W., Ross, C. A., Van Wagoner, J. C., eds., Sea-Level Changes – an Integrated Approach, SEPM Special Publication No. 42.

Ridgeway, K. D., Trop, J. M., and Jones, D. E., 1999, Petrology and provenance of the Neogene Usibelli Group and the Nenana Gravel: Implications for the denudation history of the central Alaska Range. *Journal of Sedimentary Research*, v. 69, n. 6, p. 1262-1275.

Roberts, E. M., 1999, Sedimentology, taphonomy, and alluvial sequence stratigraphy of the lower Two Medicine Formation (Campanian) near Choteau, Montana. Unpublished Masters Thesis, University of Montana, Missoula, 1999.

Roberts, S. B., Flores, R. M., Perry, W. J. Jr., and Nichols, D. J., 1991, Preliminary paleogeographic interpretations of Paleocene coal basins, Rocky Mountain region. *Abstracts with Programs - Geological Society of America*. 23; 4, p.87.

Roberts, S. B., 1998, An overview of the stratigraphic and sedimentologic characteristics of the Paleocene Fort Union Formation, southern Bighorn basin, Wyoming. In: Keefer, W.R. and Goolsby, J.E., eds., Cretaceous and lower Tertiary rocks of the Bighorn basin, Wyoming and Montana, 49th Guidebook of the Wyoming Geological Association, 1998.

Rogers, R. R., 1998, Sequence analysis of the upper Cretaceous Two Medicine and Judith River formations, Montana: nonmarine response to the Claggett and Bearpaw marine cycles. *Journal of Sedimentary Research*, v. 68, n. 4, p. 615.

Schmude, D., 1999, Interplay of uplift, erosion, sedimentation and preservation of Middle Jurassic rocks, Big Horn basin, Wyoming. *AAPG Bulletin* v. 83, n. 7, p. 1188.

Schumm, S. A., 1993, River response to baselevel change- Implications for sequence stratigraphy. *The Journal of Geology*, v. 101, p. 279-294.

Seeland, D., 1985, Oligocene paleogeography of the northern Great Plains and adjacent mountains. In: Flores, R. M. and Kaplan, S. S., eds., Cenozoic Paleogeography of West-Central United States, The Rocky Mountain section, Society of Economic Paleontologists and Mineralogists, Denver, Colorado, 1985.

Seeland, D., 1998, Late Cretaceous, Paleocene, and Early Eocene paleogeography of the Bighorn basin and Northwestern Wyoming. In: Keefer, W.R. and Goolsby, J.E., eds., Cretaceous and lower Tertiary rocks of the Bighorn basin, Wyoming and Montana, 49th Guidebook of the Wyoming Geological Association, 1998

Shanley, K. W., and McCabe, P. J., 1991, Predicting facies architecture through sequence stratigraphy-An example from the Kaiparowits Plateau, Utah. *Geology*, v. 19 p. 742-745.

Shanley, K. W., and McCabe, P. J., 1994, Perspectives on the sequence stratigraphy of continental strata. AAPG Bulletin v. 78, n. 4, p. 544-568.

Shuster, M. W. and Steidtmann, J. R., 1988, Tectonic and sedimentary evolution of the northern Green River basin, western Wyoming. In: Interaction of the Rocky Mountain Foreland and the Cordilleran Thrust Belt, G.S.A. Memoir 171, 1988.

Sloss, L. L., 1962, Stratigraphic models in exploration. AAPG Bulletin, v. 46, p.1050-1057

Smosna, R., Bruner, K. R., and Burns, A., 1999, Numerical analysis of sandstone composition, provenance, and paleogeography. Journal of Sedimentary Research, v. 69, n. 5, p. 1063 – 1070.

Stockmal, G. S., Cant, D. J., and Bell, J. S., 1992, Relationship of the stratigraphy of the Western Canada Foreland Basin to Cordilleran tectonics: Insights from geodynamic models. In: Macqueen, R. W., and Leckie, D. A., eds., Foreland basins and fold belts, AAPG Memoir 55, p. 395-425.

Van Wagoner, J. C., Posamentier, H. W., Mitchum, R. M., Vail, P. R., Sarg, J. F., Loutit, T. S., and Hadenbol, J., 1988, An overview of the fundamentals of sequence stratigraphy and key definitions. In: Wilgus C. K, Hastings, B. S., Kendall, C. G. St. C., Posamentier, H. W., Ross, C. A., Van Wagoner, J. C., eds., Sea-level changes – an integrated approach, SEPM Special Publication No. 42.

Webb, M. W., 2000, Fluvial sheet sandstones of the basal Lance Formation, Bighorn basin, Wyoming. Abstract, AAPG Bulletin v. 84, n. 8, p.1245.

Whipkey, C. E., Cavaroc, V. V., and Flores, R. M., 1991, Uplift of the Bighorn Mountains, Wyoming and Montana – A sandstone provenance study. U.S.G.S. Bulletin 1917-D.

Wiemer, R. J., Howard, J. D., and Lindsay, D. R., 1982, Tidal flats and associated tidal channels. In: Scholle, P.A and Spearing, D., eds., Sandstone Depositional Environments, AAPG Memoir 31.

Wiemer, R. J., 1988, Record of relative sea-level changes, Cretaceous Western Interior, USA, In: Wilgus C. K, Hastings, B. S., Kendall, C. G. St. C., Posamentier, H. W., Ross, C. A., Van Wagoner, J. C., eds., Sea-Level Changes, and Integrated approach, SEPM Special Publication No. 42.

Wing, S. L., and Bown, T. M., 1985, Fine scale reconstruction of Late Paleocene-Early Eocene paleogeography in the Bighorn basin of northern Wyoming. In: Flores, R. M., and Kaplan, S. S., eds., Cenozoic Paleogeography of West-Central United States. The Rocky Mountain section, Society of Economic Paleontologists and Mineralogists, Denver, Colorado, 1985.

Wiltchko, D. W., and Dorr, J. A. Jr., 1983, Timing of deformation in the overthrust belt and foreland of Idaho, Wyoming, and Utah. *AAPG Bulletin* v. 67, n. 8, p. 1304 -1322.

Wright, V. P., and Marriot, S. B., 1993, The sequence stratigraphy of fluvial depositional systems: the role of floodplain sediment storage. *Sedimentary Geology*, v. 86, p. 203-210.

Yuretich, R. F., and Hickey, L. J., 1984, Lacustrine deposits in the Paleocene Fort Union Formation, northern Bighorn basin, Montana. *Journal of Sedimentary Petrology*, v. 54, n. 3, p. 836 – 852.

Yuretich, R. F., and Hicks, J. F., 1986, Sedimentology and facies relationships of the Belfry Member, Fort Union Formation, northern Bighorn basin. MGS-YRBA Field Conference.

Zhang, Z., Sun, K., Yi, J., 1997, Sedimentology and sequence stratigraphy of Shanxi Formation (Lower Permian) in the northwestern Ordos basin, China; an alternative sequence model for fluvial strata. *Sedimentary Geology* v.112, p. 123-136.